POWER EVACUATION STUDIES FOR GRID INTEGRATED WIND ENERGY CONVERSION SYSTEM

March 2014

Project Number: RD-RD-192-10



Dr. R.P.Kumudini Devi Dr.P.Somsundaram Mrs.S.V.Anbuselvi Associate Professor Associate Professor Associate Professor

Department of Electrical and Electronics Engineering Anna University Chennai – 600025

NOTICE

This report was prepared as an account of the work sponsored by Centre for Wind Energy Technology (C-WET). Neither C-WET nor any of their employees, makes any warranty, express or implied, or assumes any legal liability or responsibility for the accuracy, completeness, or usefulness of any information, apparatus, product, or process disclosed, or represent that its use would not infringe privately owned rights. Reference herein to any specific commercial product, process, or service by trade name, trademark, manufacturer, or otherwise does not necessarily constitute or imply its endorsement, recommendation, or favoring by C-WET. The views and opinions of authors expressed herein do not necessarily state or reflect those of C-WET.

No part of this report shall be either reproduced or otherwise be used in any form without the written permission of the C-WET and the proponent.

Available electronically at http://www.cwet.res.in

ACKNOWLEDGEMENTS

The Centre for Wind Energy Technology (C-WET) would like to acknowledge the experts from Anna University, Chennai - 600025, who have authored this report. C-WET also thanks the Ministry of New and Renewable Energy (MNRE) for their financial and technical support for the research and production of this report.

Major contributors in alphabetical order include :

Anbuselvi.S.V Associate Professor Kumudini Devi.R.P Associate Professor Somsundaram.P Associate Professor

TABLE OF CONTENTS

| TERMS OF REFERENCE | 8 | | | |
|--|----|--|--|--|
| SCOPE OF WORK | 9 | | | |
| EXECUTIVE SUMMARY | | | | |
| ROAD MAP OF THE PROJECT | 11 | | | |
| 1. INTRODUCTION | 12 | | | |
| 2. FIELD VISIT AND DATA COLLECTION | 13 | | | |
| 2.1 Introduction | 13 | | | |
| 2.2 Generation details in Tirunelveli region | | | | |
| 2.3 Substation details in Tirunelveli region | 15 | | | |
| 2.4 Summary | 17 | | | |
| 3. POWER FLOW ANALYSIS | 18 | | | |
| 3.1 Introduction | 18 | | | |
| 3.2 Aggregated model for grid connected wind farms | 18 | | | |
| 3.3 Voltage profile and line over loading | | | | |
| 3.4 Reactive power requirement | 23 | | | |
| 3.5 Real power losses | | | | |
| 3.6 Summary | 24 | | | |
| 4. SHORT CIRCUIT ANALYSIS | 25 | | | |
| 4.1 Introduction | | | | |
| 4.2 Short circuit assumptions | 25 | | | |
| 4.3 Systematic computation for large scale systems | | | | |
| 4.4 Strong and weak buses without wind farms | | | | |
| 4.4.1 Strong buses in the system | | | | |
| 4.4.2 Weak buses in the system | | | | |
| 4.5 Summary | 30 | | | |
| 5. POWER FLOW WITH TCSC AND VSC BASED HVDC SYSTEM | | | | |
| 5.1 Introduction to TCSC | | | | |
| 5.2 TCSC Fundamental impedance | | | | |
| 5.3 TCSC Power flow model | 33 | | | |

| | 5.3.1 TCSC Impedance as a function of firing angle | 33 |
|-----|--|--|
| | 5.3.2 Firing angle initial condition | 35 |
| | 5.3.3 Truncated adjustments | 36 |
| | 5.3.4 Limits revision | 36 |
| | 5.4 VSC based HVDC Transmission for wind power evacuation | 37 |
| | 5.4.1 VSC based HVDC Transmission | 37 |
| | 5.4.2 Why VSC based HVDC transmission for wind power evacuation? | 37 |
| | 5.4.3 World wide VSC installations for wind power evacuation | 38 |
| | 5.4.4 Modeling of VSC based HVDC link for power flow studies | 39 |
| | 5.4.5 Control modes | 41 |
| | 5.5 Incorporation of VSC based HVDC in power flow analysis | 42 |
| | 5.6 VSC MTDC system | |
| | 5.7 Power flow analysis with TCSC | 49 |
| | 5.7.1 Power flow with 80% wind power penetration (without TCSC) | 50 |
| | 5.7.2 Power flow with 80% wind power penetration (with TCSC) | 50 |
| | 5.7.3 Installed TCSC projects in India | 51 |
| | 5.8 Power flow analysis with VSC-HVDC | 52 |
| | 5.8.1 Results from power flow analysis (Lines overloaded >100%) | 52 |
| | 5.9 VSC MTDC System power flow results | 54 |
| | 5.10 Summary | 56 |
| _ | 5. TRANSIENT STABILITY ANALYSIS | |
| U). | | |
| | | |
| | 6.1 Introduction | 57 |
| | 6.1 Introduction | 57 57 |
| | 6.1 Introduction | 57 57 59 |
| | 6.1 Introduction | 57 57 59 |
| | 6.1 Introduction 6.1.1 Classification of power system stability 6.2 Transient stability analysis 6.3 Modelling of power system components for stability studies 6.3.1 Synchronous machine model | 57 57 59 59 |
| | 6.1 Introduction 6.1.1 Classification of power system stability 6.2 Transient stability analysis 6.3 Modelling of power system components for stability studies 6.3.1 Synchronous machine model 6.3.2 Transmission line model | 57 57 59 59 60 |
| | 6.1 Introduction 6.1.1 Classification of power system stability 6.2 Transient stability analysis 6.3 Modelling of power system components for stability studies 6.3.1 Synchronous machine model 6.3.2 Transmission line model 6.3.3 Load model | 57 57 59 59 60 |
| | 6.1 Introduction 6.1.1 Classification of power system stability 6.2 Transient stability analysis 6.3 Modelling of power system components for stability studies 6.3.1 Synchronous machine model 6.3.2 Transmission line model 6.3.3 Load model 6.3.4 Wind turbine model | 57 57 59 59 60 60 |
| | 6.1 Introduction 6.1.1 Classification of power system stability 6.2 Transient stability analysis 6.3 Modelling of power system components for stability studies 6.3.1 Synchronous machine model 6.3.2 Transmission line model 6.3.3 Load model 6.3.4 Wind turbine model 6.3.5 Induction generator model | 57 57 59 59 60 60 61 |
| | 6.1 Introduction 6.1.1 Classification of power system stability 6.2 Transient stability analysis 6.3 Modelling of power system components for stability studies 6.3.1 Synchronous machine model 6.3.2 Transmission line model 6.3.3 Load model 6.3.4 Wind turbine model 6.3.5 Induction generator model 6.3.6 Transient model of IG | 57 57 59 60 60 61 62 |
| | 6.1 Introduction 6.1.1 Classification of power system stability 6.2 Transient stability analysis 6.3 Modelling of power system components for stability studies 6.3.1 Synchronous machine model 6.3.2 Transmission line model 6.3.3 Load model 6.3.4 Wind turbine model 6.3.5 Induction generator model 6.3.6 Transient model of IG 6.4 Initialization | 57 59 59 60 61 62 63 |
| | 6.1 Introduction 6.1.1 Classification of power system stability 6.2 Transient stability analysis 6.3 Modelling of power system components for stability studies 6.3.1 Synchronous machine model 6.3.2 Transmission line model 6.3.3 Load model 6.3.4 Wind turbine model 6.3.5 Induction generator model 6.3.6 Transient model of IG 6.4 Initialization 6.5 Algorithm to advance simulation by one time step | 57 57 59 59 60 61 62 63 65 |
| | 6.1 Introduction 6.1.1 Classification of power system stability 6.2 Transient stability analysis 6.3 Modelling of power system components for stability studies 6.3.1 Synchronous machine model 6.3.2 Transmission line model 6.3.3 Load model 6.3.4 Wind turbine model 6.3.5 Induction generator model 6.3.6 Transient model of IG 6.4 Initialization 6.5 Algorithm to advance simulation by one time step 6.6 Handling network discontinuities | 5759596061626365 |
| | 6.1 Introduction | 57 57 59 60 61 62 63 65 66 66 66 |
| | 6.1 Introduction 6.1.1 Classification of power system stability 6.2 Transient stability analysis 6.3 Modelling of power system components for stability studies 6.3.1 Synchronous machine model 6.3.2 Transmission line model 6.3.3 Load model 6.3.4 Wind turbine model 6.3.5 Induction generator model 6.3.6 Transient model of IG 6.4 Initialization 6.5 Algorithm to advance simulation by one time step 6.6 Handling network discontinuities 6.7 Effect of wind generator on transient stability 6.7.1Low Voltage Ride Through (LVRT) | 575960616365666666 |
| | 6.1 Introduction | 57596061626365666970 |
| | 6.1 Introduction 6.1.1 Classification of power system stability 6.2 Transient stability analysis 6.3 Modelling of power system components for stability studies 6.3.1 Synchronous machine model 6.3.2 Transmission line model 6.3.3 Load model 6.3.4 Wind turbine model 6.3.5 Induction generator model 6.3.6 Transient model of IG 6.4 Initialization 6.5 Algorithm to advance simulation by one time step 6.6 Handling network discontinuities 6.7 Effect of wind generator on transient stability 6.7.1Low Voltage Ride Through (LVRT) 6.8 Wind farm behaviour without LVRT capability 6.8.1 Fault at KANYAKUMARI Bus | 575960616365666970 |
| | 6.1 Introduction | 57 57 59 60 61 62 63 65 66 69 70 70 |

| 6.8.4 Fault at AMDAPURAM Bus | 72 |
|---|----|
| 6.9 Wind farm behaviour LVRT capability | 72 |
| 6.9.1 Fault at KANYAKUMARI Bus | 72 |
| 6.9.2 Fault at SR PUDUR21 Bus | 74 |
| 6.9.3Fault at VEERAN21 Bus | |
| 6.9.4 Fault at AMDAPURAM Bus | |
| 6.10 Summary | 79 |
| oilo Sammary | |
| 7. Conclusions and Recommendations | 80 |
| 7. Conclusions and Recommendations | 80 |
| 7. Conclusions and Recommendations | 80 |
| 7. Conclusions and Recommendations | |

ABBREVIATIONS

WTGs Wind turbine generators

IG Induction generator

FACTS Flexible AC Transmission Systems

TCSC Thyristor Controlled Series Compensator

VSC Voltage Source Converter

HVDC High Voltage Direct current

PWM Pulse Width Modulation

WECS Wind energy conversion systems

LVRT Low Voltage Ride Through

LIST OF SYMBOLS

- f Operating Frequency, 50Hz
- R_a Armature resistance of the synchronous machine
- X_d Synchronous reactance of d-axis winding of the synchronous machine
- x_d ' Transient reactance of d-axis winding of the synchronous machine
- X_q Synchronous reactance of q-axis winding of the synchronous machine
- X_q ' Transient reactance of q-axis winding of the synchronous machine
- T_{d0} Open circuit time constant of the d-axis winding of the synchronous machine
- T_{q0} Open circuit time constant of the q-axis winding of the synchronous machine
 - δ Load angle in degree
 - E' Internal voltage of synchronous machine
 - R_s Stator resistance of induction machine
 - R_r Rotor resistance of induction machine
- X_s Stator leakage reactance of induction machine
- X_r Rotor leakage reactance of induction machine
- X_m Magnetizing reactance of induction machine
- I₁ Stator current of induction machine
- I₂ Rotor current of induction machine
- V Terminal voltage of induction machine
- s Slip
- N_t Number of wind turbine generators
- E'r E'm Internal voltages of induction machine
 - P_a Air gap power
 - θ Pitch angle
 - ω Wind turbine shaft speed
 - R Radius of the wind turbine rotor

- $\omega_{\rm s}$ Synchronous speed
- ω_r Angular speed of the rotor
- λ Tip speed ratio
- I_{Norton} Norton current source
 - α⁰ Initial Firing angle of TCSC
 - α Firing angle of TCSC
- P_{spec} Specified real power flow at HVDC terminal
- Q_{spec} Specified reactive power flow at HVDC terminal
- P_{HVDC1} Calculated real power flow at converter 1.
- P_{HVDC2} Calculated real power flow at converter 2.
- Q_{HVDC1} Calculated reactive power flow at converter 1.
- Q_{HVDC2} Calculated reactive power flow at converter 2.
 - Z_{VR} Impedence of converter transformer
 - Y_{VR} Admittance of converter transformer
 - V_k AC voltage at bus k
 - θ_k Voltage angle at bus k
 - \overline{V}_{VR} Voltage at fictitious bus
 - δ_{VR} Voltage angle of fictitious bus
 - X_{TCSC} TCSC equivalent reactance
 - Z Bus impedance matrix
 - Y Bus admittance matrix
 - B Susceptance
 - H_t Inertia of the turbine
 - H_g Inertia of the generator

TERMS OF REFERENCE

A project team from Anna University is formed to analyze the power evacuation problems for grid integrated wind energy conversion system. Accordingly a project proposal was submitted to Center for Wind Energy Technology (C-WET), Chennai. C-WET had allotted a project namely "Power Evacuation Studies for Grid Integrated Wind Energy Conversion System" to the Head of the Department of Electrical and Electronics Engineering (DEEE) through appropriate authorities of Anna University (AU) to study the Power Evacuation for a part of southern grid (Tirunelveli /Tamil Nadu). A project team was formed whose composition is given below:

1. Dr.R.P.Kumudini Devi, Associate Professor, DEEE, AU. Principal Investigator

2. Dr.P.Somasundaram, Associate Professor, DEEE, AU. Co-Investigator

3. Mrs.S.V.Anbuselvi, Assistant Professor, DEEE, AU. Co-Investigator

SCOPE OF WORK

The project was agreed to be executed in following five phases:

- Phase I: To collect the data for the particular area in TNEB grid through field visit.
- **Phase II**: To model the wind turbine generators (WTGs) for power flow studies and develop source code by considering suitable model for squirrel cage induction generator.
- **Phase III**: To model the wind turbine generators for short circuit studies and to identify the weak and strong points for addition of WTGs.
- **Phase IV**: To model the TCSC and VSC based HVDC system for power flow studies and to analyze the enhancement of power evacuation from WTGs.
- **Phase V**: To develop a transient stability model of WTGs and to analyze the system stability with wind energy conversion system (WECS).

EXECUTIVE SUMMARY

- Tirunelveli region is considered for the analysis. The data pertaining to this region is collected through field visits.
- Power flow analysis is carried out for two different cases by varying the wind power penetration from 40% to 80% of the installed capacity and the over loaded transmission lines are identified.
- Short circuit analysis is carried out without WTGs to determine the fault level. The strong buses are identified for the future capacity addition in this region. Addition of WTGs can be avoided to the identified weak buses

.

- Power flow analysis is carried out with TCSC and VSC based HVDC system for future expansion of WTGs installation and to alleviate the power evacuation problems.
- Transient stability analysis with WTGs is carried out to study the effect of WTGs on the system stability.
- Conclusions and Recommendations are drawn based on the analysis.

ROAD MAP OF THE PROJECT

| Phase | Activity Block | Time Required (in months) |
|-------|--|---------------------------|
| I | Data collection for the particular area in TNEB grid. | 6 |
| II | Modeling of wind Generators for power flow studies Source code development by considering suitable model for squirrel cage Induction generator Power flow results for the system | 6 |
| III | Modeling of wind generators for short circuit studies Short circuit study for system considered to identify the weak points | 6 |
| IV | Power flow modeling of TCSC and VSC based HVDC system Power flow study with TCSC/VSC based HVDC system | 6 |
| V | Development of stability model for wind Energy conversion systems. Transient stability analysis for the system considered. Report preparation and training for Practicing Engineers. | 6 |
| | Dura | tion: 30 months |

1. INTRODUCTION

In the year 2010-11, the installed capacity of wind generators is 7134 MW (as on 31-09-2012) and an additional capacity of 6000 MW targeted under 12th five year plan by the Department of Energy, Government of Tamil Nadu. The additional wind power generation may require enhancement in the line capacity and VAR compensation in the grid. Therefore power evacuation studies are necessary to assess the technical feasibility of the grid to evacuate wind power from wind turbine generators. Power evacuation studies comprise of Power flow, short circuit and transient stability studies.

Planning, operation and control of WTG integrated power systems poses a variety of challenging problems. The solution of which requires extensive analysis of power system with WTGs. This project aims at carrying out the power flow, short circuit and transient stability studies for a part of Tamil Nadu grid with WTGs.

Power-flow studies are of great importance in planning and designing the future expansion of power systems as well as in determining the best operation of existing systems. The principal information that can be obtained from the power flow analysis is the reactive power consumption and loading of lines with respect to the wind power penetration. Short-circuit studies are essential to arrive at the possible locations for future wind power penetration to the grid. Transient stability analysis of the power system with WTGs is necessary as it provides the information regarding the fault ride through/low voltage through capabilities of WTGs.

From literature, it is noted that power transfer capabilities of transmission lines and VAR management are enhanced with the help of FACTS/VSC based HVDC link. Hence an attempt is made to include the FACTS/VSC based HVDC link in the network considered for analysis.

2. FIELD VISIT AND DATA COLLECTION

2.1 Introduction

During the first field visit, the Tirunelveli network details are obtained from the Superintending Engineer, Wind Energy Development Cell, Tirunelveli. The single line diagram of wind farm and distribution substations in Tirunelveli region is shown in Figure 2.1.

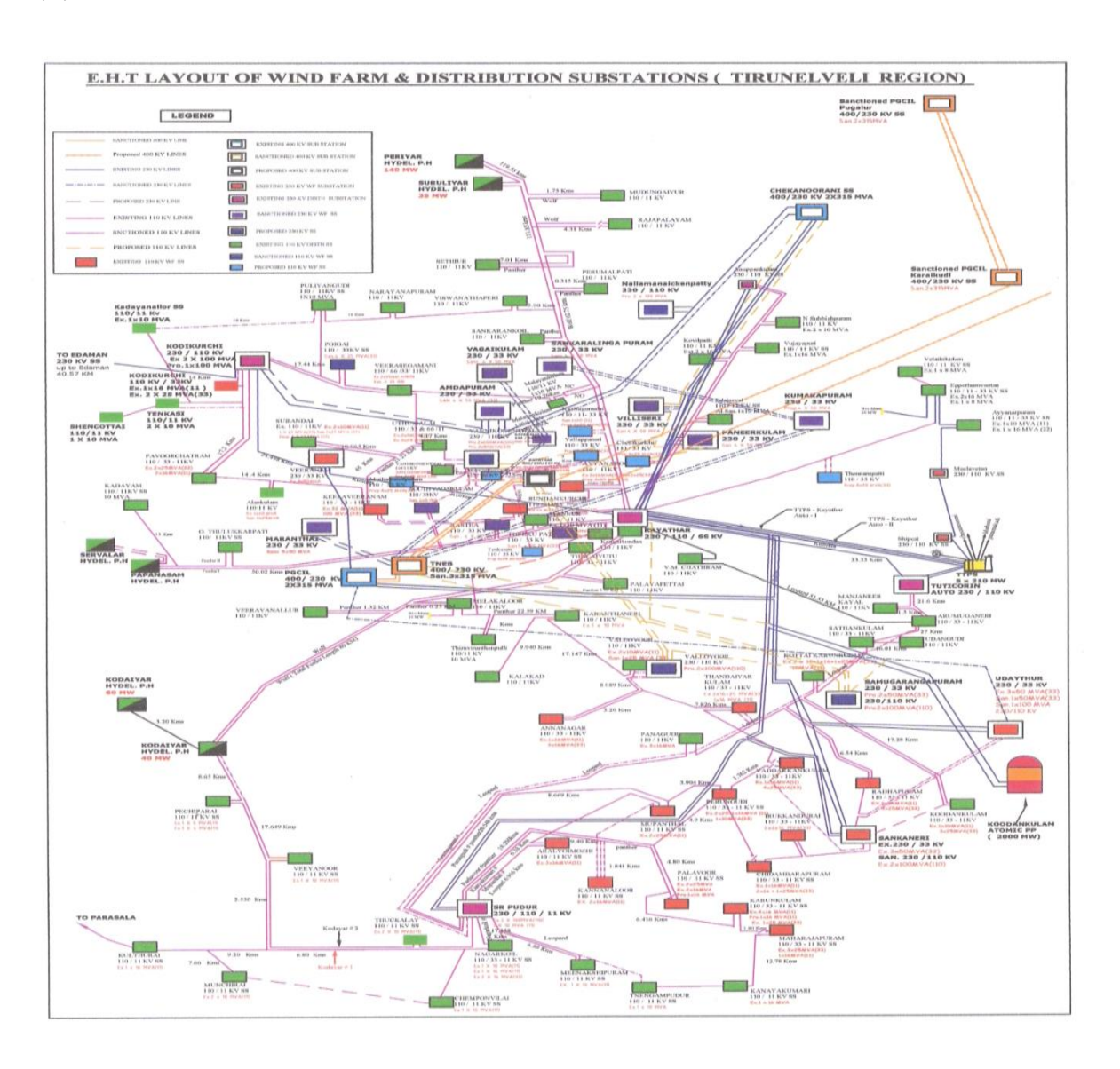


Figure 2.1 EHT layout of wind farm and distribution substations in Triunelveli study system

Tirunelveli region consists of 44 substations out of which 22 are dedicated for wind farms. The wind farms consist of different rating of induction generators of 225kW, 250kW, 500kW, 750kW, 900kW up to 2.1MW.

The wind generators data such as rated power of each wind turbine, rated apparent power, rated wind speed, cut-in wind speed, cut-out wind speed, rated voltage, rated current, short circuit ratio, synchronous speed, rated slip, magnetizing reactance of generator, stator resistance and leakage reactance, stator reactance, rotor resistance and leakage reactance, rotor reactance are collected.

The wind turbine transformer data such as transformer voltage ratio, percentage impedance, winding connection and tap settings are collected.

In the second visit, wind farm related data like wind farm sub-station details, generation data, load data, load shedding, peak return, private generation and full returns for 2010 are collected.

The data required for analysis such as generator data, substation data, bus data, transmission line data, shunt elements data, power transformer data, load data and conductor data are collected from TANGEDCO and are tabulated in Appendix – A and Appendix – B.

2.2 Generation details in Tirunelveli region

The Tirunelveli network comprises of a mix of various generations such as thermal, hydro, biomass and wind. The conventional generation details in the Tirunelveli region are tabulated in Table 2.1.

Table 2.1 Generation details of Tirunelveli region

| S.No | Generator Name | Installed capacity (MW) = (No.of units installed in MW) X (Capacity of single unit) | Total(MW) |
|------|--|---|-----------|
| 1 | Tuticorin Thermal Power Station (TTPS) | 5x210 | 1050 |
| 2 | Ind-Bharath Captive Thermal Power plant | 1X210 | 210 |
| 3 | Kodayar-I Hydro Generator | 1x60 | 60 |
| 4 | Kodayar-II Hydro Generator | 1x40 | 40 |
| 5 | Suruliyar Hydro Generator | 1x35 | 35 |
| 6 | Periyar Hydro Generator | 4x35 | 140 |
| 7 | Servalar Hydro Generator | 1x20 | 20 |
| 8 | Papanasam Hydro Generator | 1x32 | 32 |
| 9 | Biomass Eppothumventran Generator | 1X21 | 21 |
| 10 | Biomass Melakaloor Generator | 1X21 | 21 |
| | 1 | Total | 1608 |

2.3 Substation details in Tirunelveli region

The total installed capacity of WTGs in Tirunelveli region is 2857.70 MW (up to September 2010). The total number of wind turbine generators is 5106 (up to September 2010). The Table 2.2 shows substation-wise total number of connected wind turbine generators and their installed capacity (MW).

Table: 2.2 Substation details

| Sl.No | Name of the substation | Number of WTGs | Installed capacity in MW |
|-------|-----------------------------------|-------------------|--------------------------|
| 1 | Ayyanaruthu 110/11 kV SS | 174 | 81.78 |
| 2 | Kayathar 66/11 kV SS | 29 | 10.765 |
| 3 | Chettikurichy 66/11 kV SS | 3 | 4.4 |
| 4 | Perungudi 110/33-11 kV SS | 346 | 102.455 |
| 5 | Vadakkankulam 110/33-11 kV SS | 272 | 134.98 |
| 6 | Kottaikarungulam 110/33-11 kV SS | 91 | 65.025 |
| 7 | Radhapuram 110/33-11 kV SS | 180 | 139.215 |
| 8 | Muppandal 110/11 kV SS | 223 | 55.125 |
| 9 | Panagudi 110/11 kV SS | 96 | 47.875 |
| 10 | Aralvoimozhi 110/11 kV SS | 211 | 53.565 |
| 11 | Pazhavoor 110/11 kV SS | 315 | 91.505 |
| 12 | Karunkulam 110/33-11 kV SS | 321 | 113.155 |
| 13 | Koodankulam 110/33-11 kV SS | 83 | 90.25 |
| 14 | Kottaram 110/11 kV SS | 15 | 7.45 |
| 15 | Anna Nagar 110/33-11 kV SS | 119 | 66.775 |
| 16 | Sankaneri 230/110 kV SS | 137 | 152.3 |
| 17 | Chenbagaramanputhoor 110/11 kV SS | 9 | 2.25 |
| 18 | Chidambarapuram 110/33-11 kV SS | 228 | 79.75 |
| 19 | Maharajapuram 110/33-11 kV SS | 136 | 84.73 |

| 20 | Kannanallur 110/11 kV | 148 | 36.225 |
|----|----------------------------------|------|---------|
| 21 | SPIC 230 / 110 / 22 KV SS | 20 | 1.1 |
| 22 | Irrukkanthurai 110/33 kV SS | 26 | 29.2 |
| 23 | Udayathur 230/110kV SS | 130 | 196.55 |
| 24 | Thandaiyarkulam 110/33-11 kV SS | 170 | 104.2 |
| 25 | Vannikonendal 66/11 kV SS | 40 | 12.545 |
| 26 | Sundankurichi 110/33-11 kV SS | 104 | 91.5 |
| 27 | Keelaveeranam 110/33-11 kV SS | 324 | 144.275 |
| 28 | Veeranam 230/33KV SS | 182 | 201.6 |
| 29 | Alankulam 110/11 kV SS | 89 | 61.55 |
| 30 | Uthumalai 110/33-11 kV SS | 78 | 92.75 |
| 31 | Surandai 110/11 kV SS | 82 | 50.95 |
| 32 | P V Chatram 110/33-11 kV SS | 102 | 71.4 |
| 33 | Kodikuruchi 110/33-11 kV SS | 148 | 68.425 |
| 34 | Tenkasi 110/11 kV SS | 35 | 16.9 |
| 35 | Shencottah 110/11 kV SS | 25 | 10.045 |
| 36 | Kadayanallur 110/11 kV SS | 54 | 23.66 |
| 37 | Veerasigamani 110/66-33-11 kV SS | 221 | 98.57 |
| 38 | Amuthapuram 230/33 kV SS | 54 | 87.6 |
| 39 | Rastha 110/33 kV SS | 16 | 24 |
| 40 | Manur 110/11KV SS | 53 | 42.4 |
| 41 | Mandapam 110/33-11 kV SS | 4 | 0.9 |
| 42 | Rameshwaram 110/11 kV SS | 2 | 0.5 |
| 43 | Gangaikondan 110/11 KV SS | 1 | 0.055 |
| 44 | Kanyakumari 110/11kV SS | 10 | 7.45 |
| | Total | 5106 | 2857.70 |

2.4 Summary

The data required for power evacuation studies such as power flow analysis, short circuit analysis and stability analysis are collected through field visit for the Tirunelveli region.

3. POWER FLOW ANALYSIS

3.1 Introduction

The Tirunelveli network consists of 156 buses, 210 transmission lines, 44 transformers and 5106 WTGs. The network comprises of a mix of various generations such as thermal, hydro, biomass and wind. As the network consists of large number of WTGs it is necessary to go for an aggregated model to reduce the simulation time. This chapter deals with aggregated model for grid connected wind farms and power flow analysis.

3.2 Aggregated model for grid connected wind farms

Wind farms with wind turbine generators can be simulated by a complete model including the modeling of all the wind turbines and the wind farm electrical network. To represent wind turbines in wind farms without increasing unnecessarily the model order, reduced models have been used. But this complete model presents a high order model if a wind farm with high number of wind turbines is modeled and therefore the simulation time is long.

To reduce the complexity of the wind farm model and the simulation time when simulating wind farms with wind turbines in power systems, aggregated models of wind farms have been developed by the aggregation of wind turbines with identical wind into an equivalent wind turbine. The aggregation of wind turbine generators with identical wind speeds into an equivalent wind turbine generator experiencing that wind speed has been considered. This equivalent wind turbine presents the same per unit model and parameters of that of individual wind turbine generator.

The two main assumptions made while reducing the wind park to a single equivalent are:

- All wind turbines have same operating point.
- If difference in operating point exists it is not too large.

When reducing the aggregate model of the large wind farm for the purpose of simulation studies the following criteria shall be fulfilled:

 The MVA-rating (S_{Agg}) of the aggregated wind farm equivalent is the sum of the MVA- ratings of individual WTGs in the system.

$$S_{\text{Agg}} = \sum_{i=1}^{IG} S_i$$

where S_i, is the MVA rating of the individual WTGs in the system.

• The wind farm equivalent supplies the same amount of electric power which is given as,

$$P_{\text{Agg}} = \sum_{i=1}^{IG} P_i$$

where P_i is the electric power supplied by individual wind turbine generator.

A simple aggregated model is considered in all the studies (Power flow analysis, Short circuit analysis and Transient stability analysis) for representing wind farms. Simple aggregation is explained by considering the Kayathar wind farm. By assuming the direction of the wind velocity as shown in Figure 3.1.a and neglecting the wake effect, the wind farm is represented by its simple aggregated model as shown in Figure 3.1.b. The parameters of WTG's in simple aggregated model is explained in Table3.1

 Table3.1 Parameters of Detailed and Simple aggregated model

| Sl.No | Nomenclature | Detailed model of | Simple aggregation model of | |
|---|---|-------------------|-----------------------------|--|
| | | single WTG | wind farm | |
| 1. | Stator Resistance R _s | R _s | R_s/N_t^* | |
| 2. | Stator Reactance X _s | X _s | X_s/N_t | |
| 3. | Rotor Resistance R _r | R _r | R_r/N_t | |
| 4. | Rotor Reactance X _r | X _r | X_r/N_t | |
| 5. | Mutual Reactance X _m | X _m | X_m/N_t | |
| 6. | Inertia of the turbine - H _t | H _t | $H_t * N_t$ | |
| 7. | Inertia of the generator – H _g | H_{g} | $H_g * N_t$ | |
| * N _t -Number of wind turbine generators | | | | |

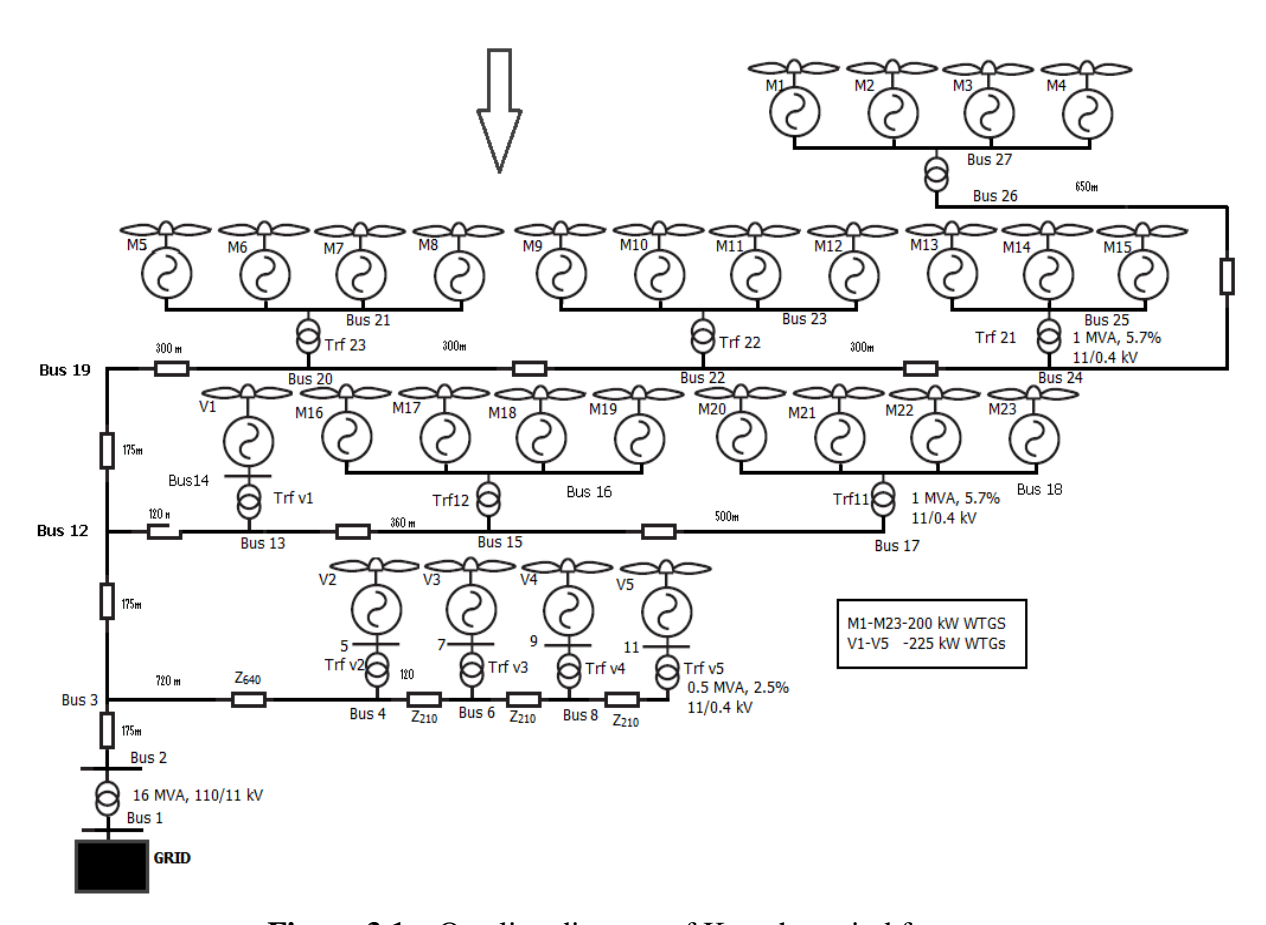


Figure 3.1.a One line diagram of Kayathar wind farm

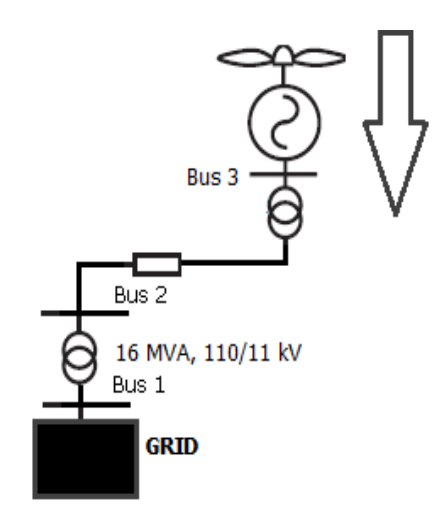


Figure 3.1.b Simple aggregation of Kayathar wind farm.

3.3 Voltage profile and line over loading

The power flow analysis is conducted for following cases:

- Case 1: 100% Hydro with nil wind power generation
- Case 2: 100% Hydro with different levels of wind power penetration.

Power flow analysis is carried out for two different cases by varying the wind power penetration from 40% to 80% of the installed capacity and the over loaded transmission lines are identified.

Case 1: 100% Hydro and nil wind power generation

In this case, Thermal generators meet the base load and the hydro generators are considered at maximum generation (six generators). The wind generation is nil. Only three lines are loaded between 75% to 100%.

Case 2: 100% Hydro with different levels of wind power penetration

The load flow analysis is carried out by varying the wind power penetration from 40% to 80% of the installed capacity of 2857.70 MW (up to September 2010).

a) Power flow with 40% wind power penetration:

Considering full hydro and up to 40% of wind power penetration, none of the transmission lines are overloaded and the voltage profile is good throughout the network.

b) Power flow with 50% wind power penetration:

Considering full hydro and 50% wind power penetration,

- Wind power penetration into the grid is 672.20 MW.
- Eight Transmission Lines are loaded from 75% to 100%.
- Low voltage is observed at PARAMAGUDI SS as 0.9352 p.u.
- Total reactive power compensation of 120.56 MVAR is provided.

c) Power flow with 70% wind power penetration

Considering full hydro and 70% wind power penetration, the lines that are overloaded are given in Table 3.2.

Table 3.2 Overloaded transmission lines at 70% of wind power penetration

| Lines | | | | | Rating |
|-----------------|---------------|----------|---------|-----------|--------|
| From substation | To substation | MW | MVAR | % Loading | (MVA) |
| SANKANE2 | SANKAN21 | -224.571 | 12.959 | 115 | 200 |
| UDAYTHR2 | UDAYTR21 | -200.807 | 19.35 | 103 | 200 |
| RADHAPUR | KOTTAIKA | 89.481 | -10.714 | 102 | 90 |
| MUPPTOFF | PERUNGUD | -92.156 | 7.071 | 104 | 90 |
| KAYATR21 | AYYANARO | -96.253 | -6.917 | 110 | 90 |
| KOTTAIKA | SATHANK | 108.734 | -21.852 | 127 | 90 |
| KEELAVEE | KAYATR21 | 104.289 | 3.75 | 115 | 90 |
| SATTURTF | OTHULUKK | -93.699 | 14.406 | 109 | 90 |
| MALAYTOF | MALAYANK | -70.729 | 7.416 | 102 | 90 |

d) Power flow with 80% wind power penetration

Considering full hydro and 80% wind power penetration, the lines that are overloaded are given in Table 3.3.Low voltage profile observed at four buses.

Table 3.3 Overloaded transmission lines at 80% of wind power penetration.

| Lines | | | | % Loading | Rating |
|-----------------|-----------------|----------|---------|-----------|--------|
| From substation | From substation | MW | MVAR | | (MVA) |
| SANKANE2 | SANKAN21 | -262.925 | 14.588 | 136 | 200 |
| UDAYTHR2 | UDAYTR21 | -234.852 | 21.478 | 122 | 200 |
| SRPUDU21 | ARALVOIM | -92.847 | 12.958 | 107 | 90 |
| SATHANK | ARUMUGAN | 86.22 | -28.587 | 105 | 90 |

| RADHAPUR | KOTTAIKA | 99.843 | -20.72 | 115 | 90 |
|----------|----------|----------|---------|-----|----|
| VALLIYUR | ANNANAGA | -87.046 | 26.12 | 103 | 90 |
| VALLIYUR | KARANTHA | 84.086 | -28.121 | 101 | 90 |
| VEERASEG | UTHUMALA | -91.679 | -8.749 | 102 | 90 |
| SRPUDU21 | MUPPTOFF | -100.62 | 3.807 | 115 | 90 |
| SRPUDU21 | PERUTOFF | -98.317 | 3.803 | 113 | 90 |
| PALATOFF | KARUNKUL | -90.018 | 4.648 | 101 | 90 |
| MUPPTOFF | PERUNGUD | -104.403 | 8.673 | 118 | 90 |
| KAYATR21 | AYYANARO | -112.464 | -2.389 | 129 | 90 |
| KOTTAIKA | SATHANK | 124.943 | -29.038 | 147 | 90 |
| KEELAVEE | KAYATR21 | 120.458 | -0.058 | 133 | 90 |
| ANUPPA21 | SATTURTF | -91.762 | 23.633 | 109 | 90 |
| SATTURTF | OTHULUKK | -105.146 | 17.486 | 122 | 90 |
| MALAYTOF | MALAYANK | -74.931 | 11.82 | 109 | 90 |

3.4 Reactive power requirement

The reactive power compensation required for different levels of wind power penetration is shown in Figure 3.2

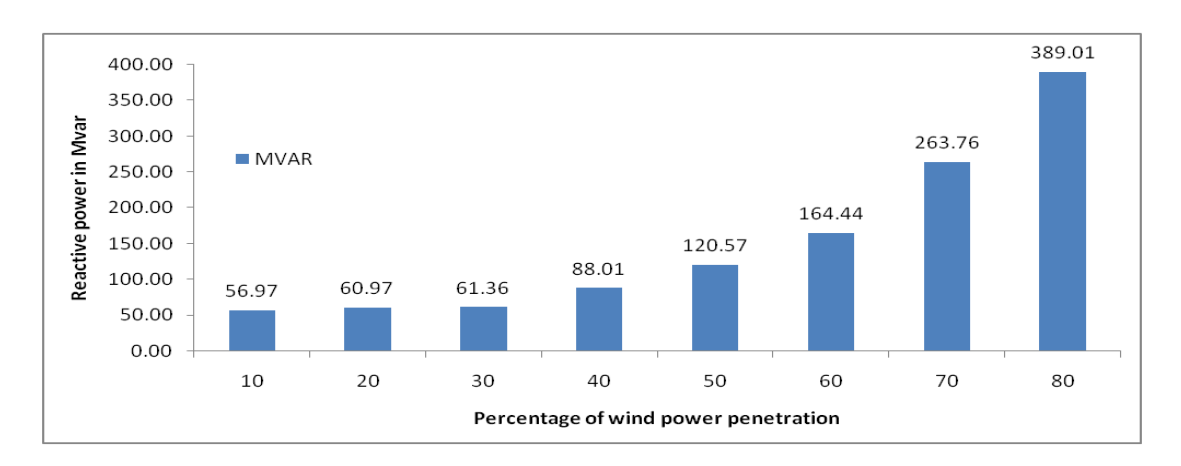


Figure 3.2 Percentage of wind power penetration Vs required reactive power

3.5 Real power losses

The real power loss with different levels of wind power penetration is shown in Figure 3.3

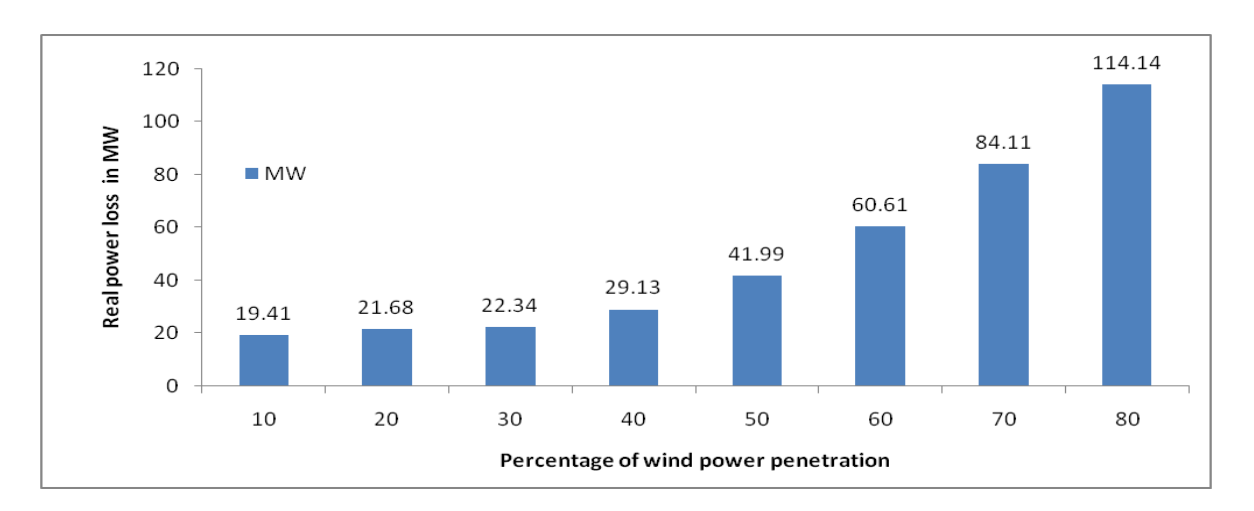


Figure 3.3 Percentage of wind power penetration Vs real power losses

3.6 Summary

Power flow analysis is carried out for Tirunelveli network with WTG's and it is observed that increasing wind power penetration leads to overloading of more number of the transmission lines and transformers.

4. SHORT CIRCUIT ANALYSIS

4.1 Introduction

Short circuit analysis of Tirunelveli system is performed to identify weak buses and strong buses in the system under disturbance. The possibilities for a short circuit in three-phase system are as follows

- a. Symmetrical three phase-to-ground fault
- b. Symmetrical three phase fault
- c. Single-line-to-ground(LG) fault
- d. Line-to-line(LL) fault
- e. Double-line-to-ground(LLG) fault

Fault of the type (a) and (b) have a symmetric impedance and/or admittance representation. Hence, for faults of these types, the system becomes a balanced three-phase network with balanced excitation. Analysis of such balanced three-phase networks can be carried out on the basis of a per phase equivalent, except that the impedances are now replaced with 'Positive sequence' impedances. In the case of unsymmetrical faults-type (c), (d), and (e) such a simplified analysis is not possible and the analysis is either carried out through sequence components.

4.2 Short circuit assumptions

In arriving at a mathematical model for short-circuit studies, a number of assumptions are made which simplify the formulation of the problem and in addition, facilitate the solution without introducing significant inaccuracies in the results. The main assumptions are as follows:

- 1. The normal loads, line charging capacitances and other shunt connections to ground are neglected. This is based on the fact that the faulted circuit has predominantly lower impedance than the shunt impedances. The saving in computational effort as a result of this assumption justifies the slight loss in accuracy
- 2. The generator is represented by a voltage source in series with a reactance that is taken as the sub-transient or transient reactance. Such a representation is adequate to compute the magnitudes of currents in the first 3-4 cycles after the fault occurrence.

- 3. All the transformers are considered to be at their nominal taps.
- 4. Since the resistances of the transmission lines are smaller than the reactance by a factor of five or more, they are neglected.

4.3 Systematic computation for large scale systems

The systematic computation procedure to be used for fault analysis of a large power systems using computer is explained below. Let us consider a symmetric fault at bus r of an n-bus system. Let us assume that the pre-fault currents are negligible.

Step 1: Draw the pre-fault per phase network of the system (positive sequence network) .Obtain the positive sequence bus impedance matrix, Z using Bus building algorithm. All the machine reactances should be included in the Z bus.

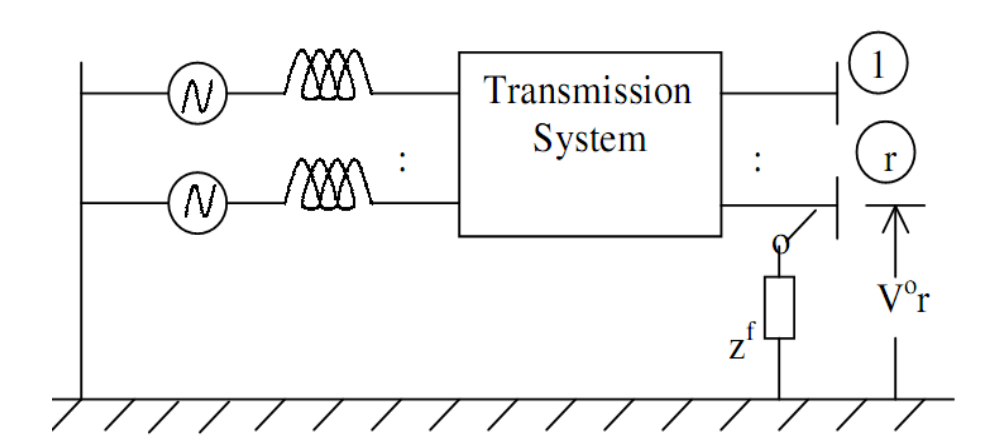


Figure 4.1 Single Line diagram with symmetrical fault

The pre-fault bus voltage vector is given by

$$\mathbf{V}^{\mathbf{o}} = \begin{pmatrix} \mathbf{V}_{1}^{\mathbf{o}} \\ \mathbf{V}_{2}^{\mathbf{o}} \\ \\ \\ \mathbf{V}_{n}^{\mathbf{o}} \end{pmatrix}$$

4.1

Step 2: Obtain the fault current using the Thevenin's equivalent of the system feeding the fault as explained below. Assume fault impedance as Z^f . The Thevenin's equivalent of the system feeding the fault impedance is given in Figure 4.2. The fault current is given by

$$I^f = V_r^o / (Z_{rr} + z^f)$$
 4.2

where Zrr is the rrth diagonal element of the bus impedance matrix.

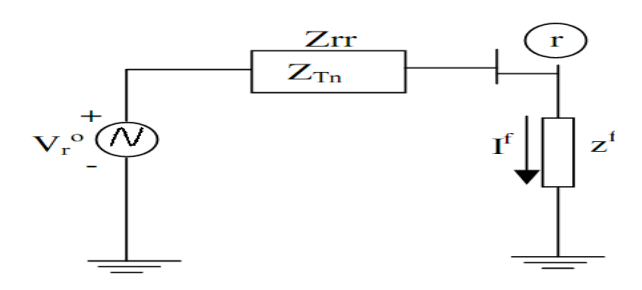


Figure 4.2 Thevenin's Equivalent of the system feeding the fault

Step 3:Obtain the Thevenin's equivalent network by inserting the Thevenin's voltage source Vr⁰ in series with the fault impedance and compute the bus voltages using network equation as explained below.

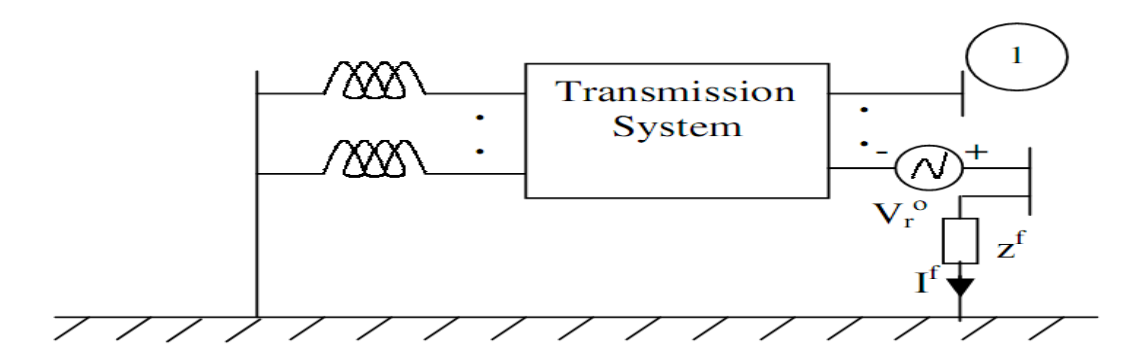


Figure 4.3 Thevenin's Network

The change in bus voltages, V_T caused by the fault at bus r is given by

$$\mathbf{V_T} = \mathbf{Z} \ \mathbf{I^f}$$

where,

Z = Bus impedance matrix of Thevenin's network including machine reactance

 I^f = bus current injection vector

$$\mathbf{I}^{\mathbf{r}} = \begin{pmatrix} \mathbf{O} \\ -\mathbf{I}^{\mathbf{r}} \\ \mathbf{O} \\ \mathbf{O} \end{pmatrix} \mathbf{r}$$

$$4.4$$

Step 4: The post fault bus voltages are given by super-position of equations

$$V^f = V^o + V_T 4.5$$

$$V^f = V^o + ZI^f$$
 4.6

Expanding, the above equation and substituting for I^f, we get the post fault voltages as

$$V_1^f = V_1^O - Z_{1r}I^f$$

$$V_n^f = V_{no} - Z_{no}I^f$$

The post fault line currents are given by $I_{ij}^f = (V_i^f - V_i^f) / Z_{ij}$ 4.7

4.4 Strong and weak buses without wind farms

The fault level of system without considering wind power generation is used to identify the strong buses and weak buses.

4.4.1 Strong buses in the system

The fault level without WTGs are computed and strong buses are identified if fault current is greater than 10 p.u and the strong buses are tabulated in Table-4.1.

 Table 4.1 Strong buses in Tirunelveli system.

| Bus No | Bus Name | Fault Level (pu) |
|--------|--------------------|------------------|
| 1 | TTPS_GENERATOR | 11.1773 |
| 2 | IBCPPGENERATOR | 10.4535 |
| 3 | SANKANERI | 10.2438 |
| 4 | UDAYTHUR | 10.1029 |
| 5 | TUTICORIN_AUTO | 11.4373 |
| 6 | ABESEKAPATTI | 10.4849 |
| 7 | KAYATHAR | 11.4743 |
| 8 | TTPS_SWITCHYARD | 11.6165 |
| 9 | STERLITE | 10.4891 |
| 10 | SIPCOT | 11.4637 |
| 11 | ANUPPANKULAM230 | 10.3857 |
| 12 | CHEKKANOORANI | 11.2668 |
| 13 | PASUMALAI | 10.8547 |
| 14 | IND BHARATH | 11.1962 |
| 15 | KODIAYAR_60 | 10.7029 |
| 16 | KODAIYAR_40 | 11.6761 |
| 17 | MELAKALOOR | 11.7073 |
| 18 | PAPANASAM HY | 11.8207 |
| 19 | SERVALAR HY | 11.8062 |
| 20 | OTHULUKKARPATTI | 10.6049 |
| 21 | KAYATHAR | 11.7881 |
| 22 | ANUPPANKULAM_110kV | 10.5867 |
| 23 | VIKRAMASINGAPURAM | 10.8681 |
| 24 | MELAKALOOR_BIOMASS | 11.609 |
| 25 | AMBASAMUTHUR | 11.2841 |
| 26 | THALAYUTHU_T1 | 10.1116 |
| 27 | THALAYUTHU_T2 | 10.4046 |
| 28 | KADAYAM_TOFF | 10.4951 |

4.4.2 Weak buses in the system

The fault levels without WTGs are computed and weak buses are identified if fault current is less is than 5 p.u and the weak buses are tabulated in Table 4.2.

Table 4.2 Fault level less than 5 p.u

| Bus No | Bus Name | Fault Level |
|--------|----------------------------------|-------------|
| | | (p.u) |
| 48 | UDANGUDI_110/11 kV | 4.5518 |
| 62 | SANKARANKOVIL_TOFF | 3.9552 |
| 80 | KADAYANALLOR_110/11 kV | 4.7205 |
| 81 | PULIYANGUDI_110/11 kV | 4.545 |
| 82 | NARAYANAPURAM_110/11 kV | 4.7205 |
| 84 | PERUMALPATTI_110/11kV SS | 4.9615 |
| 124 | KARIVALAMVANTHANALLUR_110/11kVSS | 4.2895 |

The buses which are having fault current level between 5 p.u to 9 p.u are tabulated in Appendix- C.

4.5 Summary

Short circuit study is conducted for the Tirunelveli network. Weak and strong points are identified. It is suggested that weak points are prone to power evacuation problem in case of increasing wind power penetration.

5. POWER FLOW WITH TCSC AND VSC BASED HVDC SYSTEM

5.1 Introduction to TCSC

The FACTS technology is an attractive option for increasing system operation flexibility. The recent developments in high-current, high-power electronic devices are making it possible to control the power flows on the high voltage side of the network during both steady state and transient operation. One important FACTS controller is the Thyristor Controlled Series Compensator (TCSC), which allows rapid and continuous changes of the transmission line impedance. Active power flows along the compensated transmission line can be maintained at a specified value under a range of operating conditions.

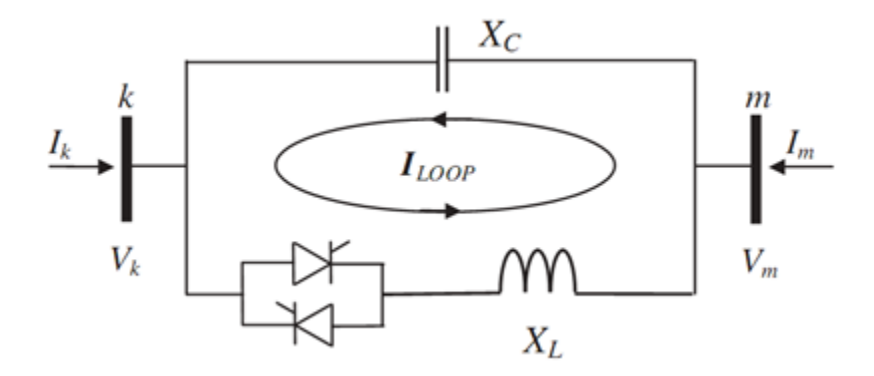


Figure 5.1.TCSC Model.

Figure.5.1 is a schematic representation of a TCSC module [Z], which consists of a series capacitor bank, in parallel with a Thyristor Controlled Reactor (TCR). The controlling element is the thyristor controller, shown as a bi-directional thyristor valve. In power flow studies, the TCSC can be represented in several forms such as the model presented is based on the concept of a variable series compensator, whose reactance is adjusted in order to constrain the power flow across the branch to a specified value. The changing reactance represents the fundamental frequency equivalent reactance of the TCSC module. The linearized TCSC power flow equations, with respect to the firing angle, are incorporated into Newton-Raphson power flow algorithm. The TCSC firing angle is combined with the nodal voltage magnitudes and angles inside the Jacobian matrix leading to very robust iterative power flow solution.

The main and basic objective of TCSC in power system is to enhance power flow and improve system stability. The deployment of TCSC in transmission line also improves subsynchronous resonance (SSR) mitigation, Power Oscillation Damping (POD) and Transient Stability (TS). In this project, the TCSC is used for power evacuation of the large scale wind farm installed capacity of around 3000 MW in Tirunelveli region.

5.2 TCSC Fundamental impedance

The voltages and currents in the TCSC circuit under the full range operating conditions is given as,

$$Z_{TCSC} = R_{TCSC} + i X_{TCSC} = V_{TCSC}/I_{line}$$
 5.1

where (bold type indicates complex quantities). V_{TCSC} is the fundamental frequency voltage across the TCSC module, I_{line} is the fundamental frequency line current and Z_{TCSC} is the TCSC impedance. The voltage V_{TCSC} is equal to the voltage across the TCSC capacitor and equation (5.1) can be written as,

$$V_{TCSC} = -i X_{TCSC} * I_{line}$$
 5.2

If the external power network is represented by an idealized current source, as seen from the TCSC terminals, this current source is equal to the sum of the currents flowing through the TCSC capacitor and inductor.

The TCSC reactance can then be expressed as,

$$X_{TCSC} = -j X_C(I_{line} - I_{TCR}) / I_{line}$$
 5.3

Substituting the expression for I_{TCR} and assuming $I_{line} = I \cos wt$, leads to the fundamental frequency TCSC equivalent reactance, as a function of the TCSC firing angle, α

$$X_{TCSC} = -X_{LC} + C_1 \{2(\pi - \alpha) + \sin 2(\pi - \alpha)\} - C_2 \cos^2(\pi - \alpha)(\omega \tan(\omega(\pi - \alpha)) - \tan(\pi - \alpha))$$
 5.4

where $\omega = 2\pi f$

$$X_{\rm LC} = \frac{X_{\rm C}X_{\rm L}}{X_{\rm C} - X_{\rm L}}$$
 5.5

$$C_1 = \frac{X_C + X_{LC}}{\pi}$$
 5.6

$$C_2 = \frac{4X_{\rm LC}^2}{X_{\rm L}\pi}$$
 5.7

 $X_L = \omega L$; $X_{C=1} / \omega C$

The overall TCSC fundamental reactance is given as

$$X_{TCR\parallel C} = (X_L^* X_C)/(X_L - X_C)/\pi \{2(\pi - \alpha) + \sin(2\alpha)\}$$
 5.8

5.3 TCSC Power flow model

The admittance matrix of the TCSC module shown in Figure 5.1 can be given as,

$$\begin{bmatrix} I_k \\ I_m \end{bmatrix} = \begin{bmatrix} jB_{kk} & jB_{km} \\ jB_{mk} & jB_{mm} \end{bmatrix} \begin{bmatrix} V_k \\ V_m \end{bmatrix}$$
 5.9

where,

$$B_{kk}=B_{mm}=B_{TCSC}=-1/X_{TCSC}$$

$$B_{km} = B_{mk} = B_{TCSC} = -1/X_{TCSC}$$
 5.10

The TCSC power equations at node k are

$$P_{k} = V_{k} V_{m} B_{TCSC} \sin(\Theta_{k} - \Theta_{m})$$

$$5.11$$

$$Q_k = V_k^2 B_{TCSC} + V_k V_m B_{TCSC} \cos(\Theta_k - \Theta_m)$$
5.12

The TCSC linearized power equations with respect to the firing angle are,

$$\frac{\partial P_k}{\partial \alpha} = P_k B_{TCSCE(1)} \frac{\partial X_{TCSC(t)}}{\partial \alpha}$$
5.13

$$\frac{\partial Q_k}{\partial \alpha} = Q_h B_{TCSC(1)} \frac{\partial X_{TCSC(1)}}{\partial \alpha}$$
 5.14

$$\frac{\partial B_{TCSC(1)}}{\partial \alpha} = B^2_{TCSC(1)} \frac{\partial X_{TCSC(1)}}{\partial \alpha}$$
5.15

$$\frac{\partial X_{TCSC(1)}}{\partial \alpha} = -2C_1 \left(1 + \cos(2\alpha) \right) \\
+ C_2 \sin(2\alpha) \left(\varpi \tan(\varpi(x - \alpha)) - \tan \alpha \right) \\
+ C_2 \left(\varpi^2 \frac{\cos^2(\pi - \alpha)}{\cos^2(\varpi(\pi - \alpha))} - 1 \right)$$
5.16

For node m exchange the subscripts k as m in (5.11)-(5.14).

When the TCSC module is controlling the active power flowing from nodes k to m, at a specified value, the set of linearized power flow equations is give as,

$$egin{bmatrix} \Delta P_k \ \Delta P_m \ \Delta Q_k \ \Delta Q_m \ \Delta P_{km} \ \end{bmatrix}$$

$$=\begin{bmatrix} \frac{\partial P_{k}}{\partial \theta_{k}} & \frac{\partial P_{k}}{\partial \theta_{m}} & \frac{\partial P_{k}}{\partial V_{k}} V_{k} & \frac{\partial P_{k}}{\partial V_{m}} V_{m} & \frac{\partial P_{k}}{\partial \alpha} \\ \frac{\partial P_{m}}{\partial \theta_{k}} & \frac{\partial P_{m}}{\partial \theta_{m}} & \frac{\partial P_{m}}{\partial V_{k}} V_{k} & \frac{\partial P_{m}}{\partial V_{m}} V_{m} & \frac{\partial P_{m}}{\partial \alpha} \\ \frac{\partial Q_{k}}{\partial \theta_{k}} & \frac{\partial Q_{k}}{\partial \theta_{m}} & \frac{\partial Q_{k}}{\partial V_{k}} V_{k} & \frac{\partial Q_{k}}{\partial V_{m}} V_{m} & \frac{\partial Q_{k}}{\partial \alpha} \\ \frac{\partial Q_{m}}{\partial \theta_{k}} & \frac{\partial Q_{m}}{\partial \theta_{m}} & \frac{\partial Q_{m}}{\partial V_{k}} V_{k} & \frac{\partial Q_{m}}{\partial V_{m}} V_{m} & \frac{\partial Q_{m}}{\partial \alpha} \\ \frac{\partial P_{km}^{\alpha}}{\partial \theta_{k}} & \frac{\partial P_{km}^{\alpha}}{\partial \theta_{m}} & \frac{\partial P_{km}^{\alpha}}{\partial V_{k}} V_{k} & \frac{\partial P_{km}^{\alpha}}{\partial V_{m}} V_{m} & \frac{\partial P_{km}^{\alpha}}{\partial \alpha} \end{bmatrix}^{i} \begin{bmatrix} \Delta \theta_{k} \\ \Delta \theta_{m} \\ \frac{\Delta V_{k}}{V_{k}} \\ \frac{\Delta V_{k}}{V_{k}} \\ \frac{\Delta V_{m}}{V_{m}} \end{bmatrix}^{i}$$

5.17

Where superscript \emph{i} indicates iteration, $\Delta P_{km} = P_{km}^{\ \alpha,reg} - P_{km}^{\ \alpha}$ is the active power flow mismatch for the TCSC module , $\Delta \alpha = \alpha^{i+1}$ - α is the incremental change in the TCSC's firing angle and $P_{km}^{\ \alpha} = P_k$.

5.3.1 TCSC Impedance as a function of firing angle

The behavior of the TCSC power flow model is influenced greatly by the number of resonant points in the TCSC impedance-firing angle characteristic, in the range of 90-180°. The number of resonant points (poles) in a TCSC module is determined by Equation (5.18).

$$\alpha = \pi \left(1 - \frac{(2n-1)\omega\sqrt{LC}}{2} \right) \quad n = 1, 2, 3...$$
 5.18

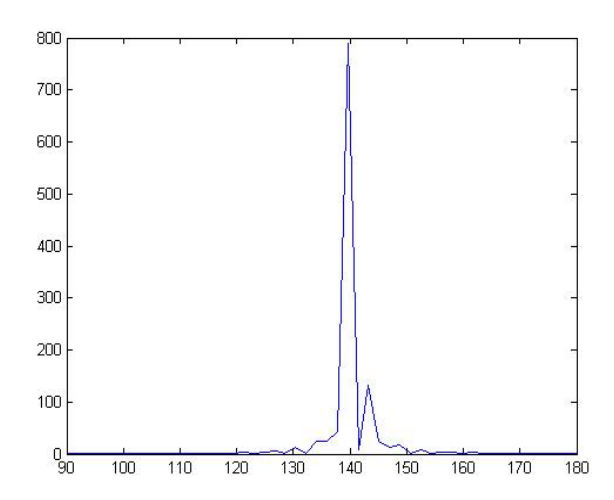


Figure 5.2 Variation of TCSC equivalent X_{Tcsc} with α

Figure 5.2 shows the fundamental frequency TCSC reactance profile, as function of the firing angle. The partial derivatives of these parameters with respect to the firing angle are also shown in these figures. As shown in Figure. 5.2, a resonant point exists at $\alpha=141.81^{0}$. This pole defines the transition from the inductive to the capacitive regions. It should be noted that near the resonant point, small variations of the firing angle will induce large changes in both X_{TCSC} and dX_{TCSC} / $d\alpha$. This, in turn, may lead to ill conditioned TCSC power equations and Jacobian terms.

5.3.2 Firing angle initial condition

The initial conditions are often responsible for Newton-Raphson power flow solution diverging or arriving at some anomalous value. In order to avoid ill conditioned Jacobians, if the customary zero voltage angle initialization is used, then TCSC is represented as a fixed reactance in the first iteration. In subsequent iterations, a small voltage angle difference at the TCSC

terminals takes place and the firing angle TCSC model is used. The initial condition for the TCSC's firing angle is selected within the range of $\pm 8^0$ from the resonant point.

5.3.3 Truncated adjustments

When solving network with TCSC, large mismatch values in ΔP , ΔQ , and ΔP_{km} , may take place in the early stages of the iterative process resulting in poor convergence. The problem is aggravated if the level of compensation required maintains a specified active power flow is near to a resonant point. In this case, large increments in the TCSC firing angle produce changes from the capacitive to the inductive regions and vice versa, causing the solution process to oscillate. In order to reduce unwanted numerical problems, the computed adjustments are replaced by truncated adjustments, if they exceed a specified limit. The size of correction in the firing angle adjustment has been limited during the backward substitution to 5°. The truncated adjustment effect is propagated throughout the remaining of the backward substitution.

5.3.4 Limits revision

The power mismatch equations are used to activate limits revision in all the controllable elements. The TCSC revision criterion is based on its active power mismatch equation,

$$\Delta P_{km}^{\alpha} = P_{km}^{\alpha,reg} + P_{km}^{\alpha}$$
 5.19

The limit revision is activated when equation (5.19) satisfies a predefined tolerance. If a limit violation takes place then the firing angle is fixed at that limit and the regulated active power flow is freed. In this situation no further attempts are made to control this active power for the remaining of the iterative process.

5.4 VSC based HVDC Transmission for wind power evacuation

5.4.1 VSC based HVDC Transmission

Voltage Source Converter based HVDC link has emerged as the latest state of art technology in medium power transmission. The developments in symmetrical turn off capability devices, especially IGBT and PWM control technique has led to this technology. Voltage Source Converter (VSC) based HVDC converters use IGBT valves with gate turn-on and turn-off capabilities eliminating the chances for commutation failure. Power flow reversal can be made easily by current reversal. Pulse Width Modulation (PWM) control enables independent control of real and reactive power in all the four quadrants. The region of control in all the quadrants is limited by the device characteristics.

5.4.2 Why VSC based HVDC transmission for wind power evacuation?

VSC-HVDC which is also called "HVDC Light" is proposed to be promising backbone for distributed and renewable generation systems, such as wind farms. Grid connection via VSC-HVDC system enables wind farms to smooth their impact on the grid stability and power quality. Trend for renewable energy makes VSC-HVDC an essential technology for the grid-connection of wind farms because wind farms are lightly populated and therefore the weakest part of a state's electricity grid. VSC- HVDC link can feed weak ac bus and also evacuate power from the weak ac systems. It also provides fast and decoupled active and reactive power control. VSC based HVDC links are extensively used for integrating large onshore/offshore wind farms with grid, used in city infeed, integration of remote small scale generations and deep sea crossings.

It offers high level of flexibility of power flow control in medium power transmission level (upto 350MW). The voltage rating of VSC based HVDC link is limited to ±300 kV due to the constraints imposed by IGBT ratings. It can also be used for supplying power to a passive grid as there are no constraints imposed by short circuit ratio. Control coordination of VSC based HVDC link is also easy, because there is no need for communication link.

It can also enhance the damping and improve the stability when a suitable additional damping controller is employed. If the dc capacitance value changes, the dc voltage at the converter end varies accordingly. By controlling the dc capacitor voltage power balance is attained in the

system. VSC is similar to synchronous source without inertia and controls active power and reactive power almost independently.

5.4.3 World wide VSC installations for wind power evacuation

The first commercial High Voltage Direct Current (HVDC) was installed to power the Island of Gotland from shore by a 96 km 100 kV subsea cable in 1955. The first commercial voltage source converter (VSC) HVDC was introduced in 1997 on the island of Gotland. This has been followed by several VSC-HVDC projects around the world. Since then ratings and applications has progressed rapidly. The world wide installation of VSC-based HVDC projects are tabulated in Table 5.1.

Table 5.1 World wide installations of VSC-HVDC projects and basic parameters.

| Project Name | Year of Commission | Power rating | Number of circuits | AC voltage | DC voltage | Length of DC cables | Comments and reasons for choosing VSC-HVDC | Topology | Semi- contactors |
|--|-----------------------|----------------------------------|--------------------|--|------------|---|--|-----------------|--------------------------|
| Hellsjön, Sweden | 1997 | 3 MW ±3 MVAr | 1 | 10 kV (both ends) | ± 10 kV | 10 km Overhead lines | Test transmission. Synchronous AC grid. | 2-level | IGBTs (series connected) |
| Gotland HVDC Light, Sweden | 1999 | 50 MW -55 to +50 MVAr | 1 | 80 kV (both ends) | ± 80 kV | 2 × 70 km Submarine cables | Wind power (voltage support). Easy to get permission for underground cables. | 2-level | IGBTs (series connected) |
| Eagle Pass, USA | 2000 | 36MW ±36 MVAr | 1 | 138 kV (both sides) | ± 15.9 kV | Back-to-back HVDC Light station | Controlled asynchronous connection for trading. Voltage control. Power exchange. | 3-level NPC | IGBTs (series connected) |
| Tjæreborg, Denmark | 2000 | 8 MVA 7.2 MW -3 to +4 MVAr | 1 | 10.5 kV (both sides) | ±9 kV | 2 × 4.3 km Submarine | Wind power. Demonstration project. Normally synchronous AC grid with variable frequency control. | 2-level | IGBTs (series connected) |
| Terrenora Interconnection (Directlink), Australia | 2000 | 180 MW -165 to +90 MVAr | 3 | 110 kV – Bungalora 132 kV – Mullumbimby | ± 80 kV | $6 \times 59 \text{ km}$ Underground cable | Energy trade. Asynchronous AC grid. Easy to get permission for underground cables. | 2-level | IGBTs (series connected) |
| MurrayLink, Australia | 2002 | 220 MW -150 to +140 MVAr | 1 | 132 kV – Berri 220 kV – Red Cliffs | ± 150 kV | 2 × 180 km Underground cable | Controlled asynchronous connection for trading. Easy to get permission for underground cables. | 3-level ANPC | IGBTs (series connected) |
| CrossSound, USA | 2002 | 330 MW ±150 MVAr | 1 | 345 kV – New- Heaven 138 kV – Shoreham | ± 150 kV | 2 × 40 km Submarine cables | Controlled synchronous connection for power exchange. Submarine cables. | 3-level ANPC | IGBTs (series connected) |
| Troll A offshore, Norway | 2005 | 84 MW -20 to +24 MVAr | 2 | 132 kV – Kollsnes 56 kV - Troll | ± 60 kV | 4 × 70 km Submarine cables | Environment, CO ₂ tax. Long submarine cable distance. Compactness of converter on platform electrification. | 2-level | IGBTs (series connected) |
| Estlink, Estonia- Finland | 2006 | 350 MW ±125 MVAr | 1 | 330 kV – Estonia 400 kV – Finland | ± 150 kV | 2 × 31 km Underground 2 × 74 km Submarine | Length of land cable, sea crossing and non- synchronous AC systems. | 2-level | IGBTs (series connected) |
| NORD E.ON 1, Germany | 2009 | 400 MW | 1 | 380 kV – Diele 170 kV – Borkum 2 | ± 150 kV | 2 × 75 km Underground 2 × 128 km Submarine | Offshore wind farm to shore. Length of land and sea cables. Asynchronous system. | | IGBTs (series connected) |
| Caprivi Link, Namibia | 2009 | 300 MW | 1 | 330 kV – Zambezi 400 kV – Gerus | 350 kV | 970 km Overhead lines | Synchronous AC grids. Long distance, weak networks | | IGBTs (series connected) |
| Valhall offshore, Norway | 2009 | 78 MW | 1 | 300 kV – Lista 11 kV – Valhall | 150 kV | 292 km Submarine coaxial cable | Reduce cost and improve operation efficiency of the field. Minimize emission of green house gases. | 2-level | IGBTs (series connected) |

5.4.4 Modeling of VSC based HVDC link for power flow studies

The PWM switching control makes VSC possible to have a simultaneous adjustment of the amplitude and phase angle of the converter ac output voltage with constant dc voltage. This control characteristic allows to represent the converter's ac output voltage at a node 'k' by a modulated ac voltage source $V_{VR} \angle \delta_{VR}$, with amplitude and phase angle limits $V_{VR}^{min} \leq V_{VR} \leq V_{VR}^{max}$ and $0 \leq \delta_{VR} \leq 2\pi$, respectively. Hence, the VSC-HVDC transmission link can be represented by the voltage source-based model given in Figure. 5.3. The coupling transformer's impedance is given by Z_{VR} . The converter's dc side is represented by the active power exchanged among the converters via the common dc link, which must be balanced at any instant, and the ac–dc side voltage converter relationships.

The ac side voltage magnitude of the converter connected at node k, V_{VR} , is related to the PWM's amplitude modulation index M_{CK} , and to the average dc capacitor voltage V_{DC} as

$$V_{VR} \angle \delta_{VR} = M_{ck} K V_{dc}$$
 5.20

where M_{ck} – Modulation index \in [0,1]

If, $M_{ck} < 1$ (under modulation); $M_{ck} > 1$ (over modulation)

K- Transformation coefficient.

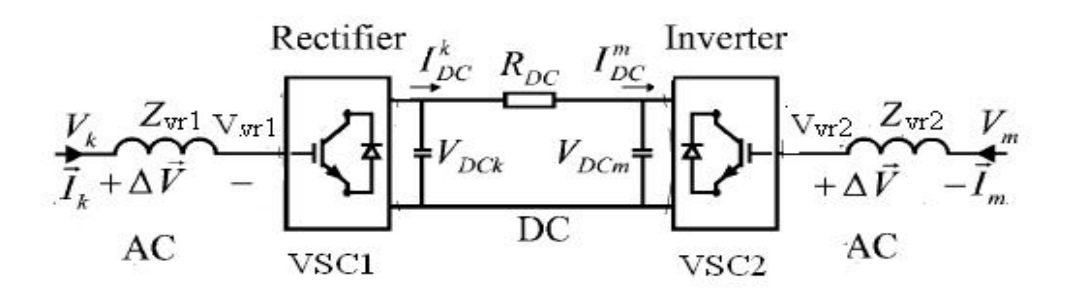


Figure 5.3 VSC-HVDC transmission link.

The power flow equations based on the equivalent circuit shown in Figure. 5.4, it is possible to obtain the power flows across the VSC-HVDC system ac terminals k and m. The powers flowing from node i to j are

$$P_{ii}^{inj} = V_i^2 G_{VRi} - V_k V_{VRi} [G_{VR} \cos(\theta_i - \delta_{VRi}) + B_{VRi} \sin(\theta_i - \delta_{VRi})]$$

$$5.21$$

$$Q_{ij}^{inj} = -V_i^2 B_{VRi} - V_i V_{VRi} [G_{ci} \sin(\theta_i - \delta_{VRi}) + B_{VRi} \cos(\theta_i - \delta_{VRi})]$$
 5.22

where, $Y_{VR} = \frac{1}{Z_{VR}}$ 5.23

$$Y_{VR} = G_{VR} + jB_{VR}$$
 5.24

Z_{VR}- Impedence of converter transformer

Y_{VR}- Admittance of converter transformer

V_k- AC voltage at bus k

 θ_k - Voltage angle at bus k

 \overline{V}_{VR} - Voltage at fictitious bus

 $\delta_{\text{VR}}\text{-}\ \text{Voltage}$ angle of fictitious bus

The power flow into the converter connected at node i=k,m are given as follows

$$P_{VRi} = V_{VRi}^2 G_{VRi} - V_{VRi} V_i [G_{VRi} \cos(\delta_{VRi} - \theta_i) + B_{VRi} \sin(\delta_{VRi} - \theta_i)]$$

$$5.25$$

$$Q_{VRi} = -V_{VRi}^2 B_{VRi} - V_{VRi} V_i [G_{VRi} \sin(\delta_{VRi} - \theta_i) - B_{VRi} \cos(\delta_{VRi} - \theta_i)]$$

$$5.26$$

The equation relating to the active power exchanged between converters is obtained by neglecting losses in the converter circuits.

For a DC link with a series resistance R_{DC} is given by,

$$Re[V_{VRK}I_{VRK}^* + V_{VRM}I_{VRM}^*] + P_{DC}^{loss} = 0$$
 5.27

where

$$P_{DC}^{loss} = (P_{VRj}^2 R_{DC}) / (V_{DCj}^{spec})^2$$
 5.28

The active power-flow direction through the dc link must be in accordance with the dc voltage magnitudes. This relation is achieved by including the Kirchhoff voltage law equation on the dc side given by (5.10), where the power flowing into the converter is considered as negative.

$$\Sigma V_{DC} = V_{DCi} - V_{DCi} + P_{VRi} R_{DC} / V_{DCi} = 0$$
 5.29

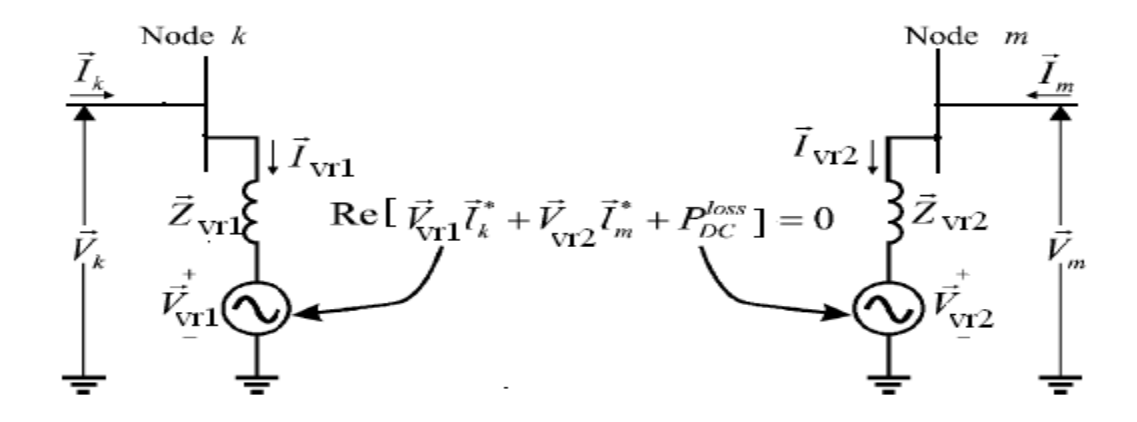


Figure 5.4 Equivalent circuit of VSC

5.4.5 Control modes

The active power exchanged between the converter and the network is controlled by adjusting the phase shift angle $\Delta\theta_i$ between the voltage on the ac bus and the fundamental frequency voltage generated by the converter,

$$\Delta\theta_{i} = \theta_{i} - \delta_{VRi}$$
 5.30

The reactive power flow is determined by controlling the difference between these voltage amplitudes,

$$\Delta V_{VRi} = V_i - V_{VRi}$$
 5.31

Hence, two independent power control loops can be used for regulation, namely active power and reactive power control loops. In the active power control loop, one converter is set to control the injected active power P_{ij}^{inj} at its ac terminal while the other is set to control the dc side voltage V_{DCj} . In the reactive power control loop, both converters have independent control over either voltage magnitude V_i or injected reactive power Q_{ij}^{inj} at their ac terminal.

Mode 1: PQ control mode

If the active and reactive powers are set to be controlled by converter i at values P_{ij}^{spec} and Q_{ii}^{spec} respectively, then the constraint equations to be satisfied are:

$$P_{ij}^{inj} - P_{ij}^{spec} = 0 ag{5.32}$$

$$Q_{ij}^{inj} - Q_{ij}^{spec} = 0 ag{5.33}$$

Mode 2: PV control mode

If the active power and ac voltage magnitude are set to be controlled by converter i, at values P_{ij}^{spec} and V_{i}^{spec} respectively, The constraint equations to be satisfied are

$$P_{ij}^{inj} - P_{ij}^{spec} = 0 ag{5.34}$$

$$V_i - V_i^{\text{spec}} = 0 ag{5.35}$$

In both cases, the other converter is set to control the dc side voltage, independently of the reactive power loop control setting. Since the dc side voltage is kept constant by converter at a value V_{DCj}^{spec} , this control action is used in the constraining equation representing the active power balance between the two converters to assess losses in the common dc link. Hence, the active power losses in the dc link are given by (5.9).

5.5 Incorporation of VSC based HVDC in power flow analysis

In the power flow analysis, both converters are set to provide PQ control. Then the residual equations are given by,

$$\Delta R(1) = P_{\text{spec}} - P_{\text{HVDC1}}$$
 5.36

$$\Delta R(2) = Q_{\text{spec}} - Q_{\text{HVDC1}}$$
 5.37

$$\Delta R(3) = P_{\text{spec}} - P_{\text{HVDC2}}$$
 5.38

$$\Delta R(4) = Q_{\text{spec}} - Q_{\text{HVDC2}}$$
 5.39

where

P_{spec}- Specified real power flow at HVDC terminal

Q_{spec}- Specified reactive power flow at HVDC terminal

P_{HVDC1}- Calculated real power flow at converter 1.

P_{HVDC2}- Calculated real power flow at converter 2.

Q_{HVDC1}- Calculated reactive power flow at converter 1.

Q_{HVDC2}- Calculated reactive power flow at converter 2.

The state variables for this power flow are the fictitious bus voltage magnitude and phase angle, as PQ control mode is chosen. State variables $(V_{VR!}, \delta_{VR1}, V_{VR2}\delta_{VR2})$.

5.6 VSC MTDC system

In literature, Multiterminal VSC based DC links, embedded on existing ac network is suggested as an ideal solution for power evacuation from renewable energy sources.

Sequential power flow analysis for VSC-MTDC system with explicit representation of dc grid is presented. The flow from ac bus to dc bus is considered as drawl in ac bus and injection in dc bus and vice versa. The dc voltages at all the buses other than dc slack bus and the dc slack bus power are obtained as result of power flow solution. The Q estimate, i.e the power flow from ac bus into fictitious VSC ac bus is calculated at the end of each iteration and updated. The fictitious ac bus voltage and angle is obtained iteratively by formulating a power balance equation.

This power balance equation is formulated by equating ac bus power to dc power with losses incorporated. A generalized converter loss model where the losses linearly and quadratically depend on current flowing through the reactor is included. The VSC parameters such fictitious VSC ac bus voltage phase shift angle α , fictitious bus voltage magnitude, dc slack bus power are included as the state variable in this power flow analysis.

Power flow of dc grid is performed by the basic nodal method. MTDC network is represented as injection/drawls of power in the power flow analysis as shown in Figure.5.7 A node in the VSC MTDC network is shown in the Figure.5.6. The voltage at nodes i and j in

Figure.5.6 are denoted by V_i and V_j respectively. The admittance between the nodes i and j is denoted by $Y_{dc_{ij}}$.

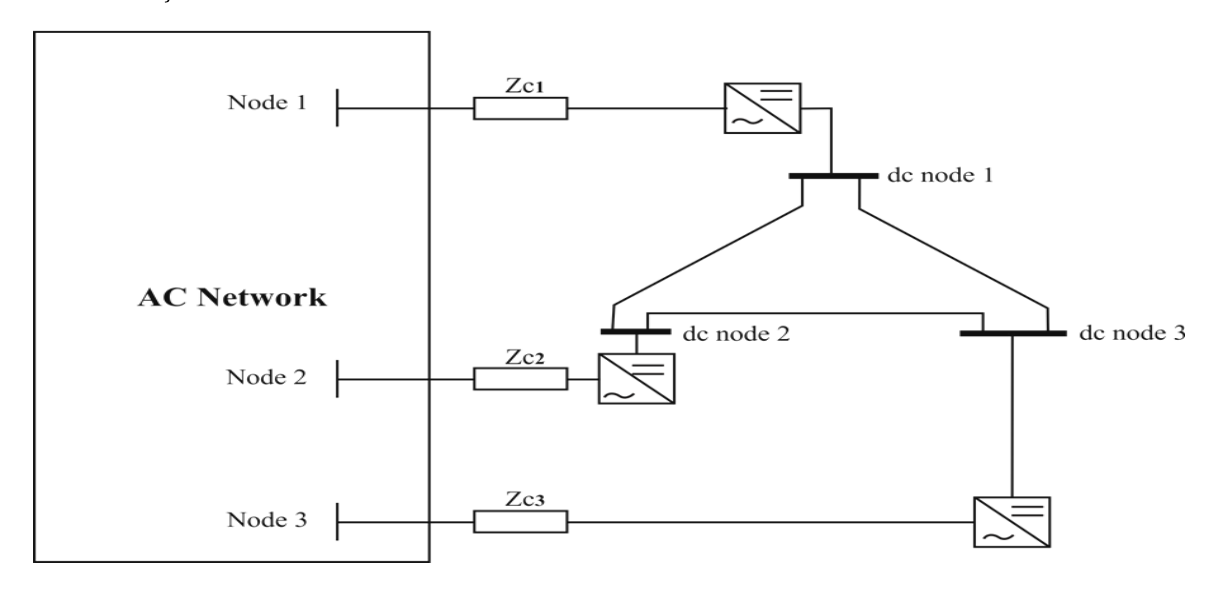


Figure. 5.5 DC network embedded on an ac network

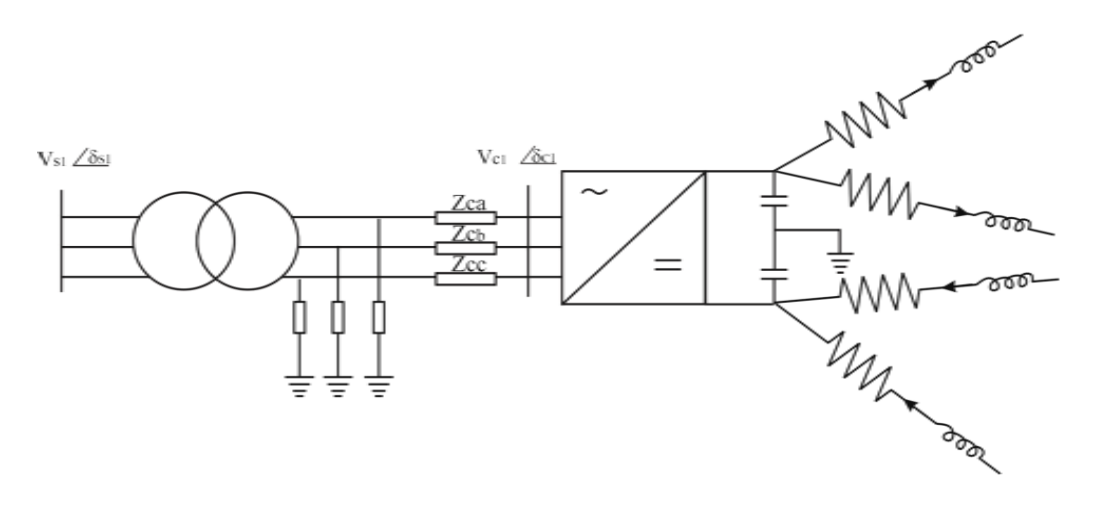


Figure.5.6 A node in a dc network

Assuming n number of nodes in the network, the injected current I_{dc_i} must be equal to the sum of the currents flowing to the other n-1 nodes,

$$I_{dc_i} = \sum_{\substack{j=1\\j\neq i}}^{n} Y_{dc_{ij}} (V_{dc_i} - V_{dc_j})$$
(5.40)

Combining the current injections in all the nodes

$$I_{dc} = Y_{dc} V_{dc} \tag{5.41}$$

The power injection or drawl at all the buses other then dc slack bus is taken to be known prior. This is justified from the basic capability of VSC-HVDC link that link powers can be fixed and the PWM controllers adjusts the phase shift angle to track the power unless the limits are hit. Strongest bus in the multiterminal link is taken to be the slack bus. The voltage magnitude of the slack bus is freed and for all the other buses flat voltage start may be assumed.

For bipolar operation, the active power injected in the ith node is given by

$$P_{dci} = 2 V_{dc_i} I_{dc_i} \tag{5.42}$$

The current injection is not known prior to dc power flow solution. DC mismatch equation is formed by equating (5.40) and (5.42).

$$I_{dc_i} - \frac{P_{dci}}{2V_{dci}} = 0 ag{5.43}$$

The vector of state variables is given by

$$X = \begin{bmatrix} P_{dc_slack} \\ V_{dc_2} \\ \vdots \\ V_{dc_n} \end{bmatrix}$$

$$(5.44)$$

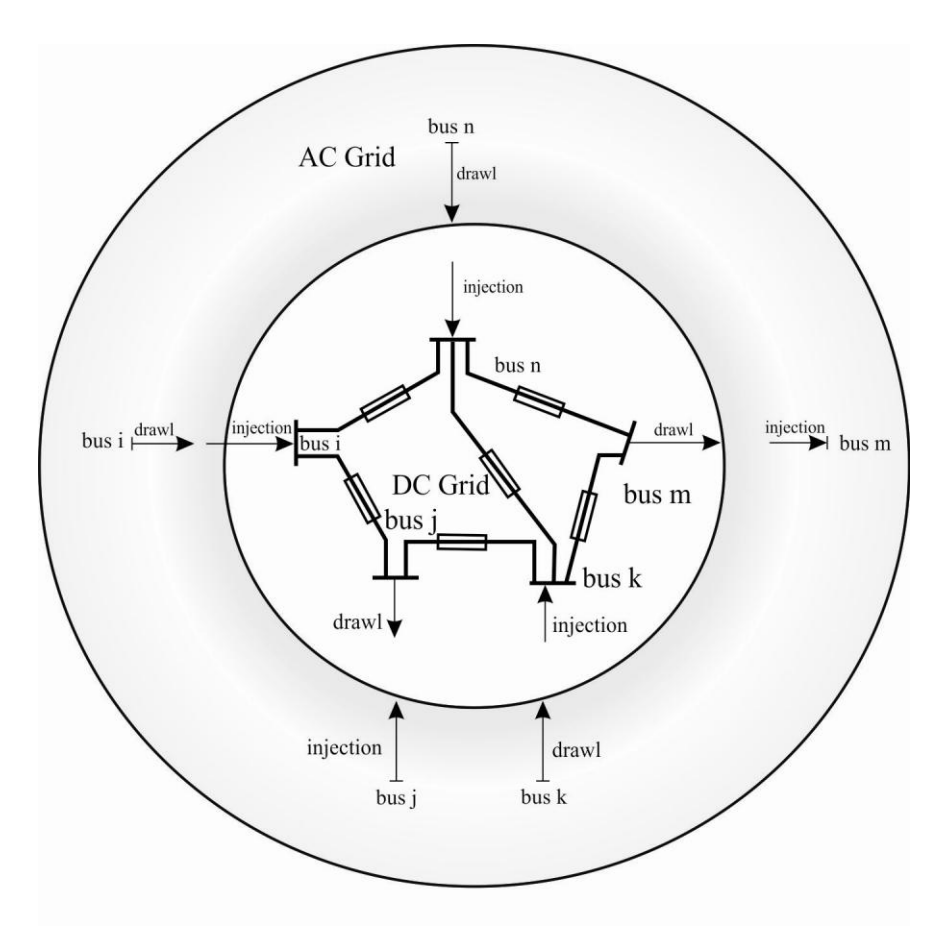


Figure. 5.7 VSC MTDC network embedded on an ac network

Thus with flat dc voltage start and the power injection/drawl at all the dc buses except the dc slack bus as known parameters the dc slack bus power and dc voltages are obtained by simple Newton-Raphson method.

5.6.1 Mathematical model of VSC MTDC link

All the dc buses are P controlled bus except the dc slack bus which takes into account of losses in the dc link and the converters. The scheduled power injection (or power drawl) from a dc bus is thus known prior. This scheduling is done based on the parallel ac lines overloading and the rating of XLPE cables. The dc ring is embedded in the existing ac network as shown in Figure. 5.7. The ac buses are connected to the voltage source converters through a coupling transformer reactance. The coupling transformer impedance is given by Z_c , where $Z_c = 1/(G_c + jB_c)$. Thus the converters are modeled as controlled voltage sources behind fictitious transformer impedances as shown in the Figure 5.8

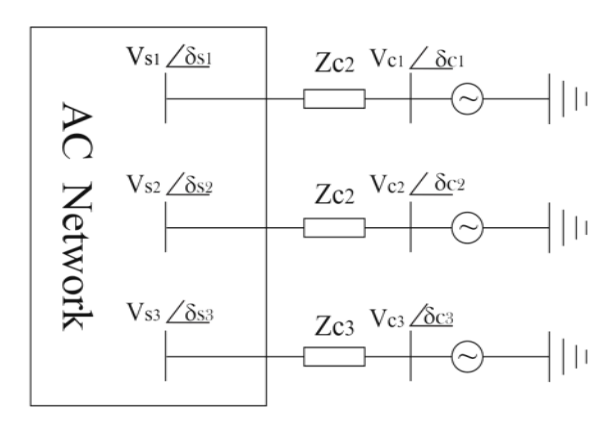


Figure.5.8 VSC station modeled as fictitious voltage source behind transformer impedance

The power flow from ac bus to converter terminal is

$$P_S = -V_S^2 G_C + V_S V_C (G_C \cos(\delta_S - \delta_C) + B_C \sin(\delta_S - \delta_C))$$
(5.45)

$$Q_s = V_s^2 B_c + V_s V_c (G_c \sin(\delta_s - \delta_c) - B_c \cos(\delta_s - \delta_c))$$
(5.46)

The power flow from converter terminal to ac bus is

$$P_c = V_c^2 G_c - V_s V_c (G_c \cos(\delta_s - \delta_c) - B_c \sin(\delta_s - \delta_c))$$
(5.47)

$$Q_c = -V_c^2 B_c + V_s V_c (G_c \sin(\delta_s - \delta_c) + B_c \cos(\delta_s - \delta_c))$$
(5.48)

with $V_s = V_s \angle \delta_c$ and $V_c = V_c \angle \delta_c$, the ac grid side and converter ac side voltage phasors respectively.

The effect of VSC-MTDC network embedded with the ac network is included as either power injection or drawl in the ac network as given in equation (5.49)

$$P_i^{sch} = P_i^g - P_i^d \pm P_i^{inj} \tag{5.49}$$

The real power balance equation is given below

$$\Delta P_i = P_i^{sch} - P_i^{cal} \tag{5.50}$$

The real power injections at all dc buses are specified except dc slack bus. The slack bus power is initialized for the first iteration and estimated subsequently. The internal dc load flow solution gives the dc slack bus power for subsequent iterations.

The reactive power flow from the ac buses to fictitious ac buses are estimated at the end of every ac iteration as it is not known prior. The reactive power balance equation is given below

$$\Delta Q_i = Q_i^{sch} - Q_i^{cal} \tag{5.51}$$

$$Q_i^{sch} = Q_i^g - Q_i^d \pm Q_i^{inj_est}$$

$$(5.52)$$

5.6.2 Fictitious ac bus power flow iterations

The VSC's are PWM controlled and thus can control the voltage magnitude, V_c and voltage angle, δ_c of the converter ac bus almost independently. The voltage magnitude and voltage angle of the fictitious ac bus are iteratively adjusted to satisfy the power balance equations. The P and Q mismatch equations (5.53) and (5.54) are formulated with losses incorporated.

$$\Delta P_c = P_{sch,dc} - P_c(V_c \delta_c) - P_{losses} \tag{5.53}$$

Losses in the converter transformer, phase reactor and filter are taken into account using transformer impedance Z_c . Converter losses are also estimated as per the loss model given in [11] and included in mismatch equation (5.53)

$$\Delta Q_c = Q_{inj_est} - Q_c(V_c \delta_c)$$
 (5.54)

The 2 x 2 Jacobian matrix (18) is formulated for every converter bus and solved sequentially.

$$\begin{bmatrix} \frac{\partial P_c}{\partial \delta_c} & \frac{\partial P_c}{\partial V_c} \\ \frac{\partial Q_c}{\partial \delta_c} & \frac{\partial Q_c}{\partial V_c} \end{bmatrix} \begin{bmatrix} \Delta \delta_c \\ \Delta V_c \end{bmatrix} = \begin{bmatrix} \Delta P_c \\ \Delta Q_c \end{bmatrix}$$
 (5.55)

The equations (5.46) and (5.47) modified by substituting $V_c \angle \alpha = k_c V_{dc} M_c \angle \alpha$ and are given as follows.

$$P_c = (k_c V_{dc} M_c)^2 G_c - V_s k_c V_{dc} M_c (G_c \cos(\delta_s - \delta_c) - B_c \sin(\delta_s - \delta_c))$$

$$(5.56)$$

$$Q_s = -(k_c V_{dc} M_c)^2 B_c + V_s k_c V_{dc} M_c (G_c \sin(\delta_s - \delta_c) + B_c \cos(\delta_s - \delta_c))$$

$$(5.57)$$

Its worth mentioning that $\alpha = \delta_c$. The mismatch equations (5.53) and (5.54). The 2 x 2 Jacobian matrix (5.58) is formulated for every converter bus and solved sequentially.

$$\begin{bmatrix} \frac{\partial P_c}{\partial \alpha} & \frac{\partial P_c}{\partial V_{dc}} \\ \frac{\partial Q_c}{\partial \alpha} & \frac{\partial Q_c}{\partial V_{dc}} \end{bmatrix} \begin{bmatrix} \Delta \alpha \\ \Delta V_{dc} \end{bmatrix} = \begin{bmatrix} \Delta P_c \\ \Delta Q_s \end{bmatrix}$$
 (5.58)

5.7 Power flow analysis with TCSC

A MATLAB program has been written for the TCSC firing angle-dependent model to incorporate in our power flow program. The program has been applied to the solution of power networks of different sizes. The Tirunelveli test system consists of 156 buses, 187 transmission lines, 2860 installed wind generators and 22 transformers. This network has enough complexity to show the robustness of the TCSC model towards the convergence.

Mechanically switched series capacitors are used to compensate the line. A Static Var Compensator (SVC) is installed at node 31 to regulate voltage magnitude. This line is of slightly different design. For the purpose of this project, the mechanically switched series capacitors are replaced by TCSC's and used to control active power flow. The TCSC's are set to control the active power flow through transmission line. The TCSC electric parameters are those given in Table 5.2. The power mismatch tolerance was set at 10⁻⁸. The firing angle of TCSC is initialized at 140° and convergence was obtained in five iterations.

Table 5.2 shows the maximum absolute power mismatch, firing angle and the fundamental frequency TCSC equivalent impedance at node 31. These values are given in degrees and p.u. respectively. In order to validate these results, the same case was simulated with the variable series compensator model and convergence was obtained in 5 iterations. It should be noted that when this model is used, the firing angles are calculated after the power flow has converged by resorting to an additional iterative process.

Table 5.2 Power mismatch and TCSC parameter value

| Iterations | ΔP_{L1} | α degree | X _{TCSC} p.u |
|------------|-----------------|----------|-----------------------|
| 0 | 5.4 | 150.00 | -0.0183 |
| 1 | 0.406 | 150.00 | -0.0183 |
| 2 | 1.012 | 146.82 | -0.0298 |
| 3 | 0.084 | 148.00 | -0.0232 |
| 4 | 0.00001 | 148.04 | -0.0237 |
| 5 | 0.00000001 | 148.04 | -0.0237 |

TCSC is carefully designed to exhibit a single resonant point. However, changes in the original parameters may take place due to the ageing of capacitors. It is not unlikely that TCSC's may exhibit more than one resonant point. This has provided the motivation for analyzing the behavior of the power flow algorithm when solving systems that contain TCSC's with more than one resonant point. When the fundamental frequency TCSC reactance presents multiple resonance points, different values of firing angle give the compensation levels required to achieve a specific active power flow.

5.7.1 Power flow with 80% wind power penetration (without TCSC)

For 80% of installed capacity of wind generation and with 64-shunt capacitors. It is observed that 110kV -17 Transmission lines are overloaded (>100%) and 230/110 kV -2 transformers are overloaded.

5.7.2 Power flow with 80% wind power penetration (with TCSC)

A single module TCSC is installed in one of the circuit in 400kVdouble circuit between Abisekapatty to Chekkanoorani. The Figure 5.9 shows the TCSC Module of Abisekapatty to Chekkanoorani. The TCSC module is provided with 27 % fixed compensation and 8% to 20 % of variable compensation.

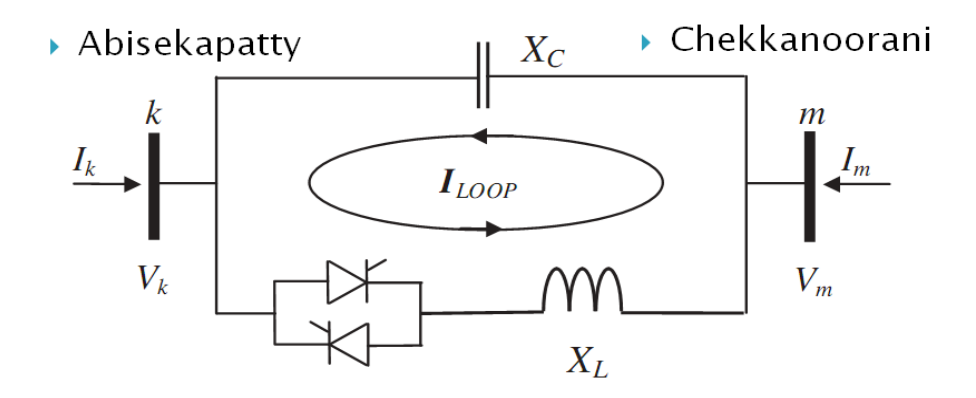


Figure 5.9 TCSC Module of Abisekapatty to Chekkanoorani

The Table 5.3 shows the power flow comparison with / without TCSC considering 80% wind power generation.

Table 5.3 Comparison of power flow results

| S.No | Quantity | Without TCSC | With TCSC | Comments |
|------|-------------|--------------|-----------|------------------------|
| 1 | Real power | 225.51 MW | 307.5 MW | 81.99 MW power flow is |
| | Transferred | | | enhanced |

5.7.3 Installed TCSC projects in India

Table 5.4 –TCSC projects-Data1

| TCSC | K | | $\omega = \operatorname{sqrt}(X_c/X_l)$ | Reasonance | Boost Factor |
|-------------|-----|-------|---|--------------|---------------------|
| Projects | FSC | TCSC | | region in | |
| | | | | Degree | |
| Kanpur- | 27% | 8-20% | 2.7452 | 147°-147.5° | 1:2.5 |
| Ballabhgarh | | | | | |
| Rourkela- | 40% | 5-15% | 2.5007 | 143.5° -144° | 1:3 |
| Raipur | | | | | |
| Purnea- | 40% | 5-15% | - | - | 1:3 |
| Gorakhpur | | | | | |

Table 5.5 –TCSC projects-Data2

| TCSC | Capacitive | Capacitive | Max.Power Transfer in pu | |
|-------------|-------------------|---------------|--------------------------|-------------|
| Projects | operating | operating | | |
| | range in Ω | range in deg. | With FSC | With |
| | | | | FSC+TCSC |
| Kanpur- | 10.40-26.12 | 180°-151.15° | 1.370 | 1.506-1.621 |
| Ballabhgarh | | | | |
| Rourkela- | 6.81-20.81 | 180°-148° | 1.667 | 1.791-1.884 |
| Raipur | | | | |

5.8 Power flow analysis with VSC-HVDC

5.8.1 Results from power flow analysis (Lines overloaded >100%)

The Table 5.6 tabulates the results obtained by power flow with VSC based HVDC.

Table 5.6 Results from power flow analysis (lines overloading >100%)

| Sl No | From Bus | To Bus | Percentage of |
|-------|----------|----------|-----------------|
| | | | Overloading (%) |
| 1 | CHEKKA42 | SIPCOT2 | 112.7807 |
| 2 | SRPUDU21 | ARALVOIM | 102.8457 |
| 3 | RADHAPUR | KOTTAIKA | 111.0518 |
| 4 | VEERASEG | UTHUMALA | 108.8940 |
| 5 | RAJAPALA | RAJTOFF2 | 100.0837 |
| 6 | SRPUDU21 | MUPPTOFF | 110.2754 |
| 7 | SRPUDU21 | PERUTOFF | 109.5918 |

| 8 | PALATOFF | KARUNKUL | 108.1888 |
|----|----------|----------|----------|
| 9 | MUPPTOFF | PERUNGUD | 119.6111 |
| 10 | KAYATR21 | AYYANARO | 146.7240 |
| 11 | KOTTAIKA | SATHANK | 133.7107 |
| 12 | KEELAVEE | KAYATR21 | 133.9105 |
| 13 | VADDAKKA | SANKAN21 | 104.3723 |
| 14 | KOODATOF | SANKAN21 | 107.9203 |
| 15 | SURULIYA | RAJTOFF2 | 105.7389 |

The transmission line1 (Kayathar21-Ayyanaroothu) has to transfer 1.3924+0.5570j p.u of power from Ayyanaroothu to Kayathar21. The line is loaded 176.22% for this operation. The overloading transmission line can be replaced by either VSC based HVDC link, or by providing addition 110 KV line with existing line, in order to reduce the loading of the transmission line.

The DC link has to carry the real power which is transmitted when the line is an AC link. The line taken for the HVDC link is Copper conductor in air. The maximum power that can be handled by this type is 312.95 MW. A detail of other types of conductors is given in Appendix. The different loading levels, if the overloading line is replaced with DC link or double circuited are given in Table 5.7.

 Table 5.7 Comparison between double circuit AC link Vs VSC-HVDC

| Sl.no | From | То | Percentage of loading (%) (with dc link) | Percentage of loading (%) (with double circuit ac line) |
|-------|------------------|------------------|--|---|
| 1 | Kayathar21 | Ayyanaroothu | 44.5 | 88.11 |
| 2 | KottaiKarunkulam | Sathankulam | 37.6 | 66.24 |
| 3 | Sattur | O.Thulukkarpatty | 38.7 | 66.64 |
| 4 | Veerasegamani | Uthumalai | 27.33 | 59.34 |
| 5 | Anuppankulam | Sattur_Toff | 34.15 | 59.67 |
| 6 | S.R Pudur | Aralvaimozhi | 29.22 | 69.78 |

As the overloading line is upgraded, the power handling capacity of that line increases. For example the transmission line between Kayathar to Ayyanaroothu is loaded to 176.22% for the given loading condition. If it is replaced with HVDC link, the loading of the line reduces to 44.5% and for double circuited line, the value is 88.11%. From the above results, it is inferred that the transmission lines can be loaded further till its maximum capacity.

5.9 VSC MTDC System power flow results

A dc ring is formulated as shown in the Figure 5.8 to relieve the overloading in four lines.

Bus n- S R Pudur; Bus m – Aralvaimozhi; Bus k- Muppantal Toff;

Bus j-Perungudi ; Bus i-Perungudi Toff

The AC power generated from all the wind forms are converted into DC and fed into the DC grid at Muppanthal Toff, Aralvaimozhi, Pegungudi and Perungudi-Toff. It is inverted at SR Pudur and the inverter is connected to the existing AC grid. The additional wind farms, if installed can be connected to the DC grid. VSC-MTDC is cost effective compared to two terminal VSC links.

Table 5.8 Flow in the AC lines with DC ring embedded

| Lines | MW | MVAR | Percentage |
|----------------------------|--------|------------|------------|
| Emes | 172 77 | 141 4 1114 | loading(%) |
| Aralvaimozhi to SR Pudur | 54.61 | -32.35 | 70.52 |
| Muppanthal to Aralvaimozhi | 49.36 | -19.06 | 58.79 |
| Muppanthal to MuppanToff | 31.93 | -7.41 | 36 .42 |
| Perungudi to MuppanToff | 71.99 | -27.81 | 85.76 |
| Perunkudi to PeruToff | 23.86 | -8.29 | 28.06 |
| PeruToff to SRPudur | 65.41 | -27.67 | 78.91 |
| MuppanToff to SRPudur | 68.27 | -27.61 | 81.81 |

Table 5.9 Flows in DC ring

| Lines | MW |
|--------------------------------|-------|
| Aralvaimozhi to SR Pudur | 74.35 |
| MuppanthalToff to Aralvaimozhi | 40.06 |
| Perungudi to MuppanToff | 50.6 |
| Perunkudi to PeruToff | 59.94 |
| PeruToff to SRPudur | 60.09 |

5.10 Summary

A TCSC power flow model has been presented. The TCR's firing angle is taken as state variable, which is regulated in order to obtain the level of compensation required to achieve a specified active power flow. The test system has been taken for the power evacuation study. If the transmission line is long (>250 km) then we can go for the Thyristor Controlled Series Compensator (TCSC) for power flow enhancement. This Series compensation (Thyristor Controlled Series Compensator) avoids the overloading of transmission lines for 60% to 90% of wind power penetration. TCSC can enhance the power around 310 MW for transmission line between Abisekapatti to Chekkanoorani. But the line length is 162km so it comes under medium transmission line. Hence a dedicated 400 kV transmission corridor from Chekkanoorani to the load centre (>250 kms) may be proposed with TCSC installation.

Two terminal VSC HVDC link and VSC-MTDC models have been presented. A dc ring is proposed to relieve the four overloaded lines. The power flow analysis reveals that the burden can be taken by the dc ring embedded on the ac network. Thus capacity addition can be done along the dc ring and overloading of the ac lines can be avoided.

6. TRANSIENT STABILITY ANALYSIS

6.1 Introduction

The power supply and power demand in the system must always be satisfied and be in equilibrium conditions during normal and dynamic changes in the system. Particularly during pre and post dynamic events, the system voltage, frequency and equipment loadings shall be within normal limits ensuring quality of power supply and acceptability of system operation.

- The operating limits of the equipments shall remain within normal operating limits or shall quickly return to normal limits following dynamic events. These dynamic events can be large disturbances following which the system should be able to continue and service the loads without loss of quality, loss of load. The response of the system to large disturbances and its ability to return to normal operating conditions is generally termed transient stability or large signal performance of the system.
- The heterogeneous system of synchronous machines and their controllers together with load and other system dynamic characteristics shall be stable, so that the system can transit from one operating condition to another without sustained oscillations limiting power transfers. This is generally referred to us small signal stability.
- The load characteristics and the power supply characteristics of the system shall be in tune with each other so that the load voltages are always healthy without any significant low voltage problems and its consequences which may lead to loss of system load and service. This problem is generally termed voltage stability problem

6.1.1 Classification of power system stability

The Figure 6.1 gives the detailed classification of power system stability [1]

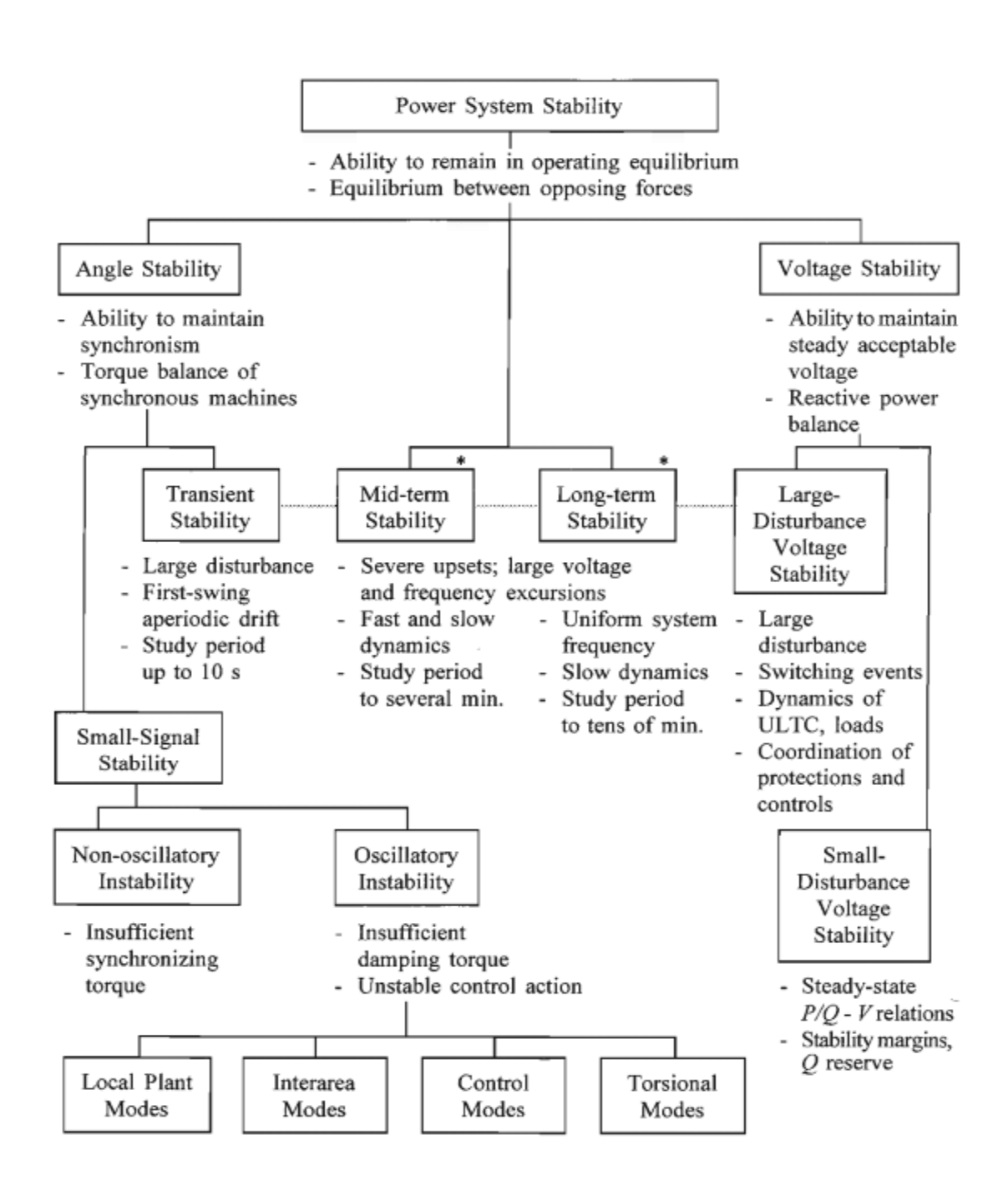


Figure 6.1 Classification of power system stability

*With availability of improved analytical techniques providing unified approach for analysis of fast and slow dynamics, distinction between mid-term and long-term stability has become less significant

6.2 Transient stability analysis

The recovery of a power system subjected to a severe large disturbance is of interest to system planners and operators. Typically the system must be designed and operated in such a way that a specified number of credible contingencies do not result in failure of quality and continuity of power supply to the loads. This calls for accurate calculation of the system dynamic behaviour, which includes the electro-mechanical dynamic characteristics of the rotating machines, generator controls, static var compensators, loads, protective systems and other controls. Transient stability analysis can be used for dynamic analysis over time periods from few seconds to few minutes depending on the time constants of the dynamic phenomenon modeled.

6.3 Modelling of power system components for stability studies

Synchronous generators form the principal source of electrical energy in power system. Therefore an accurate modelling of their dynamic performance is of fundamental importance for the study of power system stability. The synchronous generators are modelled as classical machines. Similarly the modelling of wind turbine and induction generators is of prime importance. The induction generators modelled in this section are of squirrel cage type and the analysis may be extended to Doubly Fed Induction Generators (DFIG) as a future scope.

6.3.1 Synchronous machine model

The synchronous generators are modelled as classical machines with rotor angle (δ) and speed (ω) as state variables.

$$J\frac{d\omega}{dt} = T_{\rm m} - T_{\rm e} \tag{6.1}$$

$$\frac{\mathrm{d}\delta}{\mathrm{d}t} = \omega - \omega_{\mathrm{s}} \tag{6.2}$$

The equivalent circuit for classical model of the generator is given in Figure 6.2.a. This equivalent circuit is in Thevenin's form [3], and the Norton form of the equivalent circuit is shown in Figure 6.1.b.

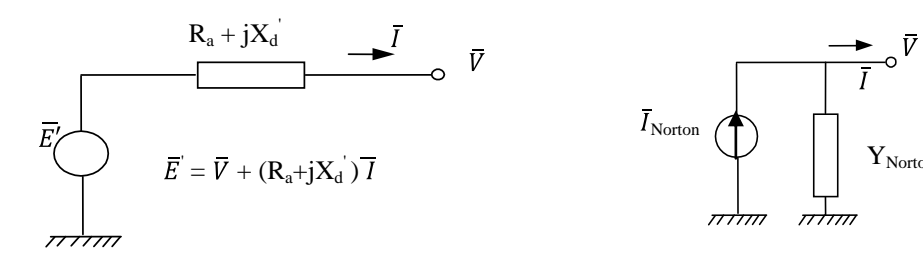


Figure 6.2 (a) The venin

Figure 6.2 (b) Norton

Figure 6.2 Generators representation for network solution

where,

X_d' - Direct axis transient reactance

I_{Norton} - Norton current source.

The expressions for the current source and the admittance are given by

$$\bar{I}_{Norton} = E' \angle \delta / (R_a + jX_d')$$
 6.3

$$Y_{\text{Norton}} = 1 / (R_a + jX_d')$$
 6.4

The Norton admittance and it gets added to the diagonal of bus admittance matrix \mathbf{Y} corresponding to the node where the generator is connected.

6.3.2 Transmission line model

The transmission lines are modeled as π -circuits using positive sequence parameters: series resistance, series reactance and half-line charging.

6.3.3 Load model

The loads are modelled as constant admittances. The admittances are computed from the initial load flow solution as shown below.

$$Y_L = (P_L - j Q_L) / |V_L|^2$$
 6.5

Where, P_L and Q_L are the active and reactive powers of the load

|V_L| is the magnitude of the voltage of the load bus computed by load flow analysis

Y_L is the load admittance and it gets added to the diagonal of bus admittance matrix Y

corresponding to the node where the load is connected.

6.3.4 Wind turbine model

The simple aerodynamic model commonly used to represent the turbine is based on the power coefficient, C_p versus the tip speed ratio, λ . The torque and power extracted from the wind turbine are given by,

$$T_{\rm m} = \frac{P_{\rm m}}{\omega_{\rm r}} \tag{6.6}$$

$$P_m = \frac{1}{2} \rho A u_w^3 C_p \tag{6.7}$$

Where, P_m - power extracted from the wind turbine, ρ - density of air, A- swept area of the blades, C_p - power coefficient, u_w - wind speed.

The tip speed ratio is given by

$$\lambda = \frac{\omega R}{u_w}$$
 6.8

Where, ω - Rotor speed of the wind turbine (low shaft speed)

R – Radius of the wind turbine rotor

The general functional representation of C_p is

$$C_{p}(\lambda,\theta) = C_{1} \left(\frac{C_{2}}{\Lambda} - C_{3}\theta - C_{4}\theta^{x} - C_{5} \right) e^{\frac{-C_{6}}{\Lambda}}$$

$$6.9$$

Where,

$$\frac{1}{\Lambda} = \frac{1}{\lambda + 0.08\theta} - \frac{0.035}{1 - \theta^3}$$

 θ -pitch angle and C_1 to C_6 and x are constants.

6.3.5 Induction generator model

The induction generator can be represented by the well-known equivalent circuit shown in Figure 6.3.a

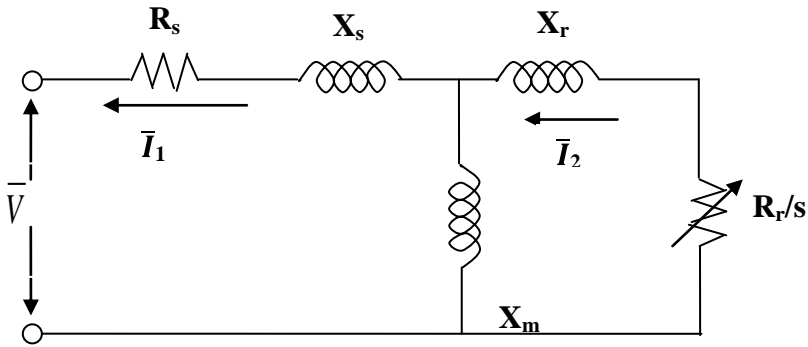


Figure 6.3.a Steady state equivalent circuit of induction generator

 R_s -Stator resistance R_r - Rotor resistance

 X_s -Stator leakage reactance X_r - Rotor leakage reactance

 X_m -Magnetizing reactance \overline{I}_l -Stator current

 \overline{I}_2 -Rotor current \overline{V} -Terminal voltage

s -Slip given by, $(\omega_s-\omega_r)/\omega_s$ N_t -Number of wind turbine generators

From Figure 6.3.a, the current I_1 can be written as,

$$\overline{I}_1 = \frac{-\overline{V}}{(R_c + R_a) + i(X_c + X_a)} \tag{6.10}$$

where,

$$R_e + jX_e = \frac{jX_m \left(\frac{R_r}{s} + jX_r\right)}{\frac{R_r}{s} + j(X_m + X_r)}$$

$$6.11$$

The per-unit active power transferred from the rotor to the stator through air gap, called air gap power, is readily calculated from the equivalent circuit as,

$$P_g = -\overline{I}_2^2 \frac{R_r}{s} \tag{6.12}$$

The electrical power developed in the rotor is,

$$P_g = -\bar{I}_2^2 \frac{R_r}{s} \ (1 - s) \tag{6.13}$$

where the slip is negative.

The electrical torque developed is then given by,

$$T_{e}(v,s) = \frac{-\overline{v}^{2}X_{m}^{2}\frac{R_{r}}{s}}{\left[\left(R_{1} + \frac{R_{r}}{s}\right)^{2} + (X + X_{r})^{2}\right]\left[R_{1}^{2} + (X_{1} + X_{m})^{2}\right]}$$

$$6.14$$

where

$$R_1 + jX_1 = \frac{jX_m(R_s + jX_s)}{R_s + j(X_s + X_m)}$$
6.15

The steady state equivalent for wind farm is obtained by replacing the parameters of individual wind generators as shown in the Figure 6.4.b

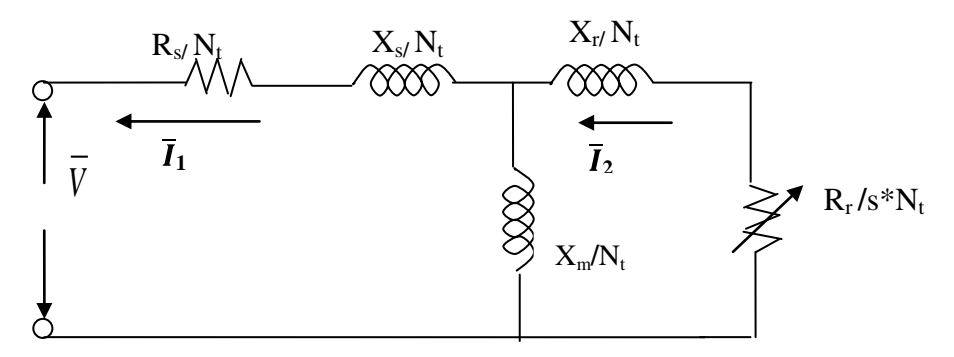


Figure 6.3.b Steady state equivalent circuit of wind farm

6.3.6 Transient model of IG

In developing the transient model of the induction machine as shown in Figure 6.4.a, it is worth noting the following aspects of its characteristics, which differ from those of the synchronous machine.

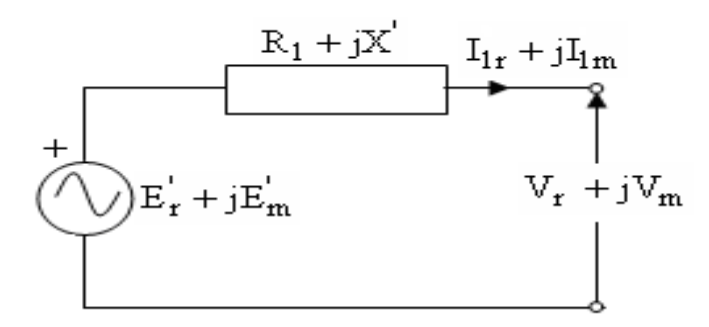


Figure 6.4.a Transient equivalent circuit of induction generator

- The rotor has symmetrical structure. This makes the d-axis and q-axis equivalent circuits identical.
- There is no excitation source applied to the rotor windings. Consequently, the dynamics of the rotor circuits are determined by slip, rather than by excitation control.
- The currents induced in the shorted rotor windings produce a field with the same number of poles as that produced by the stator winding. Rotor winding may therefore be modeled by an equivalent three-phase winding similar to the stator.
- The stator and the rotor windings are sinusoidally distributed along the air-gap as far as the mutual effect with the rotor is concerned.
- The stator slots cause no appreciable variations of the rotor inductances with rotor position.
- Magnetic hysteresis and saturation effects are negligible.

The transient state equivalent for wind farm is obtained by replacing the parameters of individual wind generators as shown in the Figure 6.4.b

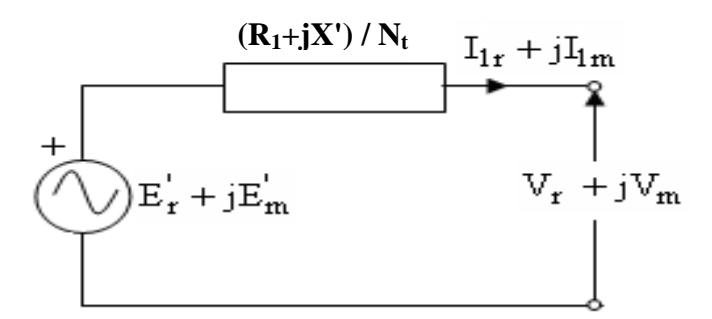


Figure 6.4.b Transient equivalent circuit of wind farm

The general expression for electrical torque is given by,

$$\overline{T}_e = E'_r I_r + E'_m I_m \tag{6.16}$$

The acceleration of the driven equipment and the generator is given by

$$\frac{2H_{Sys}}{\left(\frac{\omega_{Sm}}{\omega_{Rm}}\right)\frac{\partial \bar{s}}{\partial t}} = \bar{T}_m(s) - \bar{T}_e(s)$$

$$6.17$$

The expression for transient voltage is expressed as differential equations can be given as

$$pE'_{r} = -\frac{1}{T'_{0}} \left[E'_{r} - (X_{s} - X')I_{m} \right] + s\omega_{s} E'_{d}$$
6.18

$$pE'_{m} = -\frac{1}{T'_{0}} \left[E'_{m} + (X_{s} - X')I_{r} \right] - s\omega_{s}E'_{r}$$
6.19

$$s = (\omega_s - \omega_r)/\omega_s \tag{6.20}$$

where, H – Inertia constant in second, s – slip.

6.4 Initialization

Any dynamic study begins with a load flow which gives the initial snap shot of the system [3]. The system is assumed to be in steady state from $t = -\infty$ to t = 0. From the initial load flow solution, active and reactive powers absorbed by the generators and the terminal voltage phasor will be known. Then the initialization of other quantities can be done as shown below:

1. The stator current phasor

$$\bar{I} = \frac{P - jQ}{\bar{V}^*} \tag{6.22}$$

- 2. The state variables to be initialized for classical machines are δ and ω . In steady state, the machine speed is assumed to be synchronous speed, hence, $\omega = \omega_s$.
- 3. For classical machine, the rotor angle is initialized (t=0) as the phase angle of voltage behind transient reactance.
- 4. The transient voltage of synchronous generator is given as

$$\bar{E}' \angle \delta = \bar{V} + (R + jX_d')\bar{I}$$

$$6.23$$

5. The transient voltage of induction generator is given as

$$\bar{E}' = \bar{V} + (R + jX')\bar{I} \tag{6.24}$$

where $E'=E'_r+jE'_m$

6. The initial value of slip is obtained from load flow. Runge-Kutta (R-K) fourth order method is employed for numerical integration technique. R-K fourth order method requires calculation of four estimates for each state variable to obtain the values at the next time step. The estimates of state variables are change in phase angles (k_1,k_2,k_3,k_4) , change in speed (l_1,l_2,l_3,l_4) , change in E'_r (x_1,x_2,x_3,x_4) , change in E'_m (y_1,y_2,y_3,y_4) and change in slip (z_1,z_2,z_3,z_4) .

6.5 Algorithm to advance simulation by one time step

The stepwise computations to be performed to advance the simulation by one step from t- Δt to t are as follows [3]. The time step width (Δt) used in the algorithm is 0.001 sec.

Assumptions:

- The machines are considered to be classical(no controllers)
- Damping ignored
- Loads are assumed as constant admittances

Preparation:

- The initial conditions for δ , ω and voltage are obtained from load flow and the past history terms for δ and ω are obtained from the initial conditions.
- The initial condition synchronous generator and induction generator are calculated assuming that the system in steady state initially.

Note:

i. The loads are converted into the constant admittances and these are pushed in to diagonal elements of the corresponding load buses.

$$Y_{TRANBUS ii} = Y_{ii} + Y_{Li}$$
 Here i is for all load buses 6.25

ii. The diagonal elements of $\, Y_{\,\, bus}$ corresponding to all synchronous generators are modified as:

$$Y_{TRANBUS ii} = Y_{ii} + 1/(R_i + j X'_{di})$$
 6.26

iii. The diagonal elements of Y bus corresponding to induction generator are modified as:

$$Y_{TRANBUS ii} = Y_{ii} + 1/(R_i + j X')$$
 6.27

Assume that we have completed the simulation up to the time t- Δt , and the following quantities are known at t- Δt . State variables of induction generator (E_r ', E_m ', E_m ', E_m ') and synchronous generator (E_m)

The computational steps to advance simulation from time t- Δt to time t are given below.

Step 1: Compute the electrical power for synchronous machine.

$$P_e = \overline{V}\overline{I}^*$$
 6.28

$$\bar{I} = \frac{\bar{E}' \angle \delta - \bar{V}}{R + jX_d'}$$
 6.29

Step 2: The general expression for electrical torque of induction generator is given by,

$$Te = E'_r I_r + E'_m I_m ag{6.30}$$

$$\bar{I} = \frac{E'r + jE'm' - \bar{V}}{R + jX}$$
 6.31

where, $I=I_r+jI_m$

Step3: Compute first estimate of all state variables a follows

$$k_1 = \frac{d\delta}{dt} = \omega - \omega_s \tag{6.32}$$

Similarly compute the first estimate for other state variables (ω , Er $\dot{}$, Em $\dot{}$, s) as l_1 , x_1 , y_1 , z_1

Step 4: Calculate the Norton current

For Synchronous Generator

$$\bar{I}_{\text{Norton}} = \frac{E'/(\delta(t) + \frac{k_1}{2})}{R + jX'_d}$$
 6.33

For Induction Generator

$$\bar{I}_{\text{Norton}} = \frac{\left(\text{Er}' + \frac{x_1}{2}\right) + j\left(\text{Em}' + \frac{y_1}{2}\right)}{R + jX'}$$
 6.34

Step 5: Solve for network equations, [Y][V] = [I]

Similarly compute the second, third and fourth estimates of other state variables using Step1 to Step 4.

$$k_{2} = f\left(x_{i} + \frac{1}{2}h, y_{i} + \frac{1}{2}k_{1}h\right)$$

$$k_{3} = f\left(x_{i} + \frac{1}{2}h, y_{i} + \frac{1}{2}k_{2}h\right)$$

$$k_{4} = f\left(x_{i} + h, y_{i} + k_{3}h\right)$$

Step 6: Update the state variables $(\delta, \omega, Er', Em', s)$ and advance the time step to t+ Δt .

6.6 Handling network discontinuities

For the normal time advance and the first solution at the discontinuity, the induction generator is represented by the Norton equivalent [3]. The second solution is iterative as far as terminal voltage is concerned since slip, being a state variable, cannot change across a discontinuity. The second solution is computed using the model described by Norton equivalent.

The pre-disturbance solution at a discontinuity is called the first solution and the post disturbance solution is called the second solution.

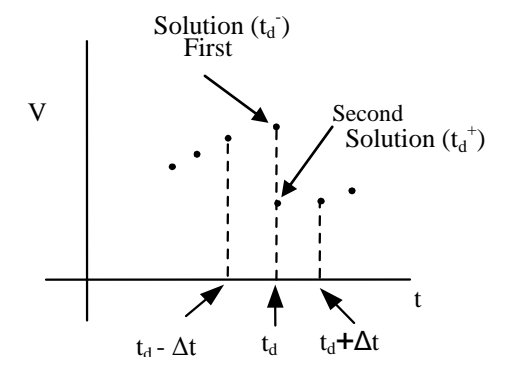


Figure 6.5 Handling network discontinuities; dots denote the points computed by the algorithm.

6.7 Effect of wind generator on transient stability

The transient stability analysis is performed for the test system by applying three phase fault at various locations of the Tirunelveli network. The transient behaviour of the wind farms is analysed without LVRT capability and with LVRT capability.

6.7.1Low Voltage Ride Through (LVRT)

The ability of a wind turbine generator to withstand voltage variations caused by grid disturbances is referred to as LVRT-capability. Large-scale wind farms, which are connected into utility grid, can be seen as conventional large generator in terms of system operation, if they are disconnected from the grid. Thus the disconnection of the wind power farms could further aggravate the situation.

Wind power farms have more limited capability to provide voltage support during faults than synchronous generating units. Accordingly, most utility has put forward requirement to dynamic voltage recovery of wind farms during grid faults under name of low voltage ride through (LVRT) requirement in their grid codes.

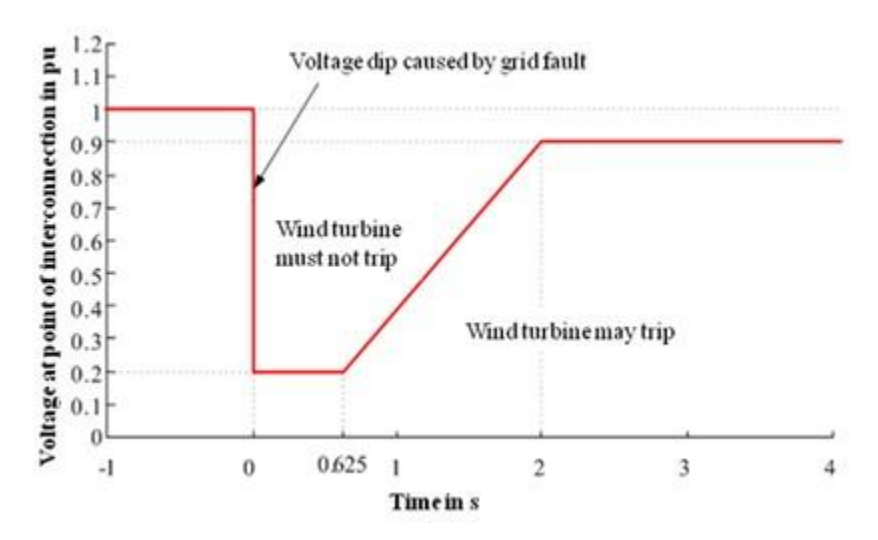


Figure 6.6 Low-Voltage Ride-Through of wind farm

LVRT is described by a voltage against time characteristic as shown in the Figure 6.6, denoting the minimum required immunity of the wind power station to dips of the system voltage. In case of dips above the residual voltage, wind farms must remain in operation, whereas they can disconnect in the event of dips below the residual limit. Transient voltage

recovery is mostly required to go back to the allowed steady state voltage drop during fault clearing time. The voltage prescribed in LVRT generally corresponds to the voltage at the grid connection point depending on the particular code requirements.

6.8 Wind farm behaviour without LVRT capability

The transient stability analysis is performed for the test system by considering wind turbine generator without LVRT capability.

6.8.1 Fault at KANYAKUMARI Bus

The Kanyakumari bus is exporting 0.2 MW power to grid which is connected to Tengampudur bus and Maharajapuram bus .When a three phase fault is applied at Kanyakumari bus at 1.0 second and cleared at 1.25 second, the variations in voltages following the disturbance are plotted in Figure 6.7.

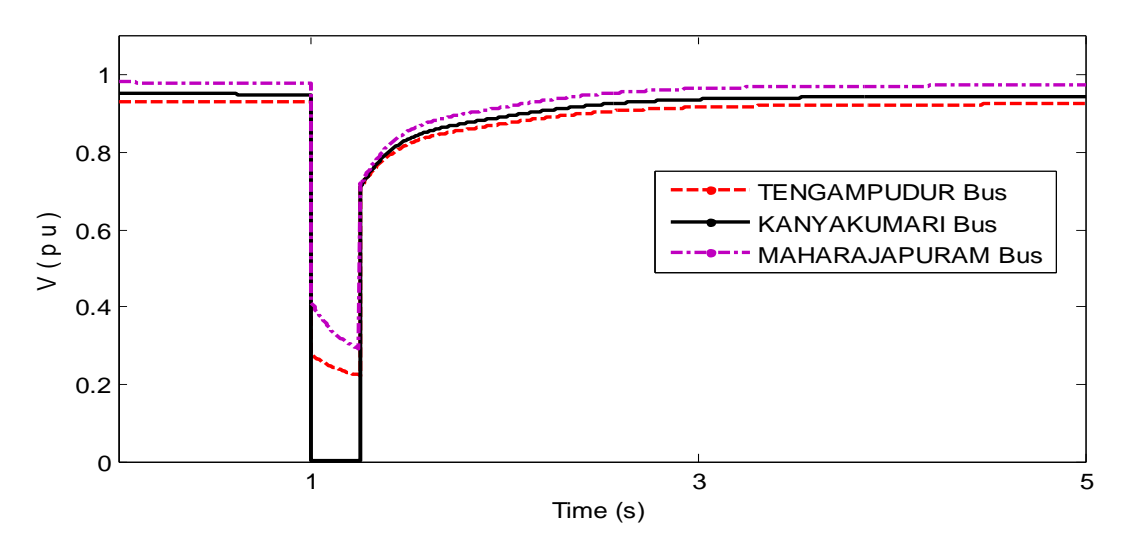


Figure 6.7 Voltage variations of Kanyakumari bus and nearer buses for three phase fault.

It is observed that fault at Kanyakumari bus has least impact on the voltages at the nearer buses. The voltage at Kanyakumari bus does not regains steady-state voltage after clearing the fault.

6.8.2 Fault at SR PUDUR21 Bus

The SR_Pudur 21 bus is exporting 1.8 MW power to grid which is connected to Thuckalay bus and Aralvoimozhi bus .When a three phase fault is applied at SR_Pudur 21 bus at 1.0 second and cleared at 1.25 second, the variations in voltages following a disturbance are plotted in Figure 6.8.

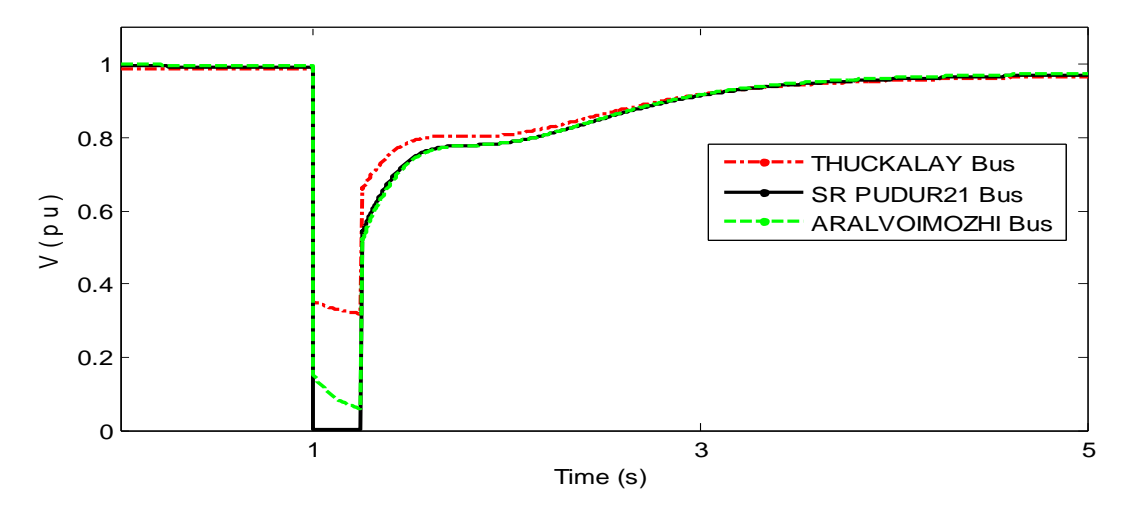


Figure 6.8 Voltage variations of SR_Pudur 21 bus and nearer buses for three phase fault.

It is observed that fault at SR_Pudur 21 bus has lesser impact on the voltages at the nearer buses. The voltage at SR_Pudur 21 bus does not regains steady-state voltage after clearing the fault.

6.8.3 Fault at VEERAN21 Bus

The Veeran21 bus is exporting 161.28 MW power to grid which is connected to Veeranm2 bus. When a three phase fault is applied at Veeran21 bus at 1.0 second and cleared at 1.25 second, the variations in voltages following a disturbance are plotted in Figure 6.9.

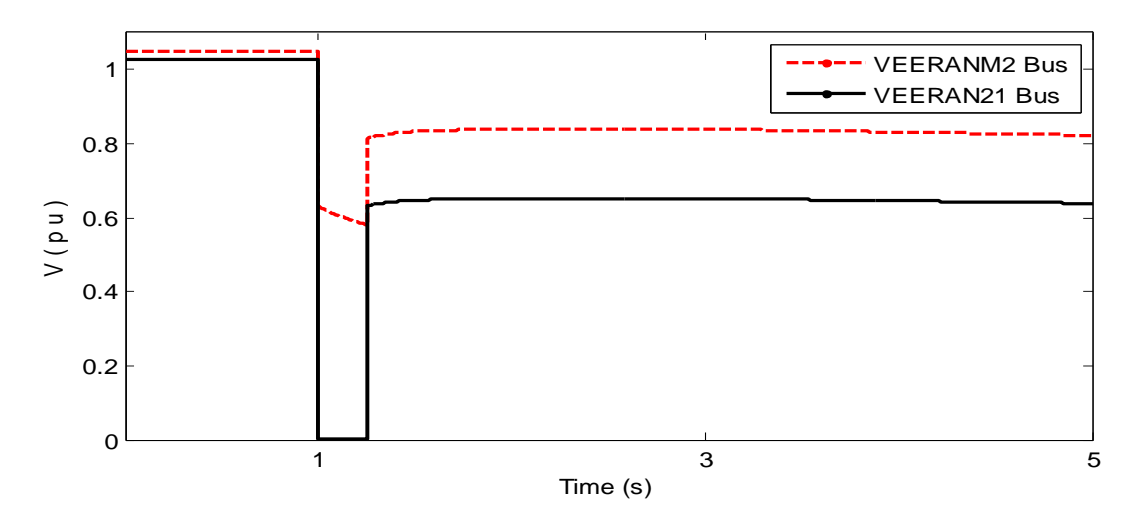


Figure6.9 Voltage variations of Veeran21 bus and nearer buses for three phase fault.

It is observed that fault at Veeran21 bus has more impact on the voltages at the nearer bus. The voltage profile at Veeran21 bus is very poor after clearing the fault.

6.8.4 Fault at AMDAPURAM Bus

The Amdapuram bus is exporting 70.8 MW power to grid which is connected to Kodikur2 bus and Chekka42 bus. When a three phase fault is applied at Amdapuram bus at 1.0 second and cleared at 1.25 second, the variations in voltages following a disturbance are plotted in Figure 6.10.

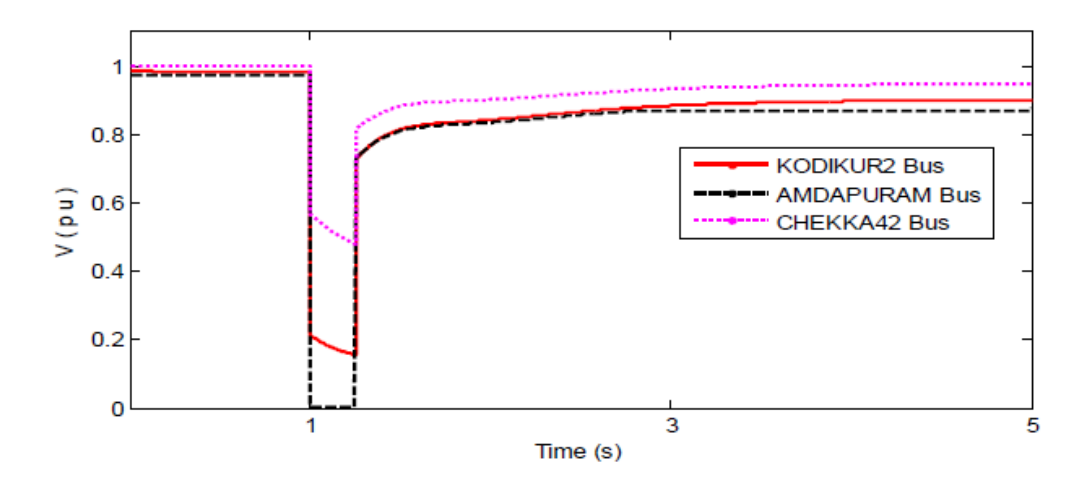


Figure 6.10 Voltage variations of Amdapuram bus and nearer buses for three phase fault.

It is observed that fault at Amdapuram bus has lesser impact on the voltages at the nearer bus. The voltage profile at Amdapuram bus does not regains to initial steady-state voltage after clearing the fault.

6.9 Wind farm behaviour with LVRT capability

The transient stability analysis is performed for the test system by considering wind turbine generator with LVRT capability.

6.9.1 Fault at KANYAKUMARI Bus

A three phase fault is applied at Kanyakumari bus at 1.0 second and cleared at 1.25 second. The variations in voltage and induction generator slip following a disturbance are plotted.

The voltage profile of Kanyakumari bus and nearby wind farm connecting buses such as Maharajapuram, SRpudur21, and Karunkulam buses are plotted in Figure 6.11.a and 6.11.b respectively.

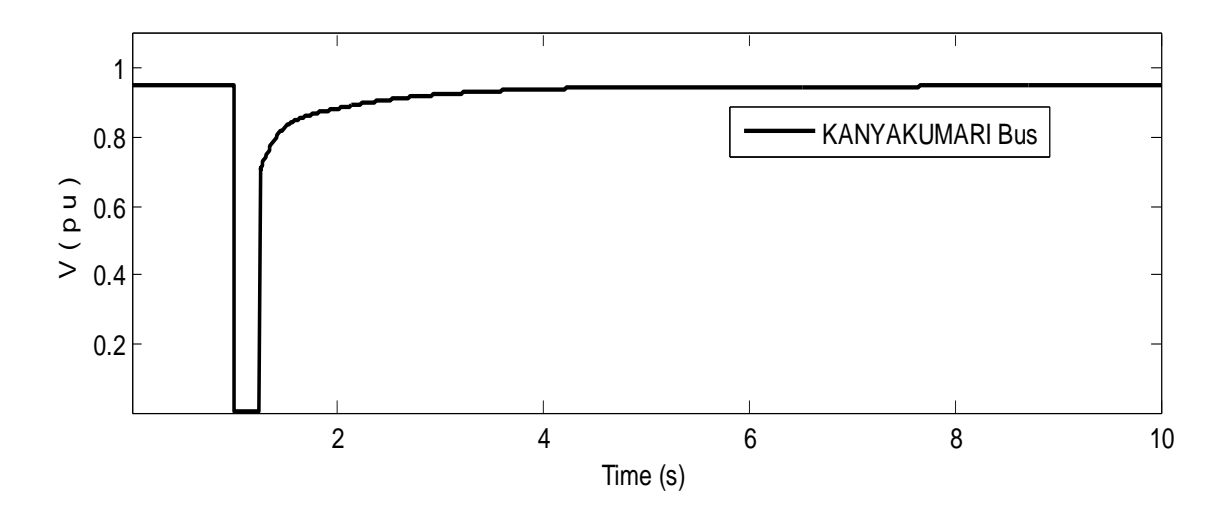


Figure 6.11.a Voltage variations at Kanyakumari bus for three phase fault

Variation of slip at Kanyakumari bus and nearer wind farm connecting bus such as Maharajapuram, SR pudur21, and Karunkulam buses are plotted in Figure 6.11.c

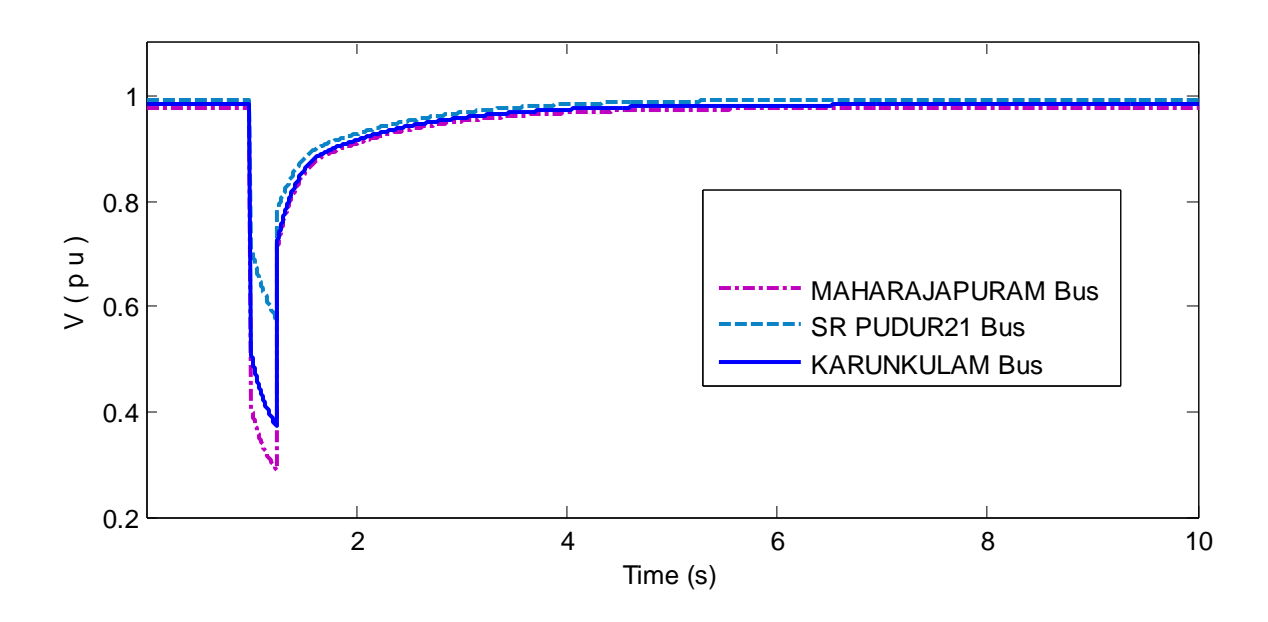


Figure 6.11.b Voltage variations of buses nearer to Kanyakumari bus for three phase fault

It is observed from Figure 6.11.a that the Kanyakumari bus voltage regains voltage to 1 p.u and reaches steady state after the removal of fault. From Figure 6.11.b it is observed that fault at Kanyakumari bus causes a sudden dip in voltage at nearby Maharajapuram bus, SR pudur21 bus and Karunkulam bus during fault and regains steady-state voltage after clearing the fault. The wind farms located at these locations have fault-ride through capability.

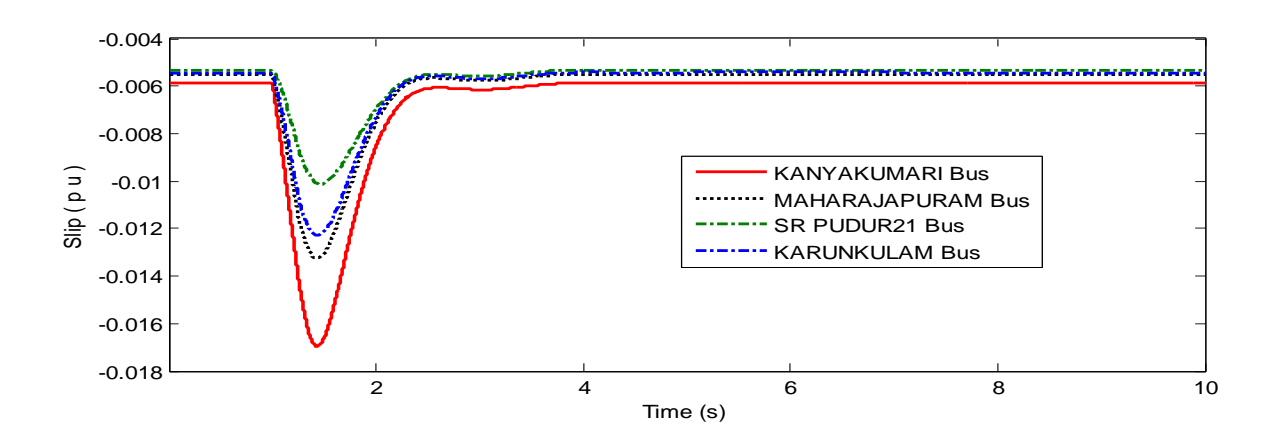


Figure 6.11.c Slip variations of Kanyakumari bus and nearer buses for three phase fault.

From Figure 6.11.c it can be noted that the wind farms at Maharajapuram bus, SR pudur 21 bus, Karunkulam bus and Kanyakumari bus undergo an increase in slip in the negative direction. Slip is increasing in the negative direction means that the induction generators rotors are over speeding beyond the rated speed. But after the clearance the machines have regained their steady-state speed. Hence, the system is stable for this fault.

6.9.2 Fault at SR PUDUR21 Bus

A three phase fault is applied at SR pudur21 bus at 1.0 second and cleared at1.25 second. The variations in voltage and induction generator slip following a disturbance are plotted.

The voltage profile of SR pudur21 bus and nearby wind farm connecting Aralvoimozhi bus is plotted in Figure 6.12.a and 6.12.b respectively.

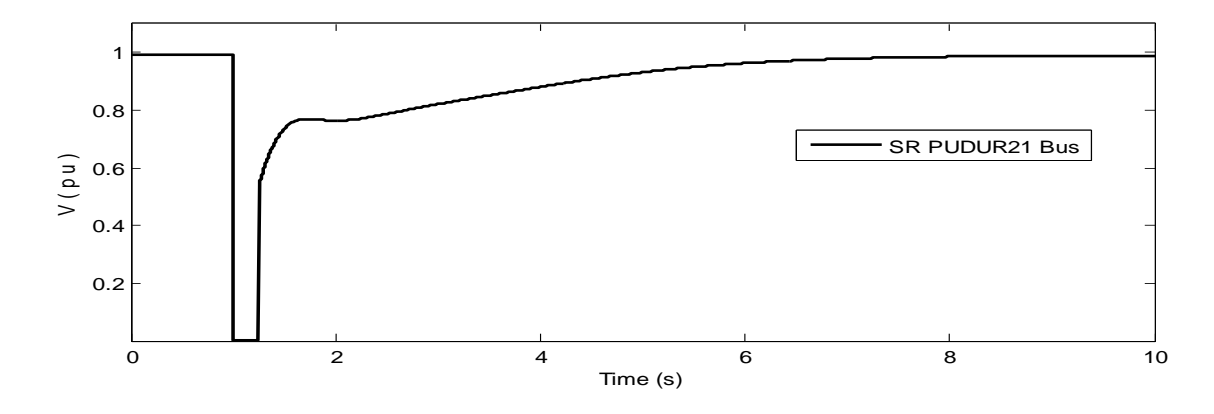


Figure 6.12.a Voltage variations at SR pudur 21 bus for three phase fault

The slip of SR pudur21 bus and nearer wind farm connecting Aralvoimozhi bus is plotted in Figure 6.12.c. It is observed that from Figure 6.12.a the SR pudur21 bus voltage regains to 1 p.u and reaches steady state after the removal of fault.

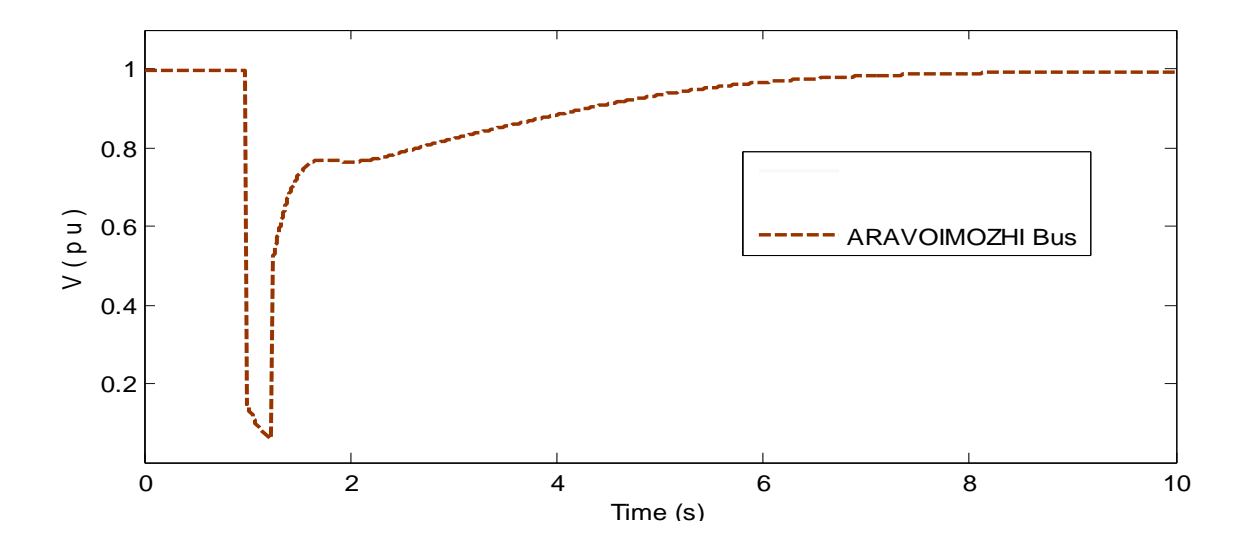


Figure 6.12.b Voltage variations at Aralvoimozhi bus for three phase fault

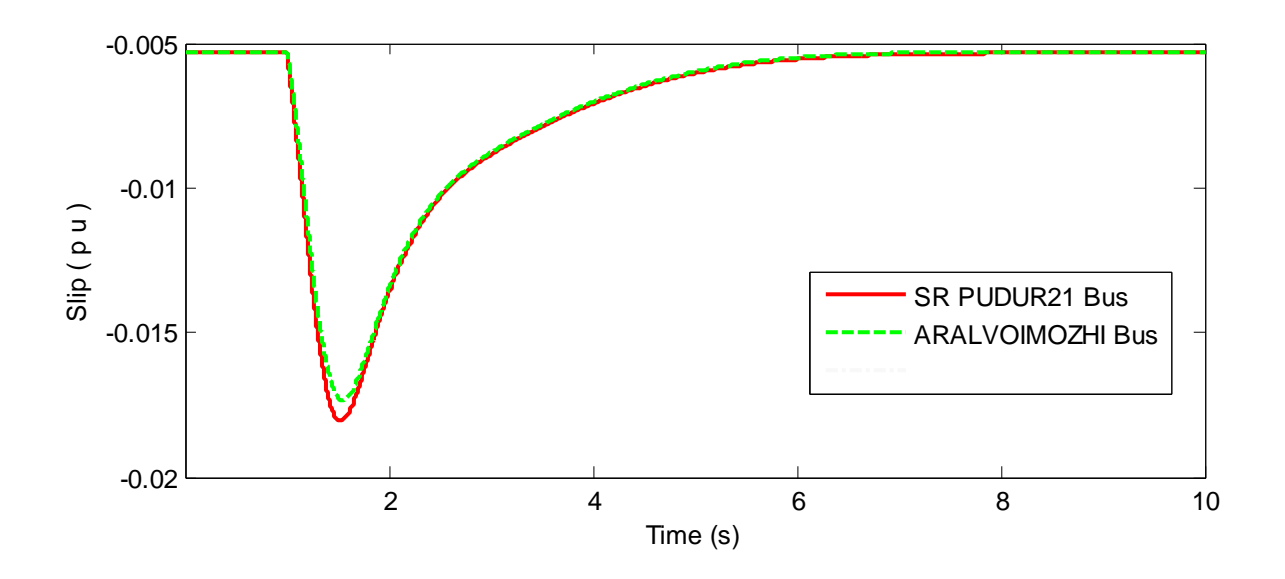


Figure 6.12.c Slip variations of SR pudur 21 bus and Aralvoimozhi bus for three phase fault.

It is also observed from Figure 6.12.b that fault at SR pudur21 bus causes a sudden dip in voltage at nearby Aralvoimozhi bus during fault and regains steady-state voltage after clearing the fault. The wind farms located at these locations have fault-ride through capability.

From Figure 6.12.c it can be noted that the wind farms at SR pudur21 and Aralvoimozhi buses undergoes an increase in slip in the negative direction. Slip is increasing in the negative direction means that the induction generators rotors are over speeding beyond the rated speed. But after the clearance the machines have regained their steady-state speed. Hence, the system is stable for this fault.

6.9.3Fault at VEERAN21 Bus

A three phase fault is applied at Veeran21 bus at 1.0 second and cleared at 1.25 second. The voltage profile of Veeran21 bus and nearby wind farm connecting buses such as Veerasegamani, Kayathar21, and Kannanaloor buses are plotted in Figure 6.13.a

The slip of Veeran21bus and nearer wind farm connecting bus such as Veerasegamani, Kayatr 21, and Kannanaloor bus are plotted in Figure 6.13.b.

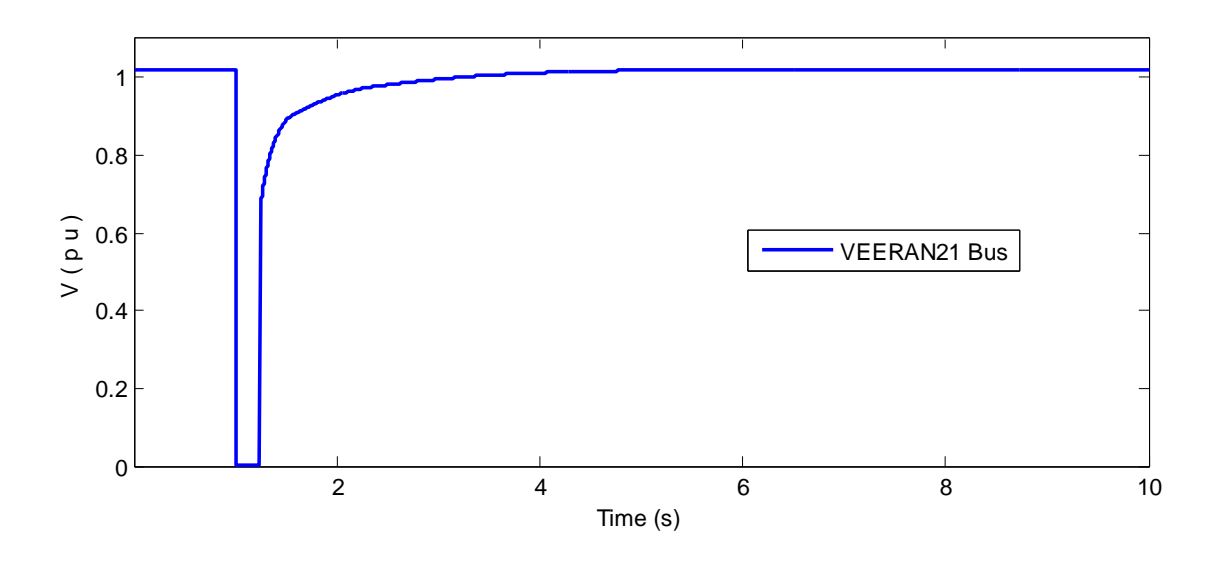


Figure 6.8.a Voltage variations at Veeran 21 bus for three phase fault

It is observed that from Figure 6.13.a the Veeran21 bus voltage regains to 1 p.u and reaches steady state after the removal of fault. It is also observed Figure 6.13.b that fault at Veeran21 bus causes a sudden dip in voltage at nearby Veerasegamani, Kayatr21, and Kannanaloor buses during fault and regains steady-state voltage after clearing the fault. The wind farms located at these locations have fault-ride through capability.

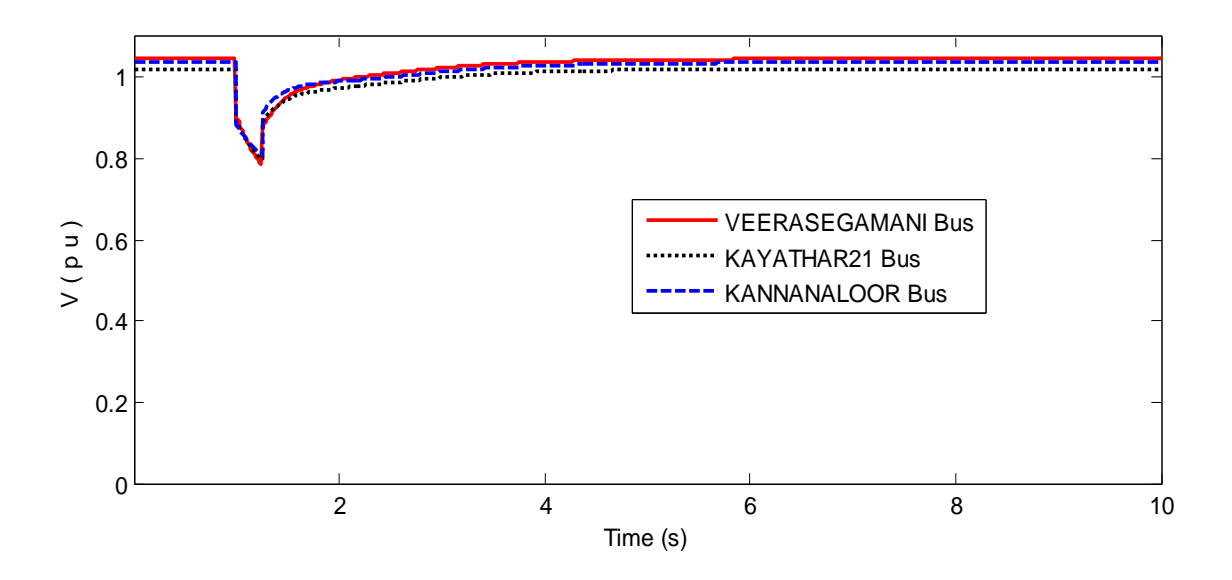


Figure 6.13.b Voltage variations of buses nearer to Veeran 21 bus for three phase fault

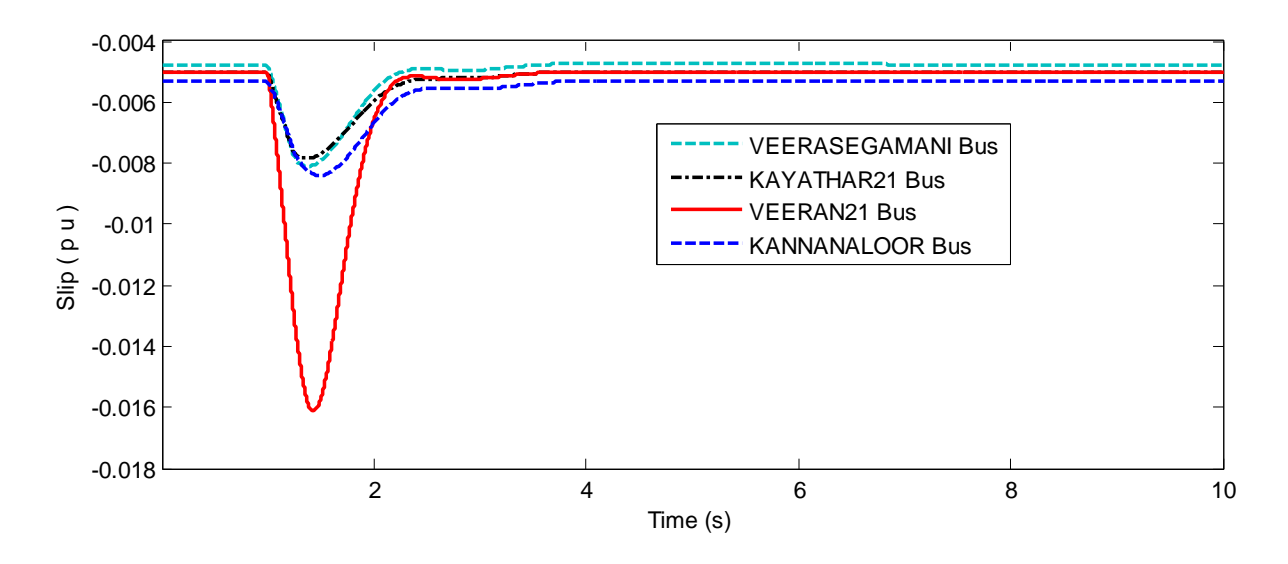


Figure 6.13.c Slip variations of Veeran 21 bus and nearer buses for three phase fault.

From Figure 6.13.c it can be noted that the wind farms at Veerasegamani, Kayatr21, and Kannanaloor buses undergo an increase in slip in the negative direction. Slip is increasing in the negative direction means that the induction generators rotors are over speeding beyond the rated speed. But after the clearance the machines have regained their steady-state speed. Hence, the system is stable for this fault.

6.9.4 Fault at AMDAPURAM Bus

A three phase fault is applied at Amdapuram bus at 1.0 second and cleared at 1.25 second. The voltage profile of Amdapuram bus and nearby wind farm connecting Veerasegamani bus is plotted in Figure 6.14.a and 6.14.b respectively. The slip of Amdapuram bus and nearer wind farm connecting Veerasegamani bus are plotted in Figure 6.14.c

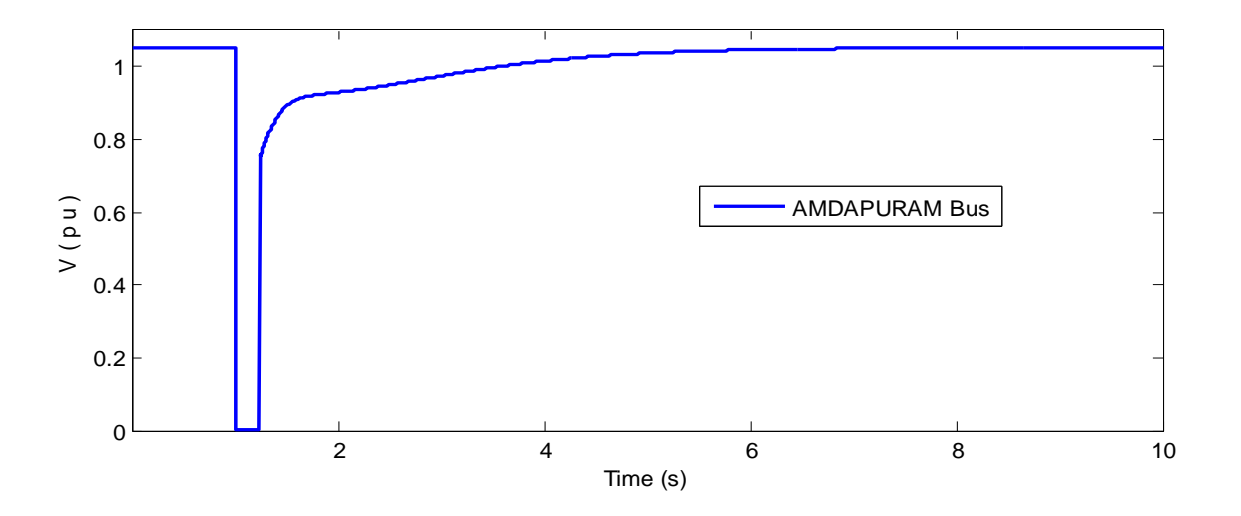


Figure 6.14.a Voltage variations at Amdapuram bus for three phase fault

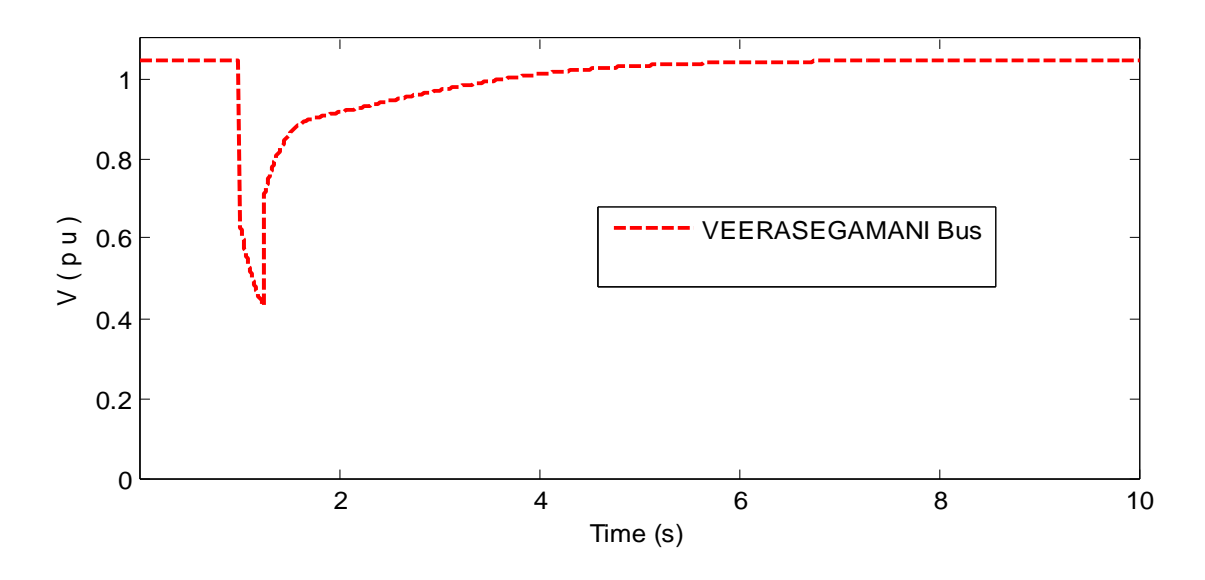


Figure 6.14.b Voltage variations at Veerasegamani bus for three phase fault

It is observed from Figure 6.14.a that the Amdapuram bus voltage regains to 1 p.u and reaches steady state after the removal of fault. It is also observed from Figure 6.14.b that fault at Amdapuram bus causes a sudden dip in voltage at nearby Veerasegamani bus during fault and regains steady-state voltage after clearing the fault. The wind farms located at these locations have fault-ride through capability.

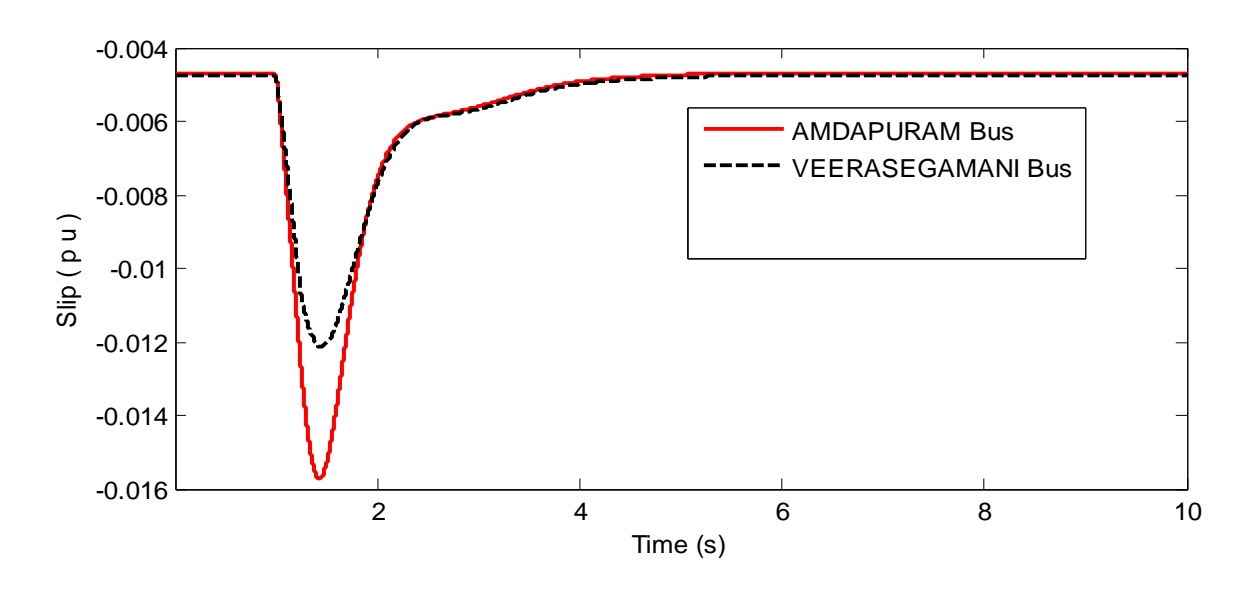


Figure 6.14.c Slip variations of Amdapuram bus and Veerasegamani bus for three phase fault.

From Figure 6.14.c it can be noted that the wind farms at Veerasegamani bus undergoes an increase in slip in the negative direction. Slip is increasing in the negative direction means that the induction generators rotors are over speeding beyond the rated speed. But after the clearance of fault the machines have regained their steady-state speed. Hence, the system is stable for this fault.

Similarly the fault is applied at various buses in Tirunelveli region and found that the system remains stable after the clearance of fault.

6.10 Summary

The dynamic models of various power system components are presented. The algorithm for analyzing the stability of the power system is described. The stability of the system and the fault-ride through capability of the wind farms are analyzed for different fault locations.

7. Conclusions and Recommendations

Based on the aforesaid analysis, the following recommendations are drawn for effective utilization of the installed wind power generation.

- When the wind penetration is below 50% the exiting transmission corridor is sufficient to evacuate the power. When it is above 50% it is observed that more number of transmission lines and transformers are overloaded. Hence, it is recommended that in order to efficiently utilize the available wind potential it is essential to establish a dedicated 765/400kV and 230 kV substations and necessary committed expansion proposals should be implemented as early as possible in the Tirunelveli region.
- The real and reactive power losses are increased as wind power penetration increases, so reactive compensation is required at the wind farm substations. Dynamic compensation at the 110 kV/230 kV substations is recommended.
- The plan for future expansion of wind turbine generators may be covered near the strong points identified in the grid.
- Weak points identified using short-circuit analysis are prone to power evacuation problem in case of increasing wind turbine generator installation.
- The transmission expansion plans in the pipe line may have a provision for installation of TCSC, as it enhances the loading of the transmission lines.
- To overcome the technical difficulties like alleviation of line over loading, reactive power compensation etc, formation of VSC based Multi terminal DC system is a viable solution.
- Stability analysis reveals that when the wind generators possess Low Voltage Ride Through (LVRT) capability there were no stability and low voltage problems. So it is necessary that the wind generators should have LVRT capability.

Appendix A

Study system data collection through field visit

| Bus details | | | | |
|-----------------------|--------|----------|-------|--------------------------------------|
| Total No of Buses | | | : 156 | |
| Number of 400kV buses | | | : 2 | |
| Number of 230kV buses | | | : 19 | |
| Number of 110kV buses | | | : 108 | |
| Actual No | Bus no | Bus Name | kV | Bus Description |
| 1 | 1 | TTPSGEN | 15 | TTPS_GENERATOR _BUS_5X210MW |
| 2 | 2 | KODAGEN6 | 11 | KODAIYAR_GENERATOR_1X60MW |
| 3 | 3 | KODAGEN4 | 11 | KODAIYAR_GENERATOR_BUS_1X40MW |
| 4 | 4 | PERIYGEN | 11 | PERIYAR_GENERATOR_1X140 |
| 5 | 5 | SURULGEN | 11 | SURULIYAR_GENERATOR_BUS_1X35MW |
| 6 | 6 | IBCPPGEN | 15 | IBCPPGENERATOR_BUS_1X200MW |
| 7 | 7 | BIOEPGEN | 11 | BIOMASS_NEAR_EPPOTHUMVENTRAN_1X20MW |
| 8 | 8 | BIOMEGEN | 11 | BIOMASS_GENERATOR_MELAKALOOR |
| 9 | 9 | SERVAGEN | 11 | SERVALAR_HYDRO_GENERATOR_BUS_1X20MW |
| 10 | 10 | PAPANGEN | 11 | PAPANASAM_HYDRO_GENERATOR_BUS_1X32MW |
| 201 | 11 | SRPUDUR2 | 230 | SRPUDUR_230/110/11kVSS |
| 202 | 12 | SANKANE2 | 230 | SANKANERI_230/110/11kVSS |
| 203 | 13 | UDAYTHR2 | 230 | UDAYTHUR_230/110 kVSS |
| 204 | 14 | KUDANKU2 | 230 | KUDANKULAM_STARTUP_BUS_230/33kV |
| 205 | 15 | TUTICOR2 | 230 | TUTICORIN_AUTO230/110 kV |
| 206 | 16 | ABPATT42 | 230 | ABPATTY_TIRUNELVELI_PGCIL400/230 kV |
| 207 | 17 | KAYATHR2 | 230 | KAYATHAR_230/110/66kVSS |
| 208 | 18 | VEERANM2 | 230 | VEERANAM230/33 kVSS |
| 209 | 19 | TTPS2 | 230 | TTPS_SWITCHYARD_230/15.75kV |
| 210 | 20 | KODIKUR2 | 230 | KODIKURCHI230/110 kVSS |

| 211 | 21 | AMDAPUR2 | 230 | AMDAPURAM230/33 kVSS |
|------|----|----------|-----|----------------------------------|
| 212 | 22 | STERLIT2 | 230 | STERLITE_230/110kV |
| 213 | 23 | SIPCOT2 | 230 | SIPCOT230/110 kV |
| 214 | 24 | ANUPKUL2 | 230 | ANUPPANKULAM230/110 kVSS |
| 215 | 25 | CHEKKA42 | 230 | CHEKKANOORANI400/230 kVSS |
| 216 | 26 | PASUMAL2 | 230 | PASUMALAI230/110kVSS |
| 217 | 27 | MEELAVE2 | 230 | MEELAVETAN230/110 kVSS |
| 218 | 28 | PARAMAG2 | 230 | PARAMAGUDI 230/110kVSS |
| 219 | 29 | IBCPP2 | 230 | IND BHARATH 230KVSY |
| 400 | 30 | CHEKKAN4 | 400 | CHEKKANURANI_400/230_KV_SS |
| 401 | 31 | ABPATTY4 | 400 | ABISHEKAPATTY_THIRUNELVELI_PGCIL |
| 1000 | 32 | CHEMPONV | 110 | CHEMPONVILAI_110/11 kV |
| 1001 | 33 | THENGAM | 110 | THENGAMPUDUR_110/11 kV |
| 1002 | 34 | KANYAKUM | 110 | KANYAKUMARI_110/11 kV |
| 1003 | 35 | MUNCHIRA | 110 | MUNCHIRAI_110/11 kV |
| 1005 | 36 | MEENAKSH | 110 | MEENAKSHIPURAM_110/11 kV |
| 1007 | 37 | KULTHURA | 110 | KULTHURAI_110/11 kV |
| 1008 | 38 | NAGARKOI | 110 | NAGARKOIL_110/11 kV |
| 1009 | 39 | THUCKALA | 110 | THUCKALAY_110/11 kV |
| 1010 | 40 | MAHARAJA | 110 | MAHARAJAPURAM_110/11 kV |
| 1011 | 41 | SRPUDU21 | 110 | SR PUDUR_230/110/11 kV_110/230kV |
| 1012 | 42 | KARUNKUL | 110 | KARUNKULAM_110/11 kV |
| 1013 | 43 | PALAVOOR | 110 | PALAVOOR_110/11 kV |
| 1015 | 44 | VEEYANOO | 110 | VEEYANOOR_110/11 kV |
| 1016 | 45 | CHIDAMBA | 110 | CHIDAMBARAPURAM_110/11 kV |
| 1017 | 46 | ARALVOIM | 110 | ARALVOIMOZHI_110/11 kV |
| 1018 | 47 | SANKAN21 | 110 | SANKANERI_230/110/11kVSS |
| 1019 | 48 | IRUKKAND | 110 | IRUKKANDURAI_110/33/11 kV SS |
| 1020 | 49 | MUPANTHA | 110 | MUPANTHAL_110/11kVSS |
| 1021 | 50 | PECHIPAR | 110 | PECHIPARAI_110/11 kV |

| 1022 | 51 | PERUNGUD | 110 | PERUNGUDI_110/33/11kVSS |
|------|----|----------|-----|------------------------------------|
| 1023 | 52 | KOODANKU | 110 | KOODANKULAM_110/11 kV_110/33kV |
| 1024 | 53 | RADHAPUR | 110 | RADHAPURAM_110/11 kV_110/33kV |
| 1025 | 54 | VADDAKKA | 110 | VADDAKKANKULAM_110/11 kV_110/33kV |
| 1026 | 55 | KODA6YAR | 110 | KODIAYAR_6SWITCHYARD |
| 1027 | 56 | PANAGUDI | 110 | PANAGUDI_110/11 kV_110/33kV |
| 1028 | 57 | ANNANAGA | 110 | ANNANAGAR_110/33/11kVSS |
| 1029 | 58 | UDAYTR21 | 110 | UDAYTHUR_230/110/33kVSS |
| 1030 | 59 | KODA4YAR | 110 | KODAIYAR_40MW_SWITCHYARD |
| 1032 | 60 | THANDAIY | 110 | THANDAIYARKULAM_110/11 kV_110/33kV |
| 1034 | 61 | KALAKAD | 110 | KALAKAD_110/11 kV |
| 1035 | 62 | KOTTAIKA | 110 | KOTTAIKARUNKULAM 110/11kVSS |
| 1037 | 63 | VALLOYOO | 110 | VALLOYOOR_110/11 kV |
| 1038 | 64 | THIRUVIR | 110 | THIRUVIRUNTHANPULLAI_110/11 kVSS |
| 1039 | 65 | SATHANK | 110 | SATHANKULAM_110/11 kV_110/33kV |
| 1040 | 66 | UDANGUDI | 110 | UDANGUDI_110/11 kV |
| 1041 | 67 | ARUMUGAN | 110 | ARUMUGANERI_110/11kV_110/33kV |
| 1042 | 68 | KARANTHA | 110 | KARANTHANERI_110/11kV |
| 1043 | 69 | MANJANEE | 110 | MANJANEER KAYAL_110/11kV |
| 1044 | 70 | VEERAVAN | 110 | VEERAVANALLUR_110/11kV |
| 1045 | 71 | MELAKALO | 110 | MELAKALOOR_110/11kVSS |
| 1047 | 72 | PALAYAPE | 110 | PALAYAPETTAI_110/11kV |
| 1048 | 73 | VMCHATHR | 110 | VMCHATHRAM_110/11kV |
| 1049 | 74 | PAPANASA | 110 | PAPANASAM HYDEL P.H_Switch yard |
| 1051 | 75 | THALAIYU | 110 | THALAIYUTU_110/11kV_110/33 |
| 1053 | 76 | SERVALAR | 110 | SERVALAR HYDEL P.H_Switch yard |
| 1055 | 77 | OTHULUKK | 110 | OTHULUKKARPATI_110/33kV_230/33kV |
| 1057 | 78 | RASTHA | 110 | RASTHA_110/33kV |
| 1058 | 79 | MANNUR | 110 | MANNUR_110/11kV |
| 1059 | 80 | KEELAVEE | 110 | KEELAVEERANAM_110/11kV_110/33kV |

| 1060 | 81 | KADAYAM | 110 | KADAYAM_110/11kV |
|------|-----|----------|-----|-----------------------------------|
| 1061 | 82 | SUNDANKU | 110 | SUNDANKURCHI_110/11kV |
| 1063 | 83 | AYYANARO | 110 | AYYAANAROOTHUR_110/11kV |
| 1064 | 84 | SANKTOFF | 110 | SANKARANKOVIL_TOFF |
| 1065 | 85 | ALANKULA | 110 | ALANKULAM_110/11kV_110/33kV |
| 1068 | 86 | PAVOORCH | 110 | PAVOORCHATRAM_110/11kV_110/33kV |
| 1069 | 87 | VANNIKON | 110 | VANNIKONENTHAL_110/11kVSS |
| 1071 | 88 | CHETTIKU | 110 | CHETTIKURICHI_110/33kV |
| 1072 | 89 | SURANDAI | 110 | SURANDAI_110/11kV |
| 1073 | 90 | UTHUMALA | 110 | UTHUMALAI_110/33kV_66/11kV |
| 1074 | 91 | AYYANAPU | 110 | AYYANAPURAM_110/11kV_110/33kV |
| 1077 | 92 | MALAYANK | 110 | MALAYANKULAM_110/11kV |
| 1078 | 93 | EPPOTHUM | 110 | EPPOTHUMVENTRAN_110/11kV_110/33kV |
| 1080 | 94 | VELATHIK | 110 | VELATHIKULAM_110/11kV |
| 1081 | 95 | TENKASI | 110 | TENKASI_110/11kV |
| 1082 | 96 | SHENKOTT | 110 | SHENKOTTAI_110/11kV |
| 1083 | 97 | KODIKU21 | 110 | KODIKURCHI_110/33kV |
| 1087 | 98 | KOVILPAT | 110 | KOVILPATTI_110/11 kV |
| 1088 | 99 | VIJAYAPU | 110 | VUJAYAPURAI_110/11 kV |
| 1089 | 100 | SANKARAN | 110 | SANKARANKOIL_110/11 kV |
| 1090 | 101 | NSUBBIAH | 110 | NSUBBIAHPURAM_110/11 kV |
| 1092 | 102 | KADAYANA | 110 | KADAYANALLOR_110/11 kV |
| 1093 | 103 | PULIYANG | 110 | PULIYANGUDI_110/11 kV |
| 1094 | 104 | NARAYANA | 110 | NARAYANAPURAM_110/11 kV |
| 1095 | 105 | VISWANAT | 110 | VISWANATHAPERI_110/11 kV |
| 1096 | 106 | PERUMALP | 110 | PERUMALPATTI_110/11kV SS |
| 1097 | 107 | SETHIUR | 110 | SETHIUR_110/11 kV |
| 1098 | 108 | RAJAPALA | 110 | RAJAPALAYAM_110/11 kV |
| 1099 | 109 | MUDUNGAI | 110 | MUDUNGAIYUR_110/11 kV |
| 1100 | 110 | SURULIYA | 110 | SURULIYAR HYDEL_Switch yard |

| 1101 | 111 | PERIYAR | 110 | PERIYAR HYDEL P.H_Switch yard |
|------|-----|----------|-----|--|
| 1102 | 112 | BIOEPPOT | 110 | BIOMASS_EPPOTHUMVANTENTRAN_BUS110kVBUS |
| 1103 | 113 | VEERASEG | 110 | VEERASEGAMANI_110/66/33kV |
| 1104 | 114 | KAYATR21 | 110 | KAYATHAR_230/110/11kVSS |
| 1105 | 115 | VEERAN21 | 110 | VEERANAM_230/110/11kVSS |
| 1106 | 116 | TUTICO21 | 110 | TUTICORIN_110kV |
| 1107 | 117 | AMDAPU21 | 110 | AMDAPURAM_110kV |
| 1108 | 118 | ANUPPA21 | 110 | ANUPPANKULAM_110kV |
| 1109 | 119 | SHIPCO21 | 110 | SHIPCOT_110kV |
| 1110 | 120 | MEELA21 | 110 | MEELAVETAN_110kV |
| 1111 | 121 | STERLT21 | 110 | STERLITE_110kV |
| 1122 | 122 | BIOMELAK | 110 | BIOMASS_MELAKALOOR |
| 1123 | 123 | MEENTOFF | 110 | MEENAKSHIPURAM_TOFF |
| 1124 | 124 | NAGATOFF | 110 | NAGARKOVIL_TOFF |
| 1125 | 125 | MARTTOFF | 110 | MARTHANDAM_TOFF |
| 1126 | 126 | AMBATOFF | 110 | AMBASAMUTHURAM_TOFF |
| 1127 | 127 | THATOFF1 | 110 | THALAYUTHU_TOFF |
| 1128 | 128 | THATOFF2 | 110 | THALAYUTHU_TOFF2 |
| 1129 | 129 | MUPPTOFF | 110 | MUPPANTHAL_TOFF |
| 1130 | 130 | PALATOFF | 110 | PALAVOOR_TOFF |
| 1131 | 131 | PERUTOFF | 110 | PERUNGUDI_TOFF |
| 1132 | 132 | TENKTOFF | 110 | TENKASI_TOFF |
| 1133 | 133 | KODITOFF | 110 | KODIKURICHI_TOFF |
| 1134 | 134 | MUNCTOFF | 110 | MUNCHIRAI_TOFF |
| 1135 | 135 | KANGAIKO | 110 | KANGAIKONDAN_110/11kVSS |
| 1136 | 136 | VISWTOFF | 110 | VISWANATHAPERI_TOFF |
| 1137 | 137 | POIGAISS | 110 | POIGAI_110/33kVSS |
| 1138 | 138 | RAJTOFF1 | 110 | RAJAPALAYAM_TOFFI_SURULIYAR |
| 1139 | 139 | RAJTOFF2 | 110 | RAJANPALAYAM_TOFF2_MUNGAIYUR |

Transformer details

| From Bus Name | To Bus Name | R (p.u) | X (p.u) | TAP | MVA |
|---------------|-------------|---------|---------|---------|------|
| PAPANASA | PAPANGEN | 0.01376 | 0.27521 | 1 | 45 |
| SERVALAR | SERVAGEN | 0.02164 | 0.43279 | 1 | 30 |
| INDBARTH | BIOEPGEN | 0.04187 | 0.83742 | 1 | 13 |
| BIOMELAK | BIOMEGEN | 0.04187 | 0.83742 | 1 | 13 |
| SANKANE2 | SANKAN21 | 0.0025 | 0.04994 | 0.99837 | 200 |
| UDAYTHR2 | UDAYTR21 | 0.0025 | 0.04994 | 0.99837 | 200 |
| TUTICOR2 | TTPSAUTO | 0.0025 | 0.04994 | 0.99837 | 200 |
| VEERANM2 | VEERAN21 | 0.0025 | 0.04994 | 0.99837 | 200 |
| KODIKUR2 | KODIKU21 | 0.0025 | 0.04994 | 0.99837 | 200 |
| SIPCOT2 | TSIPCOT1 | 0.0025 | 0.04994 | 0.99837 | 200 |
| SIPCOT2 | MEELA21 | 0.0025 | 0.04994 | 0.99837 | 200 |
| ANUPKUL2 | ANUPPA21 | 0.0025 | 0.04994 | 0.99837 | 200 |
| IBCPP2 | IBCPPGEN | 0.0012 | 0.02409 | 0.92616 | 480 |
| CHEKKAN4 | CHEKKA42 | 0.00079 | 0.01585 | 1 | 630 |
| ABPATTY4 | ABPATT42 | 0.00079 | 0.01585 | 1 | 630 |
| KAYATHR2 | KAYATR21 | 0.00166 | 0.03329 | 0.99837 | 300 |
| KODA6YAR | KODAGEN6 | 0.00459 | 0.09174 | 1 | 135 |
| KODAYAR1 | KODAGEN4 | 0.00717 | 0.14338 | 1 | 75 |
| SURULIYA | SURULGEN | 0.01872 | 0.18719 | 1 | 48 |
| PERIYAR_ | PERIYGEN | 0.01189 | 0.2378 | 1 | 42 |
| SRPUDUR2 | SRPUDU21 | 0.001 | 0.01998 | 0.99837 | 500 |
| TTPS2 | TTPSGEN | 0.00048 | 0.00963 | 0.92616 | 1200 |

Shunt connection (admittance) data

| Bus no | Bus Name | G (p.u) | B (p.u.) | MVAR |
|--------|----------|---------|----------|------|
| 1000 | CHEMPONV | 0 | 0.168 | 16.8 |
| 1003 | MUNCHIRA | 0 | 0.168 | 16.8 |
| 1002 | KANYAKUM | 0 | 0.168 | 16.8 |
| 1013 | PALAVOOR | 0 | 0.168 | 16.8 |
| 1049 | PAPANASA | 0 | 0.168 | 16.8 |
| 1038 | THIRUVIR | 0 | 0.168 | 16.8 |
| 1011 | SRPUDU21 | 0 | 0.168 | 16.8 |
| 1104 | KAYATR21 | 0 | 0.168 | 16.8 |
| 1128 | THATOFF2 | 0 | 0.168 | 16.8 |
| 1098 | RAJAPALA | 0 | 0.168 | 16.8 |
| 1040 | UDANGUDI | 0 | 0.168 | 16.8 |
| | | | 1 | |

Generator data

| S.no | Bus No | BusName | P _G MW | Qmin(MVAR) | Qmax(MVAR) | V (p.u) | MVA |
|------|--------|----------|-------------------|------------|------------|---------|-------|
| 1 | 1 | TTPSGEN | 1050 | 0 | 350 | 1.05 | 1235 |
| 2 | 2 | KODAGEN6 | 0 | 0 | 20 | 1.025 | 87.5 |
| 3 | 5 | SURULGEN | 0 | 0 | 10 | 1.025 | 68.75 |
| 4 | 3 | KODAGEN4 | 0 | 0 | 0 | 1.025 | 52.5 |
| 5 | 4 | PERIYGEN | 20 | 0 | 100 | 1.05 | 162.5 |
| 6 | 6 | IBCPPGEN | 120 | -90 | 100 | 1.025 | 247 |
| 7 | 7 | BIOEPGEN | 8 | 0 | 11 | 1 | 26 |
| 8 | 8 | BIOMEGEN | 8 | 0 | 11 | 1 | 26 |
| 9 | 9 | SERVAGEN | 20 | 0 | 5 | 1.025 | 20 |
| 10 | 10 | PAPANGEN | 8 | 0 | 20 | 1.025 | 32 |

Load data

| S.no | Bus No | BusName | P _L MW | Q _L MVAR |
|------|--------|----------|-------------------|---------------------|
| 1 | 1000 | CHEMPONV | 10 | 4.843 |
| 2 | 201 | SRPUDUR2 | 6 | 2.906 |
| 3 | 1002 | KANYAKUM | 14 | 6.781 |
| 4 | 1003 | MUNCHIRA | 27 | 13.08 |
| 5 | 1007 | KULTHURA | 24 | 11.62 |
| 6 | 1008 | NAGARKOI | 25 | 10 |
| 7 | 1009 | THUCKALA | 22 | 10.66 |
| 8 | 1010 | MAHARAJA | 1 | 0.484 |
| 9 | 1012 | KARUNKUL | 2.5 | 1.211 |
| 10 | 1015 | VEEYANOO | 20 | 9.686 |
| 11 | 1023 | KOODANKU | 14 | 6.781 |
| 12 | 1027 | PANAGUDI | 6 | 2.906 |
| 13 | 1034 | KALAKAD | 14 | 6.781 |
| 14 | 1039 | SATHANK | 34 | 16.47 |
| 15 | 1045 | MELAKALO | 15 | 7.265 |
| 16 | 1051 | THALAIYU | 16 | 7.749 |
| 17 | 1058 | MANNUR | 12 | 5.812 |
| 18 | 1059 | KEELAVEE | 9 | 4.359 |
| 19 | 1072 | SURANDAI | 7 | 3.39 |
| 20 | 1089 | SANKARAN | 16 | 7.749 |
| 21 | 1078 | EPPOTHUM | 39 | 18.89 |
| 22 | 1093 | PULIYANG | 9 | 4.359 |
| 23 | 1137 | POIGAISS | 6.3 | 3.051 |
| 24 | 1095 | VISWANAT | 10 | 4.843 |
| 25 | 1060 | KADAYAM | 11 | 5.328 |
| 26 | 1040 | UDANGUDI | 14 | 6.781 |
| 27 | 1041 | ARUMUGAN | 21 | 10.17 |
| 28 | 1044 | VEERAVAN | 15 | 7.265 |

| 29 | 1074 | AYYANAPU | 1 | 0.484 |
|----|------|----------|------|-------|
| 30 | 1081 | TENKASI | 9 | 4.359 |
| 31 | 1083 | KODIKU21 | 10.8 | 5.231 |
| 32 | 1092 | KADAYANA | 8 | 3.875 |
| 33 | 1097 | SETHIUR | 12 | 5.812 |
| 34 | 1110 | MEELA21 | 6.3 | 3.051 |
| 35 | 1099 | MUDUNGAI | 17 | 8.233 |
| 36 | 1104 | KAYATR21 | 102 | 49.4 |
| 37 | 216 | PASUMAL2 | 48 | 23.25 |
| 38 | 1106 | TUTICO21 | 13 | 6.296 |
| 39 | 213 | SIPCOT2 | 43 | 20 |
| 40 | 209 | TTPS2 | 94 | 45.53 |
| 41 | 1017 | ARALVOIM | 2 | 0.969 |
| 42 | 1020 | MUPANTHA | 1 | 0.484 |
| 43 | 1021 | PECHIPAR | 12 | 5.812 |
| 44 | 1024 | RADHAPUR | 4 | 1.937 |
| 45 | 1057 | RASTHA | 29 | 14.05 |
| 46 | 1103 | VEERASEG | 11 | 5.328 |
| 47 | 1109 | SHIPCO21 | 14 | 6.781 |
| 48 | 400 | CHEKKAN4 | -69 | -22 |
| 49 | 218 | PARAMAG2 | -36 | -12 |

Transmission Line Data

| From BUS | To BUS | R Ω/k.m | X Ω/k.m | B/2 Ω/k.m | MVA Rating | km |
|----------|----------|---------|---------|-----------|---------------|------|
| SRPUDUR2 | SANKANE2 | 0.00404 | 0.02248 | 0.02135 | 295 | 28.7 |
| SRPUDUR2 | KUDANKU2 | 0.0059 | 0.03281 | 0.03117 | 295 | 41.9 |
| SANKANE2 | UDAYTHR2 | 0.00203 | 0.0113 | 0.01073 | 295 | 14.4 |
| SANKANE2 | KAYATHR2 | 0.01292 | 0.07189 | 0.06828 | 295 | 91.9 |
| SANKANE2 | ABPATT42 | 0.01602 | 0.08918 | 0.0847 | 295 | 114 |
| UDAYTHR2 | KAYATHR2 | 0.01159 | 0.0645 | 0.06126 | 295 | 82.4 |
| ABPATT42 | KAYATHR2 | 0.00439 | 0.02256 | 0.02083 | 295 | 28.8 |
| ABPATT42 | VEERANM2 | 0.00475 | 0.02442 | 0.02255 | 295 | 31.2 |
| VEERANM2 | KAYATHR2 | 0.01359 | 0.06981 | 0.06446 | 295 | 89.2 |
| KAYATHR2 | TUTICOR2 | 0.0079 | 0.04056 | 0.03746 | 295 | 51.8 |
| KAYATHR2 | TTPS2 | 0.00396 | 0.02035 | 0.07516 | 590 | 52 |
| KAYATHR2 | ANUPKUL2 | 0.00974 | 0.05422 | 0.0515 | 295 | 69.3 |
| KAYATHR2 | CHEKKA42 | 0.01042 | 0.05798 | 0.22028 | 590 | 148 |
| VEERANM2 | KODIKUR2 | 0.00373 | 0.01917 | 0.0177 | 295 | 24.5 |
| KODIKUR2 | AMDAPUR2 | 0.00214 | 0.01192 | 0.0453 | 590 | 30.5 |
| AMDAPUR2 | CHEKKA42 | 0.00784 | 0.04365 | 0.16581 | 590 | 112 |
| CHEKKA42 | TTPS2 | 0.01042 | 0.05798 | 0.22028 | 590 | 148 |
| CHEKKA42 | SIPCOT2 | 0.0007 | 0.00391 | 0.00372 | 295 | 5 |
| CHEKKA42 | PASUMAL2 | 0.0011 | 0.00611 | 0.02321 | 590 | 15.6 |
| PASUMAL2 | TTPS2 | 0.01935 | 0.1077 | 0.10229 | 295 | 138 |
| PASUMAL2 | ANUPKUL2 | 0.01052 | 0.05854 | 0.0556 | 295 | 74.8 |
| ANUPKUL2 | STERLIT2 | 0.01306 | 0.07267 | 0.06902 | 295 | 92.9 |
| STERLIT2 | TTPS2 | 0.00229 | 0.01174 | 0.01084 | 295 | 15 |
| TTPS2 | KUDANKU2 | 0.01871 | 0.0961 | 0.08874 | 295 | 123 |
| TTPS2 | SIPCOT2 | 0.00186 | 0.00955 | 0.00882 | 295 | 12.2 |
| SIPCOT2 | PARAMAG2 | 0.0149 | 0.08296 | 0.07879 | 295 | 106 |
| TTPS2 | TUTICOR2 | 0.00035 | 0.00196 | 0.00743 | 590 | 5 |
| THENGAM | KANYAKUM | 0.01534 | 0.03942 | 0.00207 | 90 | 12 |
| MEENAKSH | NAGARKOI | 0.01541 | 0.03959 | 0.00207 | 90 | 12.1 |
| NAGARKOI | SRPUDU21 | 0.01932 | 0.04964 | 0.0026 | 90 | 15.1 |
| SRPUDU21 | THUCKALA | 0.03196 | 0.08213 | 0.0043 | 90 | 25 |
| PECHIPAR | KODAYAR1 | 0.01759 | 0.0302 | 0.00142 | 90 | 8.7 |
| VEEYANOO | KODAYAR1 | 0.02256 | 0.05798 | 0.00304 | 90 | 17.6 |
| KANYAKUM | MAHARAJA | 0.01524 | 0.03916 | 0.00205 | 90 | 11.9 |
| KARUNKUL | MAHARAJA | 0.00442 | 0.01137 | 0.0006 | 90 | 3.5 |
| PERUNGUD | PERUTOFF | 0.01662 | 0.04271 | 0.00224 | 90 | 13 |
| SRPUDU21 | ARALVOIM | 0.01405 | 0.02412 | 0.00114 | 90 | 6.9 |
| SRPUDU21 | PANAGUDI | 0.01931 | 0.04961 | 0.0026 | 90 | 15.1 |

| MUPANTHA | ARALVOIM | 0.00499 | 0.01283 | 0.00067 | 90 | 3.9 |
|----------|----------|---------|---------|---------|-----|------|
| PERUNGUD | CHIDAMBA | 0.00849 | 0.02181 | 0.00114 | 90 | 6.6 |
| IRUKKAND | CHIDAMBA | 0.00977 | 0.0251 | 0.00131 | 90 | 7.6 |
| VADDAKKA | PERUNGUD | 0.00458 | 0.01176 | 0.00062 | 90 | 3.6 |
| VADDAKKA | THANDAIY | 0.00703 | 0.01807 | 0.00095 | 90 | 5.5 |
| SATHANK | UDANGUDI | 0.02047 | 0.05259 | 0.00276 | 90 | 16 |
| SATHANK | ARUMUGAN | 0.03452 | 0.0887 | 0.00465 | 90 | 27 |
| ARUMUGAN | MANJANEE | 0.01302 | 0.03344 | 0.00175 | 90 | 10.2 |
| SANKAN21 | IRUKKAND | 0.00906 | 0.02329 | 0.00122 | 90 | 7.1 |
| RADHAPUR | PANAGUDI | 0.01598 | 0.04106 | 0.00215 | 90 | 12.5 |
| RADHAPUR | UDAYTR21 | 0.01918 | 0.04928 | 0.00258 | 90 | 15 |
| RADHAPUR | KOTTAIKA | 0.02685 | 0.06899 | 0.00361 | 90 | 21 |
| THANDAIY | ANNANAGA | 0.01215 | 0.03121 | 0.00163 | 90 | 9.5 |
| VALLIYUR | ANNANAGA | 0.01509 | 0.03876 | 0.00203 | 90 | 11.8 |
| VALLIYUR | KARANTHA | 0.02225 | 0.05716 | 0.00299 | 90 | 17.4 |
| KARANTHA | THIRUVIR | 0.02888 | 0.07421 | 0.00389 | 90 | 22.6 |
| KARANTHA | KALAKAD | 0.0166 | 0.04264 | 0.00223 | 90 | 13 |
| PALAYAPE | MELAKALO | 0.02195 | 0.05641 | 0.00295 | 90 | 17.2 |
| KODAYAR1 | MELAKALO | 0.07134 | 0.14092 | 0.007 | 90 | 41.6 |
| KODAYAR1 | VEERAVAN | 0.05114 | 0.1314 | 0.00688 | 90 | 40 |
| BIOMELAK | MELAKALO | 0.00032 | 0.00082 | 0.00004 | 90 | 0.3 |
| VMCHATHR | ARUMUGAN | 0.06152 | 0.10564 | 0.00498 | 90 | 30.3 |
| PAPANASA | SERVALAR | 0.00479 | 0.01232 | 0.00258 | 180 | 7.5 |
| EPPOTHUM | AYYANAPU | 0.02895 | 0.07438 | 0.0039 | 90 | 22.6 |
| EPPOTHUM | VELATHIK | 0.02341 | 0.06015 | 0.00315 | 90 | 18.3 |
| EPPOTHUM | INDBARTH | 0.00174 | 0.00447 | 0.00023 | 90 | 1.4 |
| PAVOORCH | KODIKU21 | 0.0206 | 0.05292 | 0.00277 | 90 | 16.1 |
| TENKASI | SHENKOTT | 0.00923 | 0.02372 | 0.00124 | 90 | 7.2 |
| TENKASI | KADAYAM | 0.02398 | 0.06163 | 0.00323 | 90 | 18.8 |
| KADAYANA | PULIYANG | 0.01279 | 0.03285 | 0.00172 | 90 | 10 |
| VEERASEG | UTHUMALA | 0.00533 | 0.0137 | 0.00072 | 90 | 4.2 |
| SURANDAI | UTHUMALA | 0.01902 | 0.04888 | 0.00256 | 90 | 14.9 |
| VANNIKON | UTHUMALA | 0.01534 | 0.03942 | 0.00207 | 90 | 12 |
| AYYANARO | SANKTOFF | 0.04475 | 0.11498 | 0.00602 | 90 | 35 |
| SURANDAI | KEELAVEE | 0.02363 | 0.06071 | 0.00318 | 90 | 18.5 |
| KEELAVEE | ALANGUW1 | 0.0039 | 0.01002 | 0.00052 | 90 | 3 |
| SUNDANKU | AYYANARO | 0.00256 | 0.00657 | 0.00034 | 90 | 2 |
| MALAYANK | VEERASEG | 0.02526 | 0.06491 | 0.0034 | 90 | 19.8 |
| VISWTOFF | SANKARAN | 0.0358 | 0.09198 | 0.00482 | 90 | 28 |
| VISWANAT | NARAYANA | 0.02005 | 0.05151 | 0.0027 | 90 | 15.7 |
| PULIYANG | NARAYANA | 0.01599 | 0.0411 | 0.00215 | 90 | 12.5 |

| | 1 | | | | | |
|----------|----------|---------|---------|---------|----|------|
| VISWTOFF | VISWANAT | 0.00511 | 0.01314 | 0.00069 | 90 | 4 |
| PERIYAR_ | SURULIYA | 0.01714 | 0.04405 | 0.00231 | 90 | 13.4 |
| PERIYAR_ | MUDUNGAI | 0.03836 | 0.09855 | 0.00516 | 90 | 30 |
| RAJAPALA | RAJTOFF2 | 0.0055 | 0.01413 | 0.00074 | 90 | 4.3 |
| MALAYTOF | SANKARAN | 0.01406 | 0.03614 | 0.00189 | 90 | 11 |
| NSUBBIAH | VIJAYAPU | 0.02055 | 0.05279 | 0.00277 | 90 | 16.1 |
| SRPUDU21 | MEENTOFF | 0.01809 | 0.03107 | 0.00146 | 90 | 8.9 |
| CHETTIKU | AYYANARO | 0.01017 | 0.01745 | 0.00082 | 70 | 5 |
| THUCKALA | MARTTOFF | 0.00869 | 0.02234 | 0.00117 | 90 | 6.8 |
| VEEYANOO | PECHIPAR | 0.02257 | 0.05798 | 0.00304 | 90 | 17.6 |
| VEEYANOO | MARTTOFF | 0.00323 | 0.00831 | 0.00044 | 90 | 2.5 |
| AMBATOFF | PAPANASA | 0.00256 | 0.00657 | 0.00034 | 90 | 2 |
| VEERAVAN | THATOFF1 | 0.03392 | 0.08715 | 0.00457 | 90 | 26.5 |
| THATOFF1 | THALAIYU | 0.00729 | 0.01873 | 0.00098 | 90 | 5.7 |
| PALAYAPE | THATOFF2 | 0.00768 | 0.01974 | 0.00103 | 90 | 6 |
| THATOFF2 | THALAIYU | 0.00729 | 0.01873 | 0.00098 | 90 | 5.7 |
| SRPUDU21 | MUPPTOFF | 0.01204 | 0.03095 | 0.00162 | 90 | 9.4 |
| MUPPTOFF | MUPANTHA | 0.0006 | 0.00154 | 0.00008 | 90 | 0.5 |
| MUPANTHA | KANNAULR | 0.00304 | 0.00782 | 0.00041 | 90 | 2.4 |
| PALATOFF | PALAVOOR | 0.00153 | 0.00394 | 0.00021 | 90 | 1.2 |
| SRPUDU21 | PERUTOFF | 0.01202 | 0.03088 | 0.00162 | 90 | 9.4 |
| SRPUDU21 | KANNAULR | 0.01667 | 0.04284 | 0.00224 | 90 | 13 |
| TENKASI | KADNATOF | 0.00895 | 0.023 | 0.0012 | 90 | 7 |
| TENKTOFF | KADNATOF | 0.00128 | 0.00329 | 0.00017 | 90 | 1 |
| VISWANAT | KADAYANA | 0.02005 | 0.05151 | 0.0027 | 90 | 15.7 |
| TENKTOFF | KODITOFF | 0.00384 | 0.00986 | 0.00052 | 90 | 3 |
| KODITOFF | KODIKU21 | 0.00256 | 0.00657 | 0.00034 | 90 | 2 |
| KODITOFF | KODIKURI | 0.00038 | 0.00099 | 0.00005 | 90 | 0.3 |
| KULTHURA | MARTHADM | 0.00588 | 0.01511 | 0.00079 | 90 | 4.6 |
| PERUTOFF | PALAVOOR | 0.00614 | 0.01577 | 0.00083 | 90 | 4.8 |
| MEENTOFF | MEENAKSH | 0.00302 | 0.00775 | 0.00041 | 90 | 2.4 |
| MEENTOFF | THENGAM | 0.01818 | 0.03121 | 0.00147 | 90 | 8.9 |
| KANNAULR | PALAVOOR | 0.00801 | 0.01375 | 0.00065 | 70 | 3.9 |
| PALATOFF | KARUNKUL | 0.00767 | 0.01971 | 0.00103 | 90 | 6 |
| MUPPTOFF | PERUNGUD | 0.00499 | 0.01281 | 0.00067 | 90 | 3.9 |
| KAYATR21 | MANURTO | 0.02595 | 0.06669 | 0.00349 | 90 | 20.3 |
| KAYATR21 | AYYANARO | 0.02557 | 0.0657 | 0.00344 | 90 | 20 |
| KAYATR21 | THATOFF2 | 0.01524 | 0.03916 | 0.00205 | 90 | 11.9 |
| ANUPPA21 | NSUBBIAH | 0.02941 | 0.07556 | 0.00396 | 90 | 23 |
| ANUPPA21 | KOVILPAT | 0.04328 | 0.1112 | 0.00583 | 90 | 33.8 |
| TSIPCOT1 | AYYANAPU | 0.01844 | 0.04737 | 0.00248 | 90 | 14.4 |

| TTPSAUTO | MANJANEE | 0.01845 | 0.0474 | 0.00248 | 90 | 14.4 |
|----------|----------|---------|---------|---------|------|------|
| TTPSAUTO | ARUMUGAN | 0.02762 | 0.07096 | 0.00372 | 90 | 21.6 |
| KODA6YAR | KODAYAR1 | 0.00767 | 0.01971 | 0.00103 | 90 | 6 |
| CHEKKAN4 | ABPATTY4 | 0.0015 | 0.01676 | 0.89633 | 1390 | 162 |
| SETHIUR | PERUMALP | 0.0179 | 0.04599 | 0.00241 | 90 | 14 |
| SETHIUR | RAJTOFF1 | 0.00936 | 0.02405 | 0.00126 | 90 | 7.3 |
| KAYATR21 | VIJAYAPU | 0.01854 | 0.04763 | 0.0025 | 90 | 14.5 |
| KOTTAIKA | SATHANK | 0.02685 | 0.06899 | 0.00361 | 90 | 21 |
| MARTTOFF | MARTHADM | 0.00767 | 0.01971 | 0.00103 | 90 | 6 |
| RASTHA | OTHULUKK | 0.03671 | 0.09432 | 0.00494 | 90 | 28.7 |
| AMBATOFF | OTHULUKK | 0.01023 | 0.02628 | 0.00138 | 90 | 8 |
| MELAKALO | THIRUVIR | 0.02888 | 0.07421 | 0.00389 | 90 | 22.6 |
| VEERASEG | POIGAISS | 0.01183 | 0.03039 | 0.00159 | 90 | 9.3 |
| VEERASEG | KODIKU21 | 0.00951 | 0.02444 | 0.00128 | 90 | 7.4 |
| VMCHATHR | KAYATR21 | 0.05114 | 0.1314 | 0.00688 | 90 | 40 |
| KEELAVEE | KAYATR21 | 0.03963 | 0.10184 | 0.00534 | 90 | 31 |
| EPPOTHUM | KAYATR21 | 0.03196 | 0.08213 | 0.0043 | 90 | 25 |
| KODIKU21 | POIGAISS | 0.01828 | 0.04698 | 0.00246 | 90 | 14.3 |
| RAJAPALA | RAJTOFF1 | 0.0055 | 0.01413 | 0.00074 | 90 | 4.3 |
| MUDUNGAI | RAJTOFF1 | 0.02301 | 0.05913 | 0.0031 | 90 | 18 |
| SIPCOT2 | IBCPP2 | 0.00105 | 0.00587 | 0.0223 | 590 | 15 |
| ABPATT42 | UDAYTHR2 | 0.01067 | 0.05478 | 0.05059 | 295 | 70 |
| KAYATHR2 | PASUMAL2 | 0.01836 | 0.10219 | 0.09706 | 295 | 131 |
| MELAKALO | SERVALAR | 0.00741 | 0.01463 | 0.00073 | 80 | 4.3 |
| MELAKALO | TIRUPULI | 0.0366 | 0.06284 | 0.00296 | 80 | 18 |
| KARANTHA | TIRUPULI | 0.02643 | 0.04538 | 0.00214 | 70 | 13 |
| VADDAKKA | SANKAN21 | 0.00813 | 0.02089 | 0.00109 | 90 | 6.4 |
| MUPANTHA | PANAGUDI | 0.00749 | 0.01925 | 0.00101 | 90 | 5.9 |
| TTPSAUTO | VAGAIKUL | 0.03235 | 0.08311 | 0.00435 | 90 | 25.3 |
| TTPSAUTO | TSIPCOTW | 0.01662 | 0.04271 | 0.00224 | 90 | 13 |
| TTPSAUTO | TSHIPCOT | 0.0351 | 0.09018 | 0.00472 | 90 | 27.5 |
| TSIPCOT1 | TSHIPCOT | 0.00288 | 0.00739 | 0.00155 | 180 | 4.5 |
| TSIPCOT1 | TUTOCORW | 0.00771 | 0.01981 | 0.00104 | 90 | 6 |
| KAYATR21 | GANKAIKO | 0.00669 | 0.01718 | 0.0009 | 90 | 5.2 |
| MANURTO | MANNUR | 0.00641 | 0.01646 | 0.00086 | 90 | 5 |
| MANURTO | RASTHA | 0.00744 | 0.01912 | 0.001 | 90 | 5.8 |
| KAYATR21 | THATOFF1 | 0.01524 | 0.03916 | 0.00205 | 90 | 11.9 |
| KAYATR21 | KOVILPAT | 0.03836 | 0.09855 | 0.00516 | 90 | 30 |
| KAYATR21 | KAZHUHU | 0.04091 | 0.10512 | 0.00551 | 90 | 32 |
| KAYATR21 | VKPURAM | 0.06831 | 0.17552 | 0.0092 | 90 | 53.4 |
| TUTOCORW | TTPSAUTO | 0.01662 | 0.04271 | 0.00224 | 90 | 13 |

| ANUPPA21 | ALANKTOF | 0.0236 | 0.06064 | 0.00318 | 90 | 18.5 |
|----------|----------|---------|---------|---------|----|------|
| ANUPPA21 | PARAPTY1 | 0.00312 | 0.00802 | 0.00042 | 90 | 2.4 |
| ANUPPA21 | SATTURTF | 0.01413 | 0.0363 | 0.0019 | 90 | 11.1 |
| SATTUR1 | SATTURTF | 0.00281 | 0.00723 | 0.00038 | 90 | 2.2 |
| ANUPPA21 | ALANKULA | 0.0236 | 0.06064 | 0.00318 | 90 | 18.5 |
| ALANKTOF | ALANKULA | 0.00038 | 0.00099 | 0.00005 | 90 | 0.3 |
| ALANKTOF | REDIYA1 | 0.00859 | 0.02208 | 0.00116 | 90 | 6.7 |
| RAJAPALA | REDIYA1 | 0.01279 | 0.03285 | 0.00172 | 90 | 10 |
| SATTURTF | OTHULUKK | 0.01305 | 0.03354 | 0.00176 | 90 | 10.2 |
| PAPANASA | VKPURAM | 0.00508 | 0.00873 | 0.00041 | 70 | 2.5 |
| KOODATOF | SANKAN21 | 0.00844 | 0.01449 | 0.00068 | 70 | 4.2 |
| MALAYTOF | MALAYANK | 0.00244 | 0.00419 | 0.0002 | 70 | 1.2 |
| MALAYTOF | AYYANARO | 0.05693 | 0.09775 | 0.00461 | 70 | 28 |
| ALANGUW1 | PAVOORCH | 0.01455 | 0.03738 | 0.00196 | 90 | 11.4 |
| PAVOORCH | TENKTOFF | 0.0179 | 0.04599 | 0.00241 | 90 | 14 |
| PERUMALP | KARIVALA | 0.01151 | 0.02957 | 0.00155 | 90 | 9 |
| SURULIYA | RAJTOFF2 | 0.03068 | 0.07884 | 0.00413 | 90 | 24 |
| PALATOFF | KANNAULR | 0.00801 | 0.01375 | 0.00065 | 70 | 3.9 |
| KADAYAM | KADAYTOF | 0.01759 | 0.0452 | 0.00237 | 90 | 13.8 |
| KADAYTOF | OTHULUKK | 0.03233 | 0.08308 | 0.00435 | 90 | 25.3 |
| KADAYTOF | PAPANASA | 0.00703 | 0.01807 | 0.00095 | 90 | 5.5 |
| UDAYTR21 | SANKAN21 | 0.0179 | 0.04599 | 0.00241 | 90 | 14 |
| KOODANKU | KOODATOF | 0.00249 | 0.00641 | 0.00034 | 90 | 2 |
| MUNCHIRA | KULTHURA | 0.00979 | 0.02516 | 0.00132 | 90 | 7.7 |
| VISWTOFF | RAJTOFF2 | 0.03836 | 0.09855 | 0.00516 | 90 | 30 |
| EMPEEDIS | OTHULUKK | 0.00895 | 0.023 | 0.0012 | 90 | 7 |

Appendix B

B1.WTGS parameters

| Object | Parameter | Value |
|------------------------|--------------------------------------|---------------------------------------|
| | Nominal output power-P | 900 kW |
| Operational parameters | Cut-in wind speed- V_{cut-in} | 3.5 m/s |
| | Rated wind speed -V _{rated} | 15 m/s |
| | Cut-out wind speed- $V_{cut-out}$ | 25 m/s |
| Rotor | Rotor diameter -2R | 52.2 m |
| | Number of blades-B | 3 |
| | Moment of inertia- J_w | 1.6*10 ⁶ kg.m ² |
| | Gear box ratio-GB | 67.5 |
| Generator | Rated power -P | 900 kW |
| | Rated voltage-V | 690 V |
| | Rated speed | 1510 rpm |
| | Power factor -cosø | 0.89 |
| | Moment of inertia- J_{G} | 35.184 kg.m ² |
| Wind wheel | Coefficients | c1=0.5 |
| | | c2=67.56 |
| | | c3=0 |
| | | c4=0 |
| | | c5=1.517 |
| | | c6=16.286 |

B.2.Induction Generator model data

| Sl.No | Parameter | Value |
|-------|--|----------------|
| 1. | Stator Resistance R _s | 0.0034Ω |
| 2. | Stator leakage Reactance X _{ls} | 0.003 Ω |
| 3. | Rotor Resistance R _r | 0.055 Ω |
| 4. | Rotor leakage Reactance X' _{lr} | 0.042 Ω |
| 5. | Magnetizing Reactance X _m | 1.6 Ω |

Appendix C

Fault current level at various buses

The buses having fault current level between 5 p.u to 9 p.u are tabulated in Table C.1.

Table C.1. Fault level between 5 p.u to 9 p.u

| Bus No | Bus Name | Fault Level (pu) |
|--------|-------------------------------------|------------------------|
| 4 | SURULIYAR_GENERATOR_BUS_1X35MW | 5.6157 |
| 6 | BIOMASS_GENERATOR_MELAKALOOR | 5.4196 |
| 14 | PARAMAGUDI 230/110kVSS | 5.7764 |
| 19 | MUNCHIRAI_110/11 kV | 5.8102 |
| 43 | KALAKAD_110/11 kV | 5.7916 |
| 65 | VANNIKONENTHAL_110/11kVSS | 5.9735 |
| 72 | VELATHIKULAM_110/11kV | 5.2786 |
| 83 | VISWANATHAPERI_110/11 kV | 5.7887 |
| 99 | VAGAIKULAM_110/11kVSS | 5.1018 |
| 105 | KAZHUHU_110/11kVSS | 5.0937 |
| 3 | PERIYAR_GENERATOR_1X140 | 6.7086 |
| 5 | BIOMASS_GENERATOR | 6.2769 |
| 18 | KANYAKUMARI_110/11 kV | 6.7699 |
| 21 | KULTHURAI_110/11 kV | 6.8801 |
| 44 | KOTTAIKARUNKULAM 110/11kVSS | 6.3314 |
| 47 | SATHANKULAM_110/11 kV_110/33kV | 6.1131 |
| 54 | VMCHATHRAM(PALAYAMKOTTAI)_110/11kV | 6.3956 |
| 66 | CHETTIKURICHI(DEVARKULAM)_110/33kV | 6.6997 |
| 74 | SHENKOTTAI_110/11kV | 6.7378 |
| 78 | SANKARANKOIL_110/11 kV | 6.7706 |
| 85 | SETHIUR_110/11 kV | 6.5563 |
| 87 | MUDUNGAIYUR_110/11 kV | 6.5652 |
| 92 | VEERANAM_230/110/11kVSS | 6.6377 |
| 100 | TSIPCOTW_110/11kVSS | 6.5334 |
| 113 | VISWANATHAPERI_TOFF | 6.3022 |
| 7 | SERVALAR_HYDRO_GENERATOR_BUS_1X20MW | 7.435 |
| 17 | THENGAMPUDUR_110/11 kV | 7.0341 |
| 20 | MEENAKSHIPURAM_110/11 kV | 7.8165 |

| 22 | NAGARKOIL_110/11 kV | 7.5047 |
|-----|--|--------|
| 24 | MAHARAJAPURAM_110/11 kV | 7.39 |
| 26 | KARUNKULAM_110/11 kV | 7.7884 |
| 36 | KOODANKULAM_110/11 kV_110/33kV | 7.641 |
| 40 | ANNANAGAR_110/33/11kVSS | 7.5609 |
| 45 | VALLIYUR_110/11 kV | 7.2237 |
| 46 | THIRUVIRUNTHANPULLAI_110/11 kV | 7.5587 |
| 49 | ARUMUGANERI_110/11kV_110/33kV | 7.9222 |
| 50 | KARANTHANERI_110/11kV | 7.8625 |
| 51 | MANJANEER KAYAL_110/11kV | 7.6056 |
| 52 | VEERAVANALLUR_110/11kV | 7.5843 |
| 56 | RASTHA_110/33kV | 7.8476 |
| 57 | MANNUR_110/11kV | 7.074 |
| 60 | SUNDANKURCHI_110/11kV | 7.3081 |
| 61 | AYYAANAROOTHUR_110/11kV | 7.701 |
| 67 | SURANDAI_110/11kV | 7.047 |
| 68 | UTHUMALAI_110/33kV_66/11kV | 7.9624 |
| 69 | AYYANAPURAM_110/11kV_110/33kV | 7.7174 |
| 70 | MALAYANKULAM_110/11kV | 7.6147 |
| 71 | EPPOTHUMVENTRAN_110/11kV_110/33kV | 7.9665 |
| 76 | KOVILPATTI_110/11 kV | 7.3454 |
| 79 | NSUBBIAHPURAM_110/11 kV | 7.8411 |
| 88 | SURULIYAR HYDEL_Switch yard | 7.627 |
| 89 | PERIYAR HYDEL P.H_Switch yard | 7.3336 |
| 90 | BIOMASS_EPPOTHUMVANTENTRAN_BUS110kVBUS | 7.7444 |
| 95 | MEELAVETAN_110kV | 7.2895 |
| 96 | TIRUPULI 110/11 kV SS | 7.9499 |
| 97 | MARTHANDAM_110/11kVSS | 7.7331 |
| 114 | POIGAI_110/33kVSS | 7.757 |
| 115 | RAJAPALAYAM_TOFF1 | 7.8738 |
| 122 | MALAYANKULAM_TOFF_110/11kV_SS | 7.6367 |
| 123 | ALANGULAMWIND FARM | 7.8805 |
| 2 | KODAIYAR_GENERATOR_BUS_1X40MW | 8.105 |
| 8 | PAPANASAM_HYDRO_GENERATOR_BUS_1X32MW | 8.1891 |
| 10 | KUDANKULAM_STARTUP_BUS_230/33kV | 8.4769 |
| 23 | THUCKALAY_110/11 kV | 8.7395 |
| 27 | PALAVOOR_110/11 kV | 8.9303 |
| 29 | CHIDAMBARAPURAM_110/11 kV | 8.3779 |
| 30 | ARALVOIMOZHI_110/11 kV | 8.9794 |
| 32 | IRUKKANDURAI_110/33/11 kV SS | 8.311 |
| 37 | RADHAPURAM_110/11 kV_110/33kV | 8.1875 |

| 39 | PANAGUDI_110/11 kV_110/33kV | 8.9088 |
|-----|------------------------------------|--------|
| 41 | UDAYTHUR_230/110/33kVSS | 8.7293 |
| 42 | THANDAIYARKULAM_110/11 kV_110/33kV | 8.385 |
| 58 | KEELAVEERANAM_110/11kV_110/33kV | 8.0139 |
| 59 | KADAYAM_110/11kV | 8.3412 |
| 64 | PAVOORCHATRAM_110/11kV_110/33kV | 8.1812 |
| 73 | TENKASI_110/11kV | 8.1105 |
| 77 | VUJAYAPURAI_110/11 kV | 8.5217 |
| 86 | RAJAPALAYAM_110/11 kV | 8.5423 |
| 91 | VEERASEGAMANI_110/66/33kV | 8.604 |
| 101 | TSHIPCOT_110/11kV SS | 8.8522 |
| 102 | TUTOCORW_110/11kV SS | 8.6177 |
| 104 | MANURTOFF | 8.0706 |
| 106 | MEENAKSHIPURAM_TOFF | 8.0804 |
| 109 | PALAVOOR_TOFF | 8.8584 |
| 110 | PERUNGUDI_TOFF | 8.8991 |
| 111 | TENKASI_TOFF | 8.7603 |
| 112 | KODIKURICHI_TOFF | 8.9285 |
| 116 | RAJANPALAYAM_TOFF2_MUNGAIYUR | 8.367 |
| 121 | REDIYARKULAM_110/11kVSS | 8.7308 |
| 125 | KADAYANALLUR_110/11kV_SS | 8.6476 |
| 126 | KODIKURICHI_110/11kVSS | 8.8465 |
| 127 | KOODANKULAM_TOFF | 8.0583 |
| 128 | EMPEE SUGARS 2*25MW COGEN | 8.4373 |
| 1 | KODAIYAR_GENERATOR_1X60MW | 9.825 |
| 9 | SRPUDUR_230/110/11kVSS | 9.7743 |
| 11 | VEERANAM230/33 kV SS | 9.9262 |
| 12 | KODIKURCHI230/110 kV SS | 9.7969 |
| 13 | AMDAPURAM230/33 kV SS | 9.5077 |
| 15 | CHEKKANURANI_400/230_KV_SS | 9.9009 |
| 16 | ABISHEKAPATTY_THIRUNELVELI_PGCIL | 9.6778 |
| 25 | SR PUDUR_230/110/11 kV_110/230kV | 9.7812 |
| 28 | VEEYANOOR_110/11 kV | 9.501 |
| 31 | SANKANERI_230/110/11kVSS | 9.2274 |
| 33 | MUPANTHAL_110/11kVSS | 9.4718 |
| 34 | PECHIPARAI_110/11 kV | 9.3855 |
| 35 | PERUNGUDI_110/33/11kVSS | 9.3588 |
| 38 | VADDAKKANKULAM_110/11 kV_110/33kV | 9.215 |
| 53 | PALAYAPETTAI_110/11kV | 9.8801 |
| 55 | THALAIYUTU_110/11kV_110/33 | 9.8829 |
| 63 | ALANKULAM_110/11kV_110/33kV | 9.1868 |

| 75 | KODIKURCHI_110/33kV | 9.1605 |
|-----|-------------------------|--------|
| 93 | TUTICORIN_110kV_SS | 9.2467 |
| 94 | SIPCOT_110kV | 9.2825 |
| 98 | KANNANALLUR_110/11kV_SS | 9.2046 |
| 103 | GANKAIKONDAN_110/11kVSS | 9.7267 |
| 107 | MARTHANDAM_TOFF | 9.2182 |
| 108 | MUPPANTHAL_TOFF | 9.469 |
| 117 | ALANKULAMTOFF | 9.2158 |
| 118 | PARAIPATTY 110 KV SS | 9.7227 |
| 119 | SATTUR TOFF | 9.7322 |
| 120 | SATTUR 110 KV SS | 9.0611 |

REFERENCES

- [1]. P. Kundur, "Power System Stability and Control", McGraw-Hill, 1994.
- [2]. N.H.Hingorani, "Understanding Flexible AC transmission systems", IEEE Spectrum, 1993.
- [3]. R.Ramanujam, "Power System Dynamics Analysis and Simulation", PHI Learning Pvt.Ltd, 2009.
- [4]. N.Christl, R. Hedin, Jhonson K, Krause P and Montoya AA "Power system studies and modelling for Kayenta 230kVsubstation advanced series compensation", proceedings of IEEE 5th International conference on Ac and DC power transmission,1991.
- [5]. Sadek, P. Llitzelberger, P. E. Krduse, S.M. McKenna, A. H. Maiitaya, and D. Togerson, "Advanced series compensation (ASC) with thyristor controlled impedance," in Int. Conf: Large High Voltage Electric Systems (CIGRE, Paris, Sept. 1992, paper 14/37/38-05).
- [6]. S. G. Helbing and G. G. Kaidy, "Investigations of an advanced form of series compensation," IEEE Trans. POWER Delivery, vol. 9, no. 2, pp.939-947, Apr. 1994.
- [7]. Dragan Jovcic, Nalin Pahalawaththa, Mohamed Zavahir, and Heba A. Hassan "SVC Dynamic Analytical Model" IEEE Trans. on Power Delivery,vol: 18, no.4, 2003, pp: 1455 1461
- [8] Z. T. Faur and C. A. Canizares, "Effects of FACTS devices an system load ability," in Proc. North American Power Symposium (NAPS), Bozeman, MT. USA, Oct. 1995, pp. 520-524.
- [9] P. Abayles and G. Arroyo, "Security assessment in the operation of longitudinal power systems," IEEE Trans. Power Systems, vol. PWRS-1, vol:1,no. 2, pp. 225-232, 1986, pp;225 232
- [10] E. Acha, C. R. Fuerte-Esquivel, H. Ambriz-Perez, and C. Angeles-Camacho, "FACTS Modelling and Simulation in Power Networks", John Wiley & Sons, Inc, 2004.
- [11] Alejandro Pizano-Martinez, Claudio R. Fuerte-Esquive, I H. Ambriz-Pérez, Enrique Acha, "Modeling of VSC-Based HVDC Systems for a Newton-Raphson OPF Algorithm", IEEE Transactions on Power Systems, Vol. 22, No. 4, November 2007,pp-1794-1803.

[12] J.Arrillaga, P. and Bodger, "Integration of HVDC links with fast- decoupled load flow Solutions." Proc. IEE, Vol. 124, No. 5, May 1977,pp-463-468.

- [13] www.tneborg.net
- [14] www.cea.nic.in
- [15] www.powergrid.in